COMPUTATIONAL MOLECULAR DESIGN OF CELLULOSE-BASED DELIVERY VEHICLES FOR VAGINAL MICROBICIDE GELS

BY

THORA WEAVER WHITMORE

Submitted to the graduate degree program in Bioengineering and the Graduate Faculty of the University of Kansas in partial fulfillment of the requirements for the degree of Doctor of Philosophy.

_____

Chairperson Dr. Sarah L. Kieweg

_____

Co-Chairperson Dr. Kyle V. Camarda

_____

Dr. P. Scott Hefty

_____

Dr. Stevin H. Gehrke

_____

Dr. Laird Forrest

Date Defended: June 13th, 2016

The Dissertation Committee for Thora Weaver Whitmore

certifies that this is the approved version of the following dissertation:

COMPUTATIONAL MOLECULAR DESIGN OF CELLULOSE-BASED DELIVERY VEHICLES FOR VAGINAL MICROBICIDE GELS

_____

Chairperson Dr. Sarah L. Kieweg

_____

Co-Chairperson Dr. Kyle V. Camarda

Date approved: July 15th, 2016

Abstract

HIV/AIDS is a global pandemic that has claimed the lives of 39 million people and currently afflicts 36.9 million more. These effects are disproportionately felt in sub-Saharan Africa which has almost 70% of those current cases and where women account for 59% of current infections. These numbers are even more disproportionate for young women and complications associated with HIV/AIDS are the leading cause of death in women aged 15-44. This creates a need for female-controlled tools to prevent infection. Microbicides are one such tool.

Microbicides are vaginally-delivered topical products that combine a therapeutic agent with activity against HIV and a delivery vehicle. The delivery vehicle can consist of many different formulations, depending on the therapeutic agent used and the delivery mechanism desired. Polymer solutions (known as "gels" in the microbicide field) have received the most attention and have been incorporated into the most formulations for use in clinical trial evaluations. There have been several high profile microbicide clinical trial failures, including nonoxynol-9 and cellulose sulfate, as well as one success, CAPRISA 004. Nonoxynol-9 failed in the direction of harm by producing host cell toxicity. The reasons for the failure of cellulose sulfate are not fully understood, but one hypothesis suggests unmeasured benefits provided by the delivery vehicle placebo caused the treatment arm to fail in the direction of harm. Conversely, CAPRISA 004 displayed moderate protection against HIV, which was highly correlated with adherence. The VOICE and FACTS 001 follow-up studies failed to prove the same efficacy, specifically citing low adherence as the reason for failure. These previous studies illustrate the need for delivery vehicles with fully understood physical properties that are safe, allow for effective microbicide delivery, and are acceptable to patients.

This study focused on rationally designing next generation microbicide delivery vehicles that are safe, effective, and acceptable. This rational design was accomplished using the methodology of computational molecular design (CMD). This process involves measuring relevant physical properties for a set of known compounds, creating structure-property correlations that relate these data to molecular structure, formulating an optimization problem that incorporates these correlations, and solving this

problem to generate novel structures that possess target physical properties. Novel delivery vehicles were designed to have ideal safety, efficacy, and adherence by creating a predictive model that considered rheology, biocompatibility, and drug compatibility.

Rheology describes the viscous and elastic character of a fluid. These properties influence the flow behavior of the fluid. The efficacy of liquid microbicide formulations depends upon the delivery vehicle flowing from the point of delivery to cover the entire epithelium to release the active therapeutic over this whole surface area as well as provide a lubricating barrier to pathogens. Additionally, patient acceptability and thus adherence is greatly influenced by how the fluid feels during insertion and use, what the consistency and color looks like, and whether the fluid leaks out prematurely. This study measured the rheology of a set of cellulose ethers, common liquid microbicide delivery vehicles, and related these data with molecular weight, molecular structure, and concentration to form the first part of the overall predictive model.

Biocompatibility characterizes the safety and incidence of harm to host cells caused by compounds. This study defined biocompatibility as *in vitro* vaginal cell cytotoxicity, inflammation represented as the upregulation of two cytokines, and inhibition of *C. trachomatis* infection. These properties were measured for the same set of cellulose ethers and correlated with molecular structure and molecular weight to form the second part of the overall predictive model.

Drug compatibility considers behavior of the active therapeutic in the delivery vehicle. This study defined drug compatibility as solubility of the drug in the delivery vehicle and release of the drug out of the delivery vehicle. Tenofovir, used in the successful CAPRISA 004 trial, was chosen as the model active therapeutic. The properties were again measured for the same set of compounds and correlated with molecular structure and molecular weight to form the final part of the predictive model.

This predictive model was finally incorporated into an optimization problem formulation along with structural feasibility constraints. Target properties for all the measured physical properties were selected and the optimization problem was solved to minimize the difference between the properties predicted by the model and these targets. This optimization process resulted in novel structures for

candidate delivery vehicles with improved properties compared to the measured set. These candidate delivery vehicles can be synthesized and incorporated into future microbicide formulations.

This dissertation is dedicated to my mother,

Joan Weaver, who died three times while

I was completing this work and came back

so I could finish.

Pierce: […] of course we didn't have the same safety standards back then so…no condoms. I tell ya, before AIDS sex was like shaking hands.

Abed: Hence AIDS.

Community, episode 108, "Home Economics"

Acknowledgements

The completion of this dissertation has been long, often immensely trying, and sometimes thrillingly satisfying. All scientific research requires collaboration, but the exceedingly interdisciplinary nature of this current work means I have a lot of people to thank. I would like to start with my advisor Dr. Sarah Kieweg who introduced me to the world of microbicides and reawaked a passion for public health outreach I hope to pursue in the future. She provided invaluable knowledge and pushed me to become a better researcher and writer. Our countless conversations made me a better scientific communicator, for which I am very grateful. In addition I need to thank my fellow graduate students as well as the several undergraduate students that populated her group, in particular Rajib Anwar, Mark Pacey, and Bin Hu who were around for most, if not all, of my journey and finished all at the same time. They helped me many times in the world of thin film flow when I felt out of my element. I need to thank Taylor Wilson who began work on this project before I ever arrived and provided much of the early rheology work that appears in chapter two.

I need to thank my *other* advisor Dr. Kyle Camarda for helping me through the initially foreign world of process design. He encouraged me to finish work, to go get things done, and to make connections outside the confines of my little office. His advice was direct and he often made lab meetings fun. I need to also thank the many graduate and undergraduate students that have filtered in and out of his group over my years, in particular Farhana Abedin, Brock Roughton, and Kyle Boone. They provided invaluable advice on numerous occasions when I encountered problems I couldn't solve on my own and often were available just to chat and listen to me rant about whatever documentary or news article was on my mind.

I need to thank a large collaborator on this work, Dr. Scott Hefty. He welcomed me into his lab and allowed me access to invaluable resources without which the third chapter of this dissertation would not exist. He devoted time to me and my work even though I wasn't his student and his constant challenging during meetings made me a better communicator and added my ability to transfer my knowledge between disciplines. I would like to thank the various members of his group I encountered

during my year and half in his lab. I would like to thank Michael Barta who took time out of his schedule to brush up my cell culture technique. I am forever indebted to Ichie Osaka who performed all the chlamydia experimental work for me that appears in chapter three. Finally, I would like to thank Kelly Harrison for being a lovely friend who commiserated with me about the trials and tribulations of grad school and also shared my deep love of cats. I'm so happy she is healthy and strong today.

I would like to thank Dr. Stevin Gehrke and the various members of his lab group. They provided me access to their shared laboratory space and, most importantly, the HPLC apparatus that allowed me to complete the experiments in chapter four. I thank the several students of his over the years that have given up their time to train me on various pieces of equipment. I would also like to thank Dr. Michael Detamore for graciously allowing me access to several pieces of equipment needed to complete the experiments in chapter four and for being so understanding to all of my requests. I would like to thank Dr. Laird Forrest for substituting onto my committee near the last minute and being so accommodating.

Finally, I would like to thank my family for putting up with me through the highs and many lows of completing this work. My cats Nellie and Tobey provided love and cuddles and only sometimes tried to keep me from working by sitting on my lap or papers or computer. My father Richard Whitmore was encouraging and always proud and most importantly made sure I had sustenance. My sister Mariah Whitmore was caring, encouraging, and endlessly optimistic. Whenever I was in the depths of frustration she assured me that everything was okay or would be okay. She helpfully pointed out that grad school was like this for everyone and my problems were no different from anyone else's. Finally, I need to thank my mother Joan Weaver. It is not hyperbole to say I would not have finished without her. She was my biggest fan, pushed me to work, cheered me on, gave me constant support, listened to my complaining on the same themes over and over, always got me tasty treats when I needed them, was incredibly flexible with my work schedule, always accommodating day and night if I needed to write or feed my cells, and most importantly let me have complete control over the DVR.

This work was supported by NIH Grant Number R21/R33 AI082697 from the National Institute of Allergy and Infectious Diseases. Hercules/Aqualon provided the samples of Natrasol HEC and Blanose

CMC. Dow Chemical provided the samples of Methocel A, E, F, and K. A colleague Dr. Miezan Ezoulin in Dr. BBC Youan's laboratory at UMKC provided the VK2/E6E7 vaginal epithelial cell line.

Table of Contents

Chapter 1

1.0 Introduction

1.1 HIV/AIDS Problem

The HIV/AIDS pandemic remains a major global health concern (1). Since the identification of the disease in 1981, an estimated 39 million people worldwide have died from HIV/AIDS or assorted complications. About 14 million (2) of those deaths had occurred by the end of 1999, while approximately 25.3 million (3) people died between 2000 and 2014. At the end of 2014 (3), an estimated 36.9 million people worldwide were living with HIV/AIDS and almost 51% were women. In that year (3), 2.0 million people were newly infected and 1.2 million died due to complications associated with the disease. This disease disproportionally affects the Global South with almost 70% of all HIV/AIDS cases occurring in sub-Saharan Africa, including 1.4 million new cases and 790,000 deaths (3). Collectively, those 44 countries have an adult prevalence of 4.8%, compared to a worldwide adult prevalence of 0.8% (3). The worst afflicted countries, such as Botswana, Lesotho, and Swaziland, had an adult prevalence around or above 25% (3). Although still formidable, these numbers indicated significant improvements in the global fight against HIV/AIDS in the last 15 years.

Great progress has been made since 2000. The worldwide new infection rate has declined 35% since 2000, from 3.1 million that year to 2.0 million in 2014 (3). The yearly death rate has decreased 42% from its peak in 2004, from 2.0 million in 2005 to 1.2 million in 2014 (3). In sub-Saharan Africa during this period new infections were down 41% and AIDS-related deaths decreased by 48% (3). These advances are due to a plethora of HIV/AIDS treatment and prevention strategies, in particular the increase in access to antiretroviral drugs. In 2000, only about 10,000 of those infected with HIV/AIDS in sub-Saharan Africa had access to HIV antiretroviral medicines with a yearly cost of $10,000 (US) (3). Worldwide, those living with HIV/AIDS who have access to antiretroviral therapy have risen from 1 million in 2001 to over 15 million in 2015, and first-line treatment regimens are only $100 (US) (3). Without increased access to antiretroviral and prevention techniques, it is hypothesized that 30 million more people would have been infected in the 15 year period from 2000 to 2015, and that 7.8 million more

would have died (3). Even with these key advancements several populations, most notably young women, are being left behind.

Worldwide, women account for just over half of all HIV/AIDS cases, but in sub-Saharan Africa they are nearly 59% of the currently infected (3). Women are more biologically susceptible to HIV infection when exposed to the virus to due differences in reproductive anatomy and fluid transfer during intercourse (4). The statistics become particularly stark for young women. In sub-Saharan Africa, among young people aged 15-24 currently infected with HIV/AIDs, 63% are women (3). For adolescents the prevalence is 1.7 times higher for females compared males, and in South Africa the prevalence is eight times higher for females aged 15-19 compared to males (5). The new infection rate continues to disproportionally impact young women. Worldwide, females account for 56% of new infections among 15-24 year olds and 62% among 15-19 year olds. In sub-Saharan Africa these figures increase to 64% and 71%, respectively (6). In South Africa, new infections for young people aged 15-24 are four times higher for females compared to males (7). HIV/AIDS-related illnesses are the leading cause of death worldwide for women of reproductive age (15-44 years), and also the leading cause of death for adolescent (10-19 years) females in sub-Saharan Africa. These disparities in HIV infection vulnerabilities are due to gender inequalities and inadequate prevention programs.

Current prevention programs include condom use, voluntary medical male circumcision (VMMC), needle-syringe programs, opioid substitution therapy for injection drug users, and antiretroviral treatment. VMMC provides a 60% reduction in female-to-male HIV transmission, comparable to vaccine-like levels (8). Needle-syringe programs that decrease the use of unsterile injection equipment decrease HIV transmission (9). Opioid substitution therapy reduced HIV incidence by an average of 54% among intravenous drug users across nine studies (10). Antiretroviral treatment, if begun as soon as a person is diagnosed, can reduce HIV transmission to a partner by 96% (11). Condom use continues to be the main prevention tool (12). There have been significant gains in regional availability, with 1.7 billion condoms procured for sub-Saharan Africa in 2014, compared to 0.4 billion in 2001 (3). However, this increase amounts to only eight condoms available per year for each sexually active individual in sub-Saharan

Africa (3), hardly enough to confer complete protection against HIV/AIDS. Indeed, in 2014 (3) only one out of every three women with multiple sexual partners reported using a condom the last time they had sex. Women are much less likely than men to use condoms in non-marital relationships, and men are less likely to know their HIV status since they are more likely to avoid being tested for HIV compared to women (13). Thus women struggle to access prevention tools, especially young women, and social inequalities prevent them from consistently using these methods.

Many barriers of access prevent young women from effectively protecting themselves from HIV/AIDS. Gender inequalities, such as power inequalities in relationships and intimate partner violence, place women at a great risk of HIV exposure compared to men (14, 15). For instance, modeling in Kenya suggests that solely eliminating sexual violence could prevent 17% of HIV infections for sex workers (16). Often, women do not have autonomy to make decisions about their health care and sexual practices. The number of women who do not have these choices in sub-Saharan Africa is over 50%, and in some countries as high as 70-80% (17). When available to women, various treatment options either confer benefits to men or are male-controlled. VMMC protects men (8); men predominately decide if and when to have sex and whether to use a condom (17); HIV-positive men are less likely to receive antiretroviral treatment compared to women, and men who are treated are less likely to adhere to antiretroviral therapy, thus putting their partners at risk (18). For all of these reasons young women urgently need a new, female-controlled prevention tool. One such tool, which depends upon a woman's decision instead of the male partner's, is vaginal gel microbicides.

1.2 A Review of Anti-HIV Microbicides in Development

Microbicides (19-22) are vaginally- (23) or rectally- (24) delivered topical products that prevent against sexually transmitted infections, or STIs. A complete formulation combines an active therapeutic and/or prophylactic agent, known as an active pharmaceutical ingredient (API), with a delivery vehicle, sometimes referred to as a drug delivery system (DDS). The delivery vehicle can consist of a polymer solution (often known as a "gel" in the microbicide field), cream, film, diaphragm, ovule, intravaginal ring, implant, injection, oral tablet, or quick dissolving tablet. Different types of delivery vehicles have

different mechanisms of protection. Delivery vehicles can either provide chronic, low doses of API for long-term protection, or brief, high doses for short-term or emergency protection (25). Both delivery mechanisms have strengths and drawbacks.

Long term delivery mechanisms remain in the same site for an extended period of time from which they produced a continuous release of the API. Long term delivery vehicles require less frequent dosing than short term mechanisms. Typically new doses are applied once a month or every few months. This strategy involves less effort from patients who do not have to adhere to a strict daily dosing schedule. Various delivery vehicles can confer this long term delivery. Subdermal injections (26-28) consist of a liquid suspension of the API. Low systemic concentrations from the injection and very short API residence times at active sites have provided challenges to this delivery mechanism (29). Integration of the API in a nanoparticle can produce constant, sustained release over the course of a month as the nanoparticle breaks down, and thus improve the efficacy of this delivery mechanism (30). Subdermal implants are modeled on the long-acting contraceptive implants (31), such as Norplant ® (32). These delivery systems confer protection in much the same way as a nanoparticle injection. The API is released at constant rate out of the polymer implant for a sustained period of time (33). A microbicide-loaded diaphragm provides an option for dual HIV-protection and contraception (34). The delivery vehicle is placed over the cervix as with a standard diaphragm and remains in place for up to six months while it releases a steady concentration of anti-HIV API. Vaginal ovules or suppositories (35, 36) are similar to commercial products that treat common vaginal infections. These delivery vehicles are similar to subdermal implants except they are applied directly to the surface of the upper vaginal tract. The benefit of these delivery vehicles is that they release a constant dose of API right at the site of infection challenge, rather than systemically. In recent years, two forms of long term protection have received a lot of attention. These include intravaginal rings and oral tablets.

As with the subdermal implants and intravaginal diaphragms, intravaginal rings for microbicide delivery (37) are modeled on contraceptive rings such as NuvaRing® (38), Progering® (39), and Fertiring® (40), and estrogen replacement therapy such as Estring® (41) and Femring® (42). These rings

are usually made from silicone elastomer, with the exception of NuvaRing® which is vinyl acetate and ethylene copolymer (43). These rings are inserted into the upper vaginal tract where they remain in place for 30 days, releasing a constant concentration of API (44). A large number of HIV antiretroviral microbicides have been formulated into these delivery vehicles (45, 46) and several are undergoing clinical trials (44), including a completed Phase I safety trial of a dapivirine (DPV) and maraviroc (MVC) combination (47), an a Phase I trial of a tenofovir (TFV) and levonorgestrel (LNG) combination HIV microbicide and contraceptive, respectively (47). Most notably was the ASPIRE trial, a Phase III safety and efficacy trial of a vaginal ring containing DPV (48). The results displayed a 27% reduction in HIV infections in the treatment arm compared to the placebo (49). When two test sites with low adherence were removed, the reduction in infection increased to 37%. Further, a 56% reduction in infection was observed for women over 21 years old while no reduction was seen in women under that age. The disparity between these figures was correlated with adherence. Although the overall benefit conferred by this study was low, these results, especially the increased protection found in those individuals with high adherence, are encouraging for the development of future microbicides.

Finally, oral tablets provide pre-exposure prophylaxis, known as PrEP, with daily dosing of antiretroviral drugs for HIV-negative individuals with HIV-positive partners (50). Daily dosing provides a steady, systemic concentration of the API. In 2012 the FDA approved a combination dose of tenofovir disoproxil fumarate (TDF) and emtricitabine (FTC), known as Truvada®, for use by sexually active, HIV-negative adults to prevent infection (51). This followed two large scale clinical trials supporting the efficacy of this dosing regimen. The iPrEx trial enrolled high risk men who have sex with men (MSM) and the overall efficacy was 44% (52). Although lower than expected, the rate of efficacy was highly dependent upon adherence such that the group with 90% adherence displayed 73% efficacy. The Partners PrEP trial observed heterosexual serodiscordant couples where one partner was HIV-infected and the other was not (53, 54). This trial observed much higher adherence overall such that the overall prevention efficacy was 73%. These results are highly encouraging and provide another prevention tool in addition to traditional prophylactic methods.

Conversely to the above delivery vehicles, short term formulations require dosing immediately before sexual intercourse and must be used repeatedly for each act. This requires more effort on the part of the patient (55). However, these vehicles can deliver a higher dose of the API at the site of infection during the period of viral challenged compared to long-term delivery vehicles. Short term delivery vehicles include gels (56-62), creams (63), films (64-70), and quick dissolving tablets (70-73). Similar to other delivery vehicles, these mechanism are based on current commercial products (74), such as vaginal contraceptive films (VCF) (75), Vagistat-1® tablets for yeast infections (76), or KY® Jelly for vaginal lubrication (77). Vaginal gels and creams are liquid formulations that are inserted with an applicator in the upper vaginal tract and then spread or flow to cover the entirety of the vaginal epithelium (78). Quick dissolving films and tablets are solid or semi-solid formulations that are inserted into the vaginal tract and quickly absorbed into the epithelium (70). These short term delivery vehicles have received a high amount of attention over the past few decades as possible ant-HIV vaginal microbicides, with variable rates of success.

1.3 History of Vaginal Gel Microbicides

The first vaginal microbicides clinically evaluated had non-specific inhibitory activity against HIV and other STIs. This class of microbicides were surfactants (79). Surfactants non-specifically destroy the integrity of lipid bilayers and thus kill cells through membrane rupture and inactivate viruses by disrupting the viral envelope. One such surfactant, nonoxynol-9 (N9), had been used since the 1960s as a lubricating contraceptive spermicide that was later used to coat latex condoms (80). The antiviral capabilities of N9 were recognized as early as 1985 (81), and the compound displayed good efficacy against HIV *in vitro* (82), and *in vivo* (83). However, clinical trials of N9 failed to prove efficacy. Early trials of sex workers in Kenya (84) and Cameroon (85) displayed no difference in infection rates between the treatment and placebo arms. However those treated with N9 had a higher incidence of genital ulcerations. In addition to failing to prove efficacy, a phase III trial of sex workers in four countries displayed an almost double HIV infection rate in the N9 arm compared to placebo in women who used the formulation more than three times a day (86, 87). The increase in vaginal toxicity, ulcerations, and

inflammation at higher doses was suggested as the cause of increase in infection rate (88). Thus N9 was discontinued from microbicide development and greater emphasis was placed on safety studies before clinical scale-up. Another surfactant, cetyl betaine and myristamine oxide (C31G), had similar antiviral activity to N9 but was assumed less cytotoxic (89). In 2005 and 2006 two trials (90) of C31G were halted for futility. The HIV infection rate was lower than anticipated and thus statistical significance could not be determined. Although it was not significant, there was a trend towards higher infection rates among the treatment arm compared to the placebo. Due to these results other classes of microbicides have been increasingly explored.

A second class of non-specific microbicides are vaginal milieu protectors (91). These prevent infection by restoring or enhancing the natural protective mechanisms inherent within the vaginal canal, particularly by maintaining the acidic pH produced by native lactobacilli. A healthy vaginal pH is in the range of 3.5 to 4.5, while HIV is inactivated at a pH between 4.0 and 5.8 (92). However, the presence of semen and some disease states neutralizes this acidity, allowing for viral penetration. One such acidifying agent is Carbopol 974P, or BufferGel. BufferGel is a polyacrylic acid that buffers twice its volume of semen to below pH 5 (93). BufferGel is spermicidal and has activity against HIV, HSV, HPV, bacterial vaginosis, and *Chlamydia trachomatis* (94). Although BufferGel was found safe in two phase I trials (95, 96), a phase II trial failed to prove efficacy over a placebo gel or no gel (97).

A final class of non-specific microbicides is anionic polymers that function as viral entry inhibitors (98). These negatively charged molecules interact with the positively charged proteins on the HIV viral envelope and prevent attachment of HIV to CD4+ cells (99). A sulfonated polymer, naphthalene sulfonate, known as PRO 2000, has *in vitro* activity against HIV, HSV, *C. trachomatis*, and *Neisseria gonorrhoeae* (100). Phase I clinical trials indicated safety of the formulation (101), although high concentrations were associated with increased intermenstrual bleeding (102). Early phase II efficacy trials demonstrated a moderate, statistically nonsignificant 30% reduction in HIV infection conferred by PRO 2000 (97). A phase III trial demonstrated safety but not efficacy (103, 104). Another sulfonated polysaccharide derived from seaweed, carrageenan, known as Carraguard, blocks HIV infection by

binding to the viral envelop and preventing HIV-infected mononuclear cells from migrating across the vaginal epithelial surface to lymph nodes (105). Once again, although this formulation was safe in early trials (106, 107), phase III trials failed to prove efficacy over the placebo (108). However, applicator dye testing indicated that adherence was low, only 42%, which might have contributed to the negative outcome. A final anionic polymer considered in large scale clinical trials was cellulose sulfate. In addition to HIV, cellulose sulfate has *in vitro* activity against HPV, *N. gonorrhoeae*, *C. trachomatis*, and *Gardnerella vaginalis* (109). However, after successful phase I safety studies (110, 111), in 2007 two large phase III trials in Africa and India had to be halted after one of them displayed 50% higher HIV infection in the cellulose sulfate arm compared to the placebo (112). As of today no satisfactory explanation exists as to why cellulose sulfate failed in the direction of harm (112). One hypothesis states that microscopic harm induced by cellulose sulfate to lactobacilli caused an inflammatory response and microscopic vaginal lesions that promoted HIV diffusion (113). Another hypothesis suggests that an unmeasured property of the placebo delivery vehicle provided non-specific benefit to the patient. The placebo could non-specifically reduce HIV infection and other STIs by non-specifically binding to pathogens, preventing pathogen diffusion through the delivery vehicle to the epithelial surface, and providing lubrication that prevents trauma and irritation to the vaginal epithelium and thus promotes the body's natural infection defenses (114). These failures create a need for both more specific APIs to prevent HIV infection that do not harm native tissues and for a more complete understanding of delivery vehicles and corresponding placebos.

In recent years there has been a shift from non-specific APIs to APIs with specific activity against HIV. This class of microbicides is antiretroviral (ARV) agents which work by preventing viral host cell entry or viral replication. These include CCR5 inhibitors, fusion inhibitors, and reverse transcriptase inhibitors (RTIs). CCR5 inhibitors target the CCR5 co-receptor located on human macrophages and thus prevent viral entry into host cells (115). Several APIs of this type have undergone preclinical evaluation, including maraviroc (116), and PSC-RANTES (117). Fusion inhibitors, such as cyanovirin-N (118),

inhibit viral envelope protein-mediated viral-cell fusion and thus prevent HIV from entry target cells (119). However, by far the most promising ARV class for microbicide development is the RTIs.

RTIs inhibit HIV infection by preventing reverse transcription of viral RNA and thus halt viral replication (120). RTIs cross host cell membranes of HIV infected cells and bind to the HIV reverse transcriptase enzyme. This blocks the conversion of viral RNA into DNA, which in turn prevents integration of this viral DNA into the host DNA, which would prompt replication of viral proteins. RTIs under consideration as vaginal microbicides include dapivirne, UC781 (121), TMC 120 (122), DABOs (123), and pyrimidinediones (124). The most widely studied of all the RTIs for the purpose of creating vaginal microbicides is tenofovir.

Tenofovir was one of the first ARV drugs evaluated for pre- and post-exposure prophylaxis in animal models (125). Successful inhibition of HIV in these models allowed tenofovir to be the first ARV assessed as a vaginal microbicide in clinical trials (126, 127). In 2010 results were released for the CAPRISA 004 randomized trial, the first microbicide trial to display efficacy over the placebo (128). CAPRISA 004, a 1% tenofovir gel, reduced HIV 39% overall in the treatment arm compared to the placebo. Efficacy was highly correlated with adherence. Those individuals with high adherence, greater than 80%, had a 54% reduction in infection. Conversely, those with moderate adherence, 50 to 80%, had a 38% reduction in infection, while those with low adherence, less than 50%, had only a 28% reduction in infection. Still, these results were very promising. However, follow-up studies have not been able to replicate these results. The 2013 VOICE study (129), which looked at oral daily treatment of TDF, oral daily treatment of TDF-FTC, or a 1% tenofovir gel as PrEP, failed to display efficacy in any treatment arm, although the infection rate was lowest for the TFV gel. Low adherence was specifically cited as the reason for the trial failure. The FACTS 001 trial (130), which assessed a 1% tenofovir gel for women aged 18-30, also failed to prove efficacy. Once again adherence was low and gel effectiveness was highest in the most adherent subgroup.

These variable successes and failures of microbicide clinical trials emphasize the need for safe and effective microbicide formulations. Neither the API nor the delivery vehicles should cause harm

during repeated use over long periods of time. Further, the delivery vehicle and placebo should be fully characterized for any potential harms or benefits that could impact efficacy of the microbicide. Finally, a formulation must be acceptable to the patient to maximize patient acceptability and thus to maximize efficacy. Additionally, a microbicide formulation should ideally prevent other STIs, such as *Chlamydia trachomatis*, which increase HIV transmission and acquisition as co-current infections.

1.4 *Chlamydia trachomatis* Infection and HIV

Chlamydia trachomatis is the most prevalent sexually transmitted bacterial infection worldwide (131). In 2012 alone there were an estimated 131 million new cases (131). *C. trachomatis* causes severe infections of the mucosal epithelium in the genital tract. These include urethritis, cervicitis, epididymitis (132), and lymphogranuloma venereum (LGV) (133), an invasive infection that spreads via macrophages to the lymph nodes. Women suffer the most severe consequences of *C. trachomatis* infection, with an estimated 10-15% of untreated infections progressing to the uterus or fallopian tubes to cause pelvic inflammatory disease (PID) (134). Complications of PID include chronic pelvic pain, life-threatening ectopic pregnancy, and tubal factor infertility (135). Additionally, *C. trachomatis* infection increases rates of HIV transmission and acquisition.

C. trachomatis infection can increase the risk of HIV infection when exposed to the virus and also increase HIV transmission to partners (136-139). As part of the normal host response to infection, *C. trachomatis* infection activates recruitment of HIV infected inflammatory cells to the genital tract mucosal surface. This increases HIV shedding in the genital tract and increases viral loads in cervical fluid and semen (136, 137). Patients with both HIV and *C. trachomatis* infections have higher viral loads and are thus more infectious compared to patients only infected with HIV (140). The recruitment of inflammatory cells to the epithelial surface also increases infection susceptibility in HIV-negative patients when challenged by the virus. *C. trachomatis* infection recruits leukocytes to the genital tract and interacts with these leukocytes to increase HIV viral replication in infected cells present in the partner's semen or cervical fluid (141). Thus, preventing and treating genital *C. trachomatis* infection serves as a prevention mechanism against HIV transmission and acquisition.

C. trachomatis is an obligate intracellular parasite and exists in two morphological forms, infectious, metabolically inactive elementary bodies (EBs) and noninfectious, metabolically active reticulate bodies (RBs) (142). Infection is caused by attachment of an EB to a host cell surface and subsequent internalization into the cell (143). Following internalization the EBs transition to RBs and undergo replication via binary fission (142). Upon completion of the development cycle the RBs differentiate back to EBs and are released from the cell either by cell lysis or as a packaged extrusion (144). The infection process continues again in neighboring cells. Thus, a microbicide that inhibited entry of the EBs into host cells would halt this process, prevent *C. trachomatis* infection, and help prevent subsequent HIV infection and transmission.

Microbicide APIs are often assessed for their activity against several STIs in addition to their anti-HIV activity. As discussed in the preceding section, cellulose sulfate (112), Carraguard (145), and PRO 2000 (103) have all been evaluated for their activity against *C. trachomatis*. However, since *C. trachomatis* is an intracellular parasite, infection can be prevented by preventing bacterial entry into host cells. Thus the microbicide delivery vehicle itself could provide activity against *C. trachomatis*. Indeed, several studies have demonstrated *in vitro* anti-chlamydial activity of compounds used in anti-HIV microbicide delivery vehicles (146, 147). In particular, one study of hydroxyethyl cellulose, a major component of the CAPRISA 004 microbicide and placebo, demonstrated inhibition of *C. trachomatis* infection in HeLa 229 cervical epithelial cells (148). A collaborator on this dissertation, Ichie Osaka, further demonstrated the inhibitory ability of this hydroxyethyl cellulose as well as several other types of cellulose ethers, which are structurally similar (149). This work further emphasizes the need to fully characterize the anti-bacterial and anti-viral activities of delivery vehicles that would confer added anti-STI activity to the microbicide formulation and thus increase anti-HIV activity by decreasing co-infections.

1.5 Properties of Ideal Microbicides

The NIH National Institute of Allergy and Infectious Diseases (NIAID) research topic on HIV/AIDS defines the optimal characteristics of a microbicide (150, 151). As mentioned above, the

microbicide formulation must be safe for use over extended periods of time whether it is used repeatedly daily, periodically, or occasionally. The formulation cannot cause harm to the host. Thus the formulation cannot exhibit toxicity to host cells, promote an inflammatory response, disrupt the vaginal epithelium or microbiota, or otherwise irritate the vaginal mucosal environment (152). While all microbicide formulations must be safe for repeated and extensive use, those formulations that confer repeated short term protection directly to the vagina require special consideration. Marginal irritations can accumulate over time and cause adverse effects, as seen with the surfactant microbicides. Micro-abrasions that are not visible during routine pelvic exams can still facilitate viral diffusion and HIV infection (153). These properties must be shared by both the API and the delivery vehicle.

The API must be effective against HIV infection. In order for the API to be effective, the delivery vehicle must release and deliver the API quickly to the proper site of action in the host tissues at the desired dose level. The delivery vehicle must be retained at the site of action for a sufficient period of time to allow for thorough API release. The delivery vehicle has another requirement to create an effective microbicide formulation. The delivery vehicle must solubilize a sufficient concentration of the API and then release the proper dose to the proper site in the body depending on the API's method of action. Additionally, it is desirable for the microbicide, whether API, formulation, or both, to have additional activity against STIs associated with increased HIV infection, such as *C. trachomatis*.

The microbicide must be acceptable to the user and their partner. The formulation should not be unpleasant to use nor decrease pleasure. The microbicide should not produce an unpleasant odor, have an undesirable color, or produce an uncomfortable sensation that would prevent a patient from using it (154). If the microbicide is prepared in a liquid formulation it must coat the vaginal epithelium, it must not have an unpleasant consistency, it must not leak prematurely, it must not be messy, and it must not change consistency or color during coitus (155, 156). If these property requirements are not met, the microbicide will be unacceptable to the patient and adherence will decrease, which in turn will decrease the efficacy of the API. To provide the required safety, efficacy, and acceptability, anti-HIV vaginal microbicides and their delivery vehicles must possess a number of optimal physical, chemical, and biological properties.

Next generation APIs and delivery vehicles should be rationally designed at the pre-clinical stage to ensure the formulation of microbicides that possess all of these properties to prevent future clinical failures. This rational design can be achieved with computational molecular design (CMD).

1.6 Computational Molecular Design

CMD (157) is an optimization methodology that generates products with near-optimal behavior by relating that behavior empirically to physical or chemical properties, and relating those physical and chemical properties to the molecular structure. Novel products are proposed by incorporating these correlations into an optimization problem formulation, and then solving the problem to generate structures that correspond to ideal properties and behavior. In brief, the process involves the creation of a model building set of test compounds, generation of structure-property correlations, development and solution of an optimization problem, and synthesis of novel molecules.

A complete CMD problem is solved using the following steps. First, a set of compounds, known as a model building set, with known molecular structures are selected. The relevant physical or chemical properties, corresponding to some desired behavior, of these compounds are then measured. At the same time structural descriptors, which numerically describe the molecular structure, are calculated for the compounds. These measured data and calculated structural descriptors are then incorporated into quantitative structure-property relationships (QSPRs), which are empirical equations that predict physical properties given molecular structure (158). These QSPRs are integrated into an optimization problem formulation along with a number of structural feasibility constraints to ensure chemically possible molecules are generated. This problem is solved to generate several novel molecular structures that possess the target physical properties that correspond to the desired behavior. CMD is an advantageous methodology because multiple properties and behaviors with conflicting targets can be considered within one problem. This problem can be solved quickly multiple times to produce many candidate molecules and thus accelerate the timeline of drug discovery and pre-clinical evaluation by minimizing the need for high-throughput screening.

CMD has been used in many pharmaceutical fields including drug discovery, protein characterization, and polymer drug delivery system design. This methodology can predict pharmaceutical properties such as solubility and permeability (159-163) to streamline high-throughput screening in drug discovery. Protein-ligand interactions (164-168) can be predicted to aid in design of more targeted drugs. New enzymes can be designed to catalyze reactions that lack naturally occurring biocatalysts (169-172). CMD can predict protein structure, folding, and stability from peptide sequence and protein secondary structure (173-176). Aggregation propensity can be predicted from protein structure (177-179). CMD can design cross-linked polymers for improved dental restorations (180) and controlled release hydrogel formulations (181). CMD accelerates the discovery and development of novel molecules and formulations, and therefore is useful for the design of microbicide delivery systems. This dissertation broadens both the fields of microbicides and CMD by using this computational methodology in a unique manner to design novel delivery vehicles for a specific microbicide API possessing the characteristics of an ideal microbicide.

1.7 Project Summary

This dissertation will use CMD to rationally design next generation delivery vehicles for a gel formulation of tenofovir that possess ideal safety, efficacy, and acceptability characteristics. Chapter 2 will assess the rheology for a model building set of delivery vehicles and relate these measurements to molecular structure in a set of QSPRs. The rheology of gel delivery vehicles influences their spreading behavior. This spreading behavior, in turn influences the efficacy of the formulation by providing a prophylactic barrier for the vaginal epithelium and determining the surface area of drug release. Further, patient acceptability depends upon how the delivery vehicle flows when applied and whether it is retained or leaks out.

Chapter 3 will assess safety for the same model building set of delivery vehicles and relate them to molecular structure in a set of QSPRs. Safety will be defined as *in vitro* cytotoxicity, upregulation of cytokine production that induces an inflammatory response, and inhibition of *C. trachomatis*. Cytotoxicity is measured using an alamarBlue® assay, which indicates cell viability by measuring aerobic

respiration. Solutions containing the delivery vehicles are applied to the surface of plated cells and incubated for a period of time, after which the impacts of the delivery vehicles on cell viability are compared to cells incubated with no delivery vehicle (182). Inflammation is measured as the upregulation of cytokines IL-6 and IL-8 using ELISA kits. Solutions containing the delivery vehicles are applied to the surface of plated cells and incubated for a period of time, after which the cell supernates are collected and the quantities of cytokines produced are measured using sandwich ELISA plates and compared to positive and negative controls (183). Inhibition of *C. trachomatis* infection conferred by the delivery vehicles is measured using a direct culture infection. Solutions containing the delivery vehicles and infectious *C. trachomatis* are applied to the surface of plated cells and incubated for a period of time and then removed. The cells are then fixed with methanol, stained, and enumerated for amount of *C. trachomatis* infection, which is compared to a negative control containing no delivery vehicle in the infectious media (184).

A variety of *in vitro* methods exist to assess cellular cytotoxicity. One mechanism measures cell membrane integrity to determine cell viability. These assays include trypan blue (185), and lactate dehydrogenase (LDH) (186). Cell viability can also be assessed by measuring overall cell metabolic activity to determine if compounds harm cells in ways other than membrane rupture. These assays include MTT (187) and alamarBlue® (182), which measure the overall reducing potential of cells. AlamarBlue® was chosen for this dissertation because this assay quantifies other types of metabolic harm in addition to membrane disruption. Many different safety biomarkers have been considered to assess preclinical inflammation, including many different cytokines and chemokines (188-192). In particular, IL-6 and IL-8 have been identified as playing important roles in the inflammatory pathways that recruit HIV target cells and have been suggested as good predictors of epithelial inflammation for evaluating vaginal microbicides (182, 193, 194). For these reasons they were chosen as the pro-inflammatory cytokines measured in this dissertation. Finally, *in vitro* assays of *C. trachomatis* infection typically rely on staining the chlamydial inclusion followed by direct enumeration via manual, visual inspection under a microscope (195). The above assay method (184) was selected for its adaptability to a high-throughput

screening format, a methodology that is advantageous when testing the many compounds that constitute a model building set.

Chapter 4 will conclude this work by measuring drug compatibility, generating the final set of QSPRs, and performing the final optimization. Delivery vehicles can promote drug efficacy by promoting compatibility with the API. This study defines drug compatibility as drug solubility in the delivery vehicle and drug release from the delivery vehicle. Drug solubility is assessed by performing incubator shaker tests. An excess of drug powder is added to solutions containing the delivery vehicles and then shaken at a constant temperature for a period of time, after which the concentration in the sample is read using an HPLC column (196). Drug release is assessed by measuring drug diffusion out of a dialysis bag. Solutions containing the delivery vehicle and drug are placed inside a dialysis bag which is incubated and shaken for a period of time. The drug diffuses through a semi-permeable dialysis membrane, which allows the drug molecules to pass but not the delivery vehicle molecules, and into a receiving medium. The final concentration of drug in this receiving medium is measured using an HPLC column (197).

To assess aqueous solubility, incubator shaker tests are standard protocol for the NIH, NIEHS, and EPA (198). The above method (196) combines this standard protocol with HPLC quantification to determine the maximum solubility of the drug in the delivery vehicle solution. Drug release is typically assessed with permeation studies (196, 199). This method involves separating a donor and receiving chamber with a tissue sample layer of cells grown to confluence, and measuring the amount of drug that travels from the donor chamber, through the cell layer, into the receiving chamber. However, this method of assessing drug release measures the overall diffusion of the drug from the formulation to the site of action. However, in this dissertation, the initial release of the drug from the delivery vehicle formulation is the property of interest. This the above method (197) was selected to measure the release of drug initially out of formulation through a semi-permeable membrane.

Also in Chapter 4, the QSPRs generated for the rheology, safety, and efficacy properties in the proceeding chapters will be incorporated into an optimization problem formulation that will be solved to generate novel delivery vehicle molecular structures that possess ideal physical properties and behavior.

The successful completion of this design problem serves as a proof of concept that CMD can be applied to this pharmaceutical field. This methodology can then be expanded to characterize and predict other types of microbicide delivery vehicles, the APIs themselves, and other small molecules and simple polymers for other drug delivery systems.

Chapter 2

Quantitative Structure-Property Relationships for Rheological Properties of Cellulose Ether Vaginal Microbicide "Gels"

2.1 Introduction

Patient acceptance, along with drug delivery effectiveness, in vaginally-delivered microbicides which contain polymer solutions (i.e. "gels") determines the success of a microbicide formulation. A recent clinical trial of CAPRISA 004 (128), a 1% tenofovir gel, resulted in an overall 39% reduction in HIV infection compared to the placebo arm. However, individuals with use adherence over 80% had a 54% reduction in infection, demonstrating the crucial impact patient adherence and acceptability have on drug product effectiveness. The subsequent VOICE clinical trial (129), which looked at daily treatment with a 1% tenofovir gel or oral tablets, and the FACTS 001 clinical trial (130), which looked at pericoital treatment with a 1% tenofovir gel, failed to reduce rates of HIV infection in any treatment arm. The studies specifically cited low adherence as the reason for a lack of efficacy.

Patient acceptability studies (154, 155) have analyzed how patient sensory perceptions of vaginal microbicide products could influence patient adherence. In particular, these studies have sought to relate these sensory perceptions to physical properties of the microbicide formulation. Patients (154) believe a specific volume of the microbicide must be placed within the vagina and this volume must be retained in order to form a barrier between the epithelium and infectious agents. If the microbicide changes color or consistency or leaks out prematurely, the patient believes it has reduced effectiveness and is less likely to use it again. This desired retention and consistency of the microbicide depends upon the rheological properties of the formulation (155). To achieve efficacy and acceptability, the microbicide must spread such that it coats the vaginal wall, without leaking. It also must be retained for a sufficient amount of time to deliver the API to the appropriate site while providing lubrication and serving as a potential barrier to infectious agents during intercourse. To achieve the desired degree of spreading, the delivery vehicle must exhibit optimal rheological properties that allow it to coat and be retained in the vagina. A next generation microbicide should include a delivery vehicle possessing these optimal properties.

This study aims to advance the field of microbicide development by illustrating how quantitative correlations relating polymer molecular structure and physical properties can be used to create a predictive model. This predictive methodology is demonstrated with a cellulose-based delivery system, but could also be expanded to other delivery vehicles. This work is initiated by selecting and characterizing a group of representative molecules to serve as the model building set. The structural and physical properties of this model building set are also measured and correlated. In later studies, these correlations are incorporated into an optimization problem to generate similar, but novel, molecular structures with target physical properties. In many pharmaceutical fields, predictive models like the one developed in this study have been successfully used in tandem CMD (157) to predict properties such as: solubility and permeability (159), controlled release from hydrogels (181), and physiochemical properties of cross-linked polymers (180). Similarly, the significance of the predictive model in this study is that it will be used, along with a final CMD model, to design improved microbicide delivery vehicles or select candidate structures that possess the best spreading behavior. When combined with predictive models for other properties (e.g. biocompatibility and drug compatibility), this predictive model will allow for the development of a microbicide formulation with target properties that lead to multiple functions (e.g. target drug loading, release, spreading behavior, inhibition of *C. trachomatis*, and minimization of cytotoxicity) with improved behavior compared to currently available products.

Cellulose ethers in aqueous solutions are a possible delivery vehicle and are currently used in several over-the-counter vaginal products available in the U.S. market, as well as the "universal placebo" used in clinical microbicide trials (200). Cellulose ethers are alkyl modifications of cellulose that vary in type of substituent, amount of substitution, and molecular weight. The molecular structure of these molecules has a great impact on their physical properties, including their rheological properties. Previous rheological characterization of cellulose ethers in the microbicide field (201-205) as well as other drug delivery fields (206-208) has examined the effects of concentration, temperature, pH, and dilution on physical properties such as viscosity and elasticity. These previous works measured rheology of one or a few cellulose ether solutions and fit these data to rheological constitutive models; some of the previous

work incorporated these rheology data into coating or squeezing flow models. In particular, Mahalingam *et. al.* (203) used mixture design of experiments theory to relate concentration of mixtures of hydroxyethyl cellulose and Carbopol 974P to physical properties and spreading performance. That study identified a gel mixture with optimal rheological properties and spreading behavior. These collective studies concluded that the physical properties of different cellulose ether solutions responded differently to variations in dilution, temperature, and concentration. However, the causes of these differences due to effects of molecular structure on rheological behavior of cellulose-based polymer solutions have not been addressed, nor have any property-structure correlations been proposed. Additionally, this current study improves upon these previous studies by measuring a wide range of cellulose ethers with unique structures, many of which have not been evaluated for use as vaginal microbicide delivery vehicles.

This study addresses this gap by focusing on molecular structure and concentration of a wide range of cellulose ether solutions. To rationally design an effective delivery vehicle using these polymers requires an understanding of how variations in molecular structure impact rheological properties, specifically those properties which determine spreading behavior of the delivery vehicle. The goal of this study is to elucidate the impact of molecular weight, concentration, substituent group, and amount of substitution on rheological properties for a wide range of cellulose ethers to aid in future delivery system design. The outcome will consist of a set of empirical correlations that will predict the rheological properties of cellulose ether solutions based on these structural factors and formulation choices. The large model building set in this study allows for the development of quantitative correlations, while previous rheology studies with more limited data sets could only elucidate general trends. This study's template of data acquisition and analysis will be used in later studies to elucidate how molecular structure impacts drug compatibility, and biocompatibility, and will be used to accomplish the final goal of designing the molecular structure of a microbicide delivery vehicle.

2.2 Materials and Methods

2.2.1 Cellulose Ethers and Rheology

Cellulose ethers are widely used in solution as rheology modifiers and to thicken formulations (209). They are utilized in a wide variety of industries including construction, oil field chemicals, personal care products, food additives, and pharmaceuticals. In the pharmaceutical field cellulose ethers are incorporated into drug tablets to create controlled release matrices (210), into saliva substitutes to relieve dry mouth (211), in mucoadhesive buccal disks for oral pro-drug delivery (212), or in ophthalmic viscosurgical devices to minimize damage in eye surgery (206). Additionally, the use of hydroxyethyl cellulose (HEC) in KY Jelly, a commercial vaginal lubricant, has led to the development of a "universal placebo" in vaginal microbicide clinical trials (200) based on Natrosol, a proprietary HEC from Hercules/Aqualon.

In order to rationally design an appropriate cellulose ether for use in a microbicide delivery vehicle, its specific rheological properties must be identified. This current study emphasizes non-Newtonian viscosity (described by consistency and shear-thinning index), shear storage modulus, and shear loss modulus. Previous studies of thin film spreading indicate that consistency and shear-thinning index have an impact on the time the solution takes to spread due to gravity (213, 214) and squeezing forces (205, 215), the length it covers, and if fingering patterns develop in the flow that would create undesired bare spots in the coverage area (216). The storage and loss moduli (also known as elastic and viscous moduli) represent the elastic and viscous effects of the moving fluid and the ratio of these values influences how the solution is retained or if it continues to flow and leak (217). These two dynamic moduli are measured under oscillatory flow conditions, which are relevant to topical drug delivery vehicles exposed to oscillatory shear stresses during application and use.

A wide range of cellulose ethers were selected to form a model building set and their rheological properties were measured over a range of shear rates and oscillatory frequencies. The "universal placebo" currently in clinical microbicide trials (200) contains HEC as the rheology modifier. This study focuses on the rheology of aqueous solutions of HECs at various molecular weights to create a model building set with a range of rheological properties. This range is further increased by the incorporation of the additional cellulose ether, sodium carboxymethyl cellulose (CMC).

2.2.1.1 Cellulose Ethers

Natural cellulose is highly crystalline, and the lower chemical potential of crystals due to hydrogen-bonding causes the molecules to be insoluble in water (218). To create aqueous cellulose solutions this crystalline order must be disrupted by the addition of side chain substitutions that prevent tight packing and expose the hydrophilic glucose repeat units to the solvent. In addition, the side chains themselves can be hydrophilic. Cellulose ethers are produced by modifying the hydroxyl groups on the glucose units in the cellulose chains. Specifically, an alkyl substituent group replaces the hydrogen atom on these hydroxyl groups. These substituent groups can include hydroxyethyl, carboxymethyl, methyl, or hydroxypropyl substitutions. The molecular structure of the cellulose ethers depends on the molecular weight, the type of substituent groups, the degree of substitution (DS), and molar substitution (MS). Degree of substitution indicates on average how many of the three hydroxyl groups on each glucose repeat unit have substitutions (see Figure 2.1). For hydroxyethyl cellulose, since the additional hydroxyl group in the substitution group can receive a substitution, the MS refers to on average how many hydroxyethyl groups are present at each substitution site. If the MS is large, this can lead to long side-group chains branching off of the main cellulose strand (219).

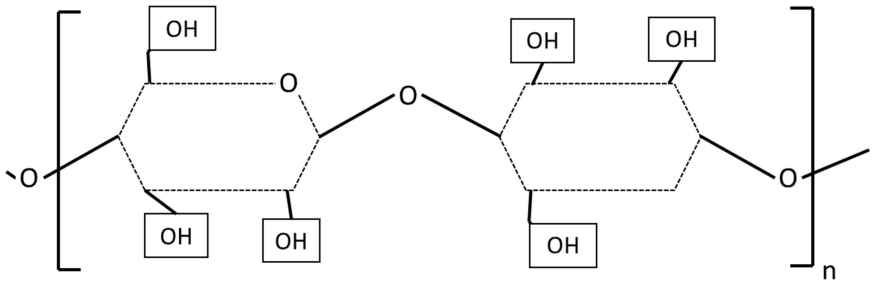

Figure 2.1: Two glucose repeat units in a cellulose chain. The ether modifications are made by replacing the hydrogen on a hydroxyl group with a substitution group.

The universal placebo (200) consists of a solution containing 2.7% HEC in water with trace amounts of sorbic acid, sodium chloride, and sodium hydroxide to increase biocompatibility with the vaginal epithelial cells and native lactobacteria. Viscosity studies conducted in our lab using the universal placebo formulation indicated that the presence of salts and preservatives had a negligible impact on the

solution viscosity (data not shown). HECs have very little viscosity variation over a pH range of 2 to 12, while CMCs have very little viscosity variation over a pH range of 4 to 10 (220). Thus, in this study, the cellulose ethers were mixed in water in the absence of buffer, salt, or any preservatives to create polymer solutions.

Several cellulose ethers were tested to vary molecular weight, substituent group, and MS/DS (see Table II.I). The average molecular weight of the molecules was obtained from commercial product information. The manufacturer-provided molecular weight values are approximate and based on average viscosity behavior, reflecting synthesized polymer batches which may have high polydispersity. These polydispersity indices may be highly variable since they are unpublished. Additionally, all cellulose ethers were tested at several concentrations to create the final model building set. The concentration range was based around the concentration of the universal placebo and increased for low viscosity solutions, corresponding to the lower molecular weight formulations. This was done to create a model building set with rheological properties that were broad, but excluded viscoelastic moduli that were too low, which would cause them to immediately leak out of the vagina, or high, which would cause them to fail to spread upon insertion. Overall, 29 polymer solutions of cellulose ethers formed the model building set, as show in Table II.I.

Table II.I: 29 Cellulose Ether Polymer Solutions[a]

Name	Molecular Weight[b]	MS/DS[b]	Concentration
Hydroxyethyl Cellulose (HEC, Natrosol 250 HX Pharm, Hercules/Aqualon)[c]	M_v=1,000,000	2.5/1.5	2.4%, 2.7%, 3.0%
Hydroxyethyl Cellulose (HEC, Sigma-Aldrich)	M_v=90,000 M_w=250,000 M_v=720,000 M_v=1,300,000	2.5/1.5 2.0/1.0 2.5/1.5 2.5/1.5	12%, 14%, 16% 2.7%, 6%, 7%, 8% 2.4%, 2.7%, 3.0% 2.4%, 2.7%, 3.0%
Carboxymethyl Cellulose (CMC, Blanose 7HF PH, Hercules/Aqualon)	M_w=700,000	NA/0.7	2.0%, 2.4%, 2.7%, 3.0%, 3.3%
Carboxymethyl Cellulose (CMC, Sigma-Aldrich)	M_w=250,000	NA/0.9 NA/1.2	2.7%, 6%, 7%, 8% 2.7%, 6%, 7%, 8%

[a]Solutions were generated by varying ether type, molecular weight, MS/DS, and/or concentration.
[b]Molecular weight and MS/DS data were obtained from Sigma-Aldrich and Hercules/Aqualon.

[c]The hydroxyethyl cellulose used in the "Universal Placebo."

2.2.1.2 Rheology

The shear-thinning viscosity and shear moduli were measured on a rheometer (TA Instruments AR2000) at 37°C. The viscosity was measured using a 40 mm 2° cone over a range of shear rates from 0.01 to 100 1/s. The mean of three replicates were then fit to the following power-law model (221) to find power-law parameters:

$$\mu = m\dot{\gamma}^{n-1} \qquad \text{Equation 2.1}$$

where μ is the viscosity, m is the consistency, $\dot{\gamma}$ is the shear rate, and n is the shear-thinning index. Several models exist to describe shear-thinning viscosity data. The power-law model captures both the consistency and shear-thinning behavior over a range of shear rates, and is used often to describe rheology of pharmaceutical formulations, e.g. (222). The power-law model was also selected for it applicability for non-cross-linked polymers and for its integration with previous and concurrent fluid mechanics studies in our research group (214, 216). Future expansion of this study may include the Ellis rheological model, which may better describe the spreading behavior of the cellulose ethers in the model building set, especially at the low shear-rate Newtonian plateau (213).

The shear moduli were measured by performing oscillatory frequency sweeps using a 40 mm plate at a constant stress in the linear viscoelastic regime over a range of frequencies from 0.01 Hz to 1 Hz. This provided frequency-dependent data for the storage modulus, *G'*, and the loss modulus, *G''*. The *G'* and *G''* data were represented as the mean of three uniquely loaded samples for each solution. In contrast to the power-law behavior for the viscosity data, it was not possible to find a robust constitutive equation to capture the frequency-dependent behavior for *G'* and *G''*, due to the wide range of samples. For this reason the data analysis focuses on representative *G'* and *G''* values at a specific frequency, while example plots show the full range of data.

2.2.2 Construction of QSPRs

These rheology data were then used to create a set of Quantitative Structure-Property Relationships (158), or QSPRs. These QSPRs relate the physical properties (consistency, shear-thinning

index, storage modulus, and loss modulus) to the molecular topology and concentration of the cellulose ethers solutions. The four structure properties used for the correlations were: the average molecular weight of the polymer chains, the polymer concentration in solution, and two zeroth-order connectivity indices.

Connectivity indices assign numerical values to the graph of a molecule to quantify its topological structure (223). They contain a wealth of information such as the numbers of atoms bonded to each non-hydrogen atom, details about the electronic structure of each atom, and larger-scale structural features in a few numbers. Connectivity indices have been shown to be highly effective for the prediction of physical properties of straight-chain polymers (223). The zeroth-order connectivity indices are group contribution descriptors which adequately describe the average repeat unit structure. They are calculated as follows:

$$^{0}\chi = \sum_i \frac{1}{\sqrt{\delta_i}} \qquad \text{Equation 2.2}$$

$$^{0}\chi^{V} = \sum_i \frac{1}{\sqrt{\delta_i{}^{V}}} \qquad \text{Equation 2.3}$$

Each non-hydrogen atom is defined as a vertex. The δ_i represents the number of bonds to non-hydrogen atoms at vertex i. The $\delta_i{}^{V}$ represents the sum of the lone pair electrons at the ith vertex plus its number of bonds to non-hydrogen atoms. Figure 2.2 shows an example calculation for a simple polymer repeat unit. This allows for the calculation of a pair of connectivity indices for each of the unique cellulose ether polymers in Table II.I. These results are shown in Table II.II.

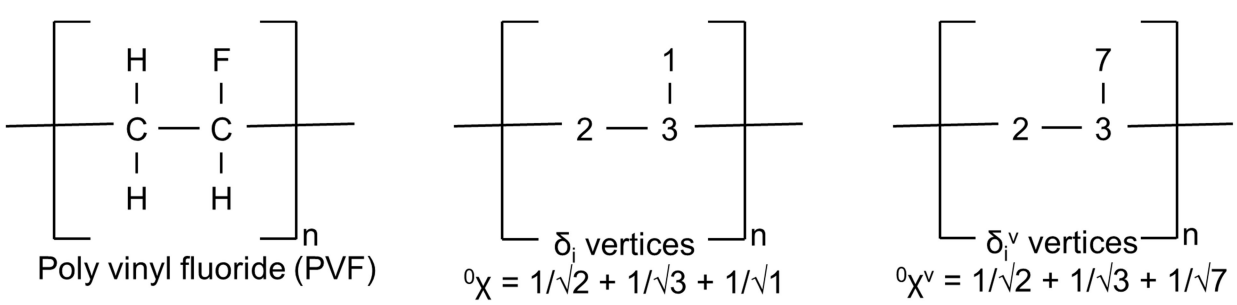

Figure 2.2: Diagram showing example calculation of zero-order connectivity indices for a simple polymer repeat unit of poly vinyl fluoride. The vertices include all non-hydrogen atoms. δ_i represents the

number of bonds to non-hydrogen atoms at each vertex *i*, while δ_i^V represents the number of bonds to non-hydrogen atoms plus lone pair electrons at the *i*th vertex. Adapted from (223).

Table II.II: Calculated Connectivity Indices for Unique Cellulose Ether Solutions[a,b]

Cellulose Ether	MS	DS	$^0\chi$	$^0\chi^V$
HEC	2.5	1.5	13.35	10.33
HEC	2.0	1.0	12.29	9.41
CMC	NA	.7	10.14	7.14
CMC	NA	.9	10.74	7.53
CMC	NA	1.2	11.64	8.11

[a] Calculations of connectivity indices were based on MS/DS values for an average glucose repeat unit.
[b] The two connectivity indices ($^0\chi$ and $^0\chi^V$) are defined in Equations 2.2 and 2.3.

To create QSPRs, the four physical measurements (consistency, shear-thinning index, storage modulus, and loss modulus) were each correlated with the four structural properties (two connectivity indices, concentration, and molecular weight). The QSPR correlations were generated using R statistical software (224). These correlations were evaluated using goodness of fit (r^2), which indicates the accuracy of the predictive model. Additionally, cross validation was performed to indicate the predictive quality of the correlations, represented as q^2, and to reduce over-fitting of descriptors in QSPR selection. The method selected was leave-one-out cross-validation, which estimates the goodness of fit on independent data sets by leaving out one data point, re-correlating the rest of the data, evaluating the new correlation using the outlier point, repeating this for each data point, and summing the resulting r^2 values to generate a q^2 value. Linear and nonlinear dependence on the four structural properties, as well as interaction terms between the structural properties, were considered when generating QSPRs. The QSPRs with the best goodness of fit and cross-validation performance were identified from these possible correlations with the three structural descriptors.

2.3 Results

In this section, the rheology results and trends are presented. The effects of several factors are isolated: concentration, molecular weight, substituent type, and MS/DS. After each of these is presented and shown how they are related, the following Discussion section will demonstrate the construction of nonlinear and interaction terms in the QSPRs.

Representative rheology data for all cellulose ether solutions in the model building set are displayed in Table II.III. These data describe the viscosity data using power-law fit parameters and the viscoelastic data by representative values taken at the maximum, minimum, and midpoint of the frequency measurement range. Rheology data points for some representative polymer solutions from Table II.I are shown in Figures 2.3 through 2.9. These figures display viscosity and storage modulus data; loss modulus plots are not shown for brevity. These figures do not represent all available data, but allow for discussion of molecular structure effects on physical properties in the following sections and identification of some trends for insight on improving the correlations.

Table II.III: Representative Viscosity Data[a,c] and Viscoelastic Data[b,d] for all 29 Cellulose Ether Solutions.

Cellulose Ether Solution	m (P*s^{n-1})	n	r^2	G' at 0.01 Hz (Pa)	G'' at 0.01 Hz (Pa)
2.4% HEC MW=1,000,000	212.79	0.5975	0.9804	1.72±0.15	4.98±0.27
2.7% HEC MW=1,000,000	376.81	0.5494	0.9782	4.18±1.25	9.66±2.14
3.0% HEC MW=1,000,000	506.58	0.5127	0.9772	5.12±0.34	11.17±0.52
12% HEC MW=90,000	30.18	0.9468	0.9999	0.0025±0.00083	0.19±0.0059
14% HEC MW=90,000	73.27	0.9335	0.9993	0.018±0.0019	0.48±0.012
16% HEC MW=90,000	170.58	0.8771	0.9983	0.13±0.0079	1.57±0.049
2.7% HEC MW=250,000	2.27	0.9406	0.9997	0.042±0.014	0.58±0.015
6% HEC MW=250,000	45.14	0.8946	0.9988	0.021±0.0014	0.34±0.014
7% HEC MW=250,000	91.17	0.8683	0.9979	0.044±0.0078	0.70±0.019
8% HEC MW=250,000	189.24	0.8260	0.9966	0.14±0.034	1.51±0.18
2.4% HEC MW=720,000	93.41	0.6658	09883	0.29±0.00067	1.22±0.014
2.7% HEC MW=720,000	128.27	0.6425	0.9873	0.52±0.068	1.87±0.11
3.0% HEC MW=720,000	191.72	0.6156	0.9857	0.85±0.0078	2.83±0.027
2.4% HEC MW=1,300,000	389.81	0.5441	0.9768	3.04±0.080	7.64±0.11
2.7% HEC MW=1,300,000	473.45	0.5202	0.9757	4.45±0.48	10.04±0.74
3.0% HEC MW=1,300,000	655.57	0.4937	0.9751	5.49±0.0051	12.03±0.036
2.0% CMC MW=700,000	118.96	0.5360	0.9820	0.76±0.045	1.33±0.031
2.4% CMC MW=700,000	395.43	0.3704	0.9597	5.01±0.051	4.74±0.026
2.7% CMC MW=700,000	533.25	0.3078	0.9571	8.72±0.32	6.41±0.14
3.0% CMC MW=700,000	914.79	0.2466	0.9679	22.46±1.52	13.07±0.70
3.3% CMC MW=700,000	1378.32	0.2212	0.9798	40.19±1.46	20.96±0.64
2.7% CMC 0.9 MW=250,000	8.10	0.9053	0.9996	0.0017±0.0012	0.051±0.0024
6.0% CMC 0.9 MW=250,000	404.91	0.5686	0.9887	2.30±0.068	3.87±0.040
7.0% CMC 0.9 MW=250,000	934.87	0.4509	0.9829	5.53±0.0078	8.00±0.040
8.0% CMC 0.9 MW=250,000	2103.82	0.3316	0.9732	26.90±0.50	22.35±0.62
2.7% CMC 1.2 MW=250,000	3.80	0.9577	0.9996	0.0018±0.00060	0.023±0.0024
6.0% CMC 1.2 MW=250,000	59.13	0.9029	0.9983	0.011±0.0014	0.42±0.0082
7.0% CMC 1.2 MW=250,000	107.79	0.8787	0.9974	0.042±0.00066	0.84±0.0086
8.0% CMC 1.2 MW=250,000	178.77	0.8522	0.9966	0.083±0.0061	1.42±0.017

Cellulose Ether Solution	*G'* at 0.1 Hz (Pa)	*G''* at 0.1 Hz (Pa)	*G'* at 1 Hz (Pa)	*G''* at 1 Hz (Pa)
2.4% HEC MW=1,000,000	14.63±0.74	24.32±0.98	76.45±7.20	74.80±6.80
2.7% HEC MW=1,000,000	29.01±6.88	41.63±7.46	126.29±23.44	111.03±16.54
3.0% HEC MW=1,000,000	32.80±1.59	45.69±167	142.80±5.35	121.77±4.90
12% HEC MW=90,000	0.10±0.0083	1.77±0.061	1.85±0.086	15.70±0.49
14% HEC MW=90,000	0.37±0.014	4.09±0.13	6.25±0.21	33.61±1.28
16% HEC MW=90,000	2.05±0.11	12.43±0.446	26.79±1.13	87.47±2.69
2.7% HEC MW=250,000	0.64±0.014	5.02±0.050	12.99±018	34.67±0.28
6% HEC MW=250,000	0.36±0.024	3.05±0.12	6.16±0.30	23.27±0.84
7% HEC MW=250,000	0.92±0.037	6.05±0.14	13.77±0.54	42.75±1.57
8% HEC MW=250,000	2.48±0.38	12.14±1.28	30.22±2.17	77.30±3.05
2.4% HEC MW=720,000	3.24±0.037	7.25±0.082	22.19±0.21	28.83±0.26
2.7% HEC MW=720,000	5.12±0.32	10.40±0.43	31.92±1.24	38.76±0.98
3.0% HEC MW=720,000	7.93±0.050	15.01±0.12	47.23±1.08	54.32±1.25
2.4% HEC MW=1,300,000	22.52±0.36	34.57±0.44	111.93±4.79	100.59±4.24
2.7% HEC MW=1,300,000	30.26±2.35	42.63±2.36	134.70±7.62	114.13±5.56
3.0% HEC MW=1,300,000	35.97±1.07	50.64±0.80	168.37±6.10	139.93±5.40
2.0% CMC MW=700,000	3.74±0.083	6.15±0.088	19.12±0.29	23.29±0.31
2.4% CMC MW=700,000	15.17±0.23	15.84±0.13	53.36±2.17	48.89±1.98
2.7% CMC MW=700,000	21.63±0.58	18.29±0.18	63.14±2.16	51.61±1.33
3.0% CMC MW=700,000	48.87±2.89	32.32±1.25	119.97±6.13	80.73±3.09
3.3% CMC MW=700,000	84.47±2.98	49.57±1.02	194.13±4.88	118.00±2.59
2.7% CMC 0.9 MW=250,000	0.041±0.0073	0.48±0.015	0.73±0.037	4.03±0.11
6.0% CMC 0.9 MW=250,000	10.38±0.050	19.07±0.11	55.82±1.21	86.63±2.15
7.0% CMC 0.9 MW=250,000	23.09±0.32	35.79±0.45	105.61±6.49	140.27±8.92
8.0% CMC 0.9 MW=250,000	73.15±3.22	74.27±3.25	245.93±11.59	249.80±12.04
2.7% CMC 1.2 MW=250,000	0.016±0.012	0.22±0.011	0.16±0.047±	2.07±0.013
6.0% CMC 1.2 MW=250,000	0.35±0.0078	3.91±0.075	7.91±0.20	31.31±0.78
7.0% CMC 1.2 MW=250,000	0.92±0.0065	7.58±0.098	17.34±0.46	57.60±1.90
8.0% CMC 1.2 MW=250,000	1.80±0.035	12.54±0.18	29.33±0.90	84.91±2.70

[a] Viscosity measurements are tabulated as the power-law parameters: *m* (consistency) and *n* (shear-thinning index).
[b] Viscoelasticity measurements are tabulated as *G'* (shear storage modulus) and *G''* (shear loss modulus) at a representative frequency.
[c] The power-law parameters were fit to the mean of triplicate data, and the $r^2$of the fit is shown.
[d] For *G'* and *G''*, the mean ± standard deviation (n=3) is given.

2.3.1 Concentration Effects

Figures 2.3 through 2.5 and Table II.III illustrate rheological property variation with solution concentration. As seen in studies with similar cellulose solutions (206-208), the viscosity, storage modulus, and loss modulus increase with increasing polymer concentration for all solutions measured while *n* decreases. The data shown in these figures indicate that this increase in physical properties is not

linear with concentration. For example, for the HEC in Figure 2.3, the increase in consistency, apparent viscosity, and elastic moduli from a concentration of 2.4% to 2.7% is greater than the increase from 2.7% to 3.0%. The nonlinear influence of concentration on viscosity is also observed in Figure 2.4a for a CMC. Figures 2.3 and 2.4 show just two examples of nonlinear variation of physical properties with concentration, but all cellulose ether solutions in Table II.III had similar trends, which indicates that standard linear regression cannot adequately relate viscosity or elasticity to concentration.

The rheological properties in Figure 2.5 for a low molecular weight HEC indicate that molecular weight moderates the concentration effects. Table II.III reveals that each increase in concentration in Figure 2.5 more than doubles the resulting rheological properties with an especially large increase in the storage modulus, but this requires a 2% increase in solution concentration. To increase the apparent viscosity at the lowest shear rate by approximately two times, the low molecular weight HEC requires a concentration increase of 2% while the high molecular weight HEC requires an increase of less than 0.6%.

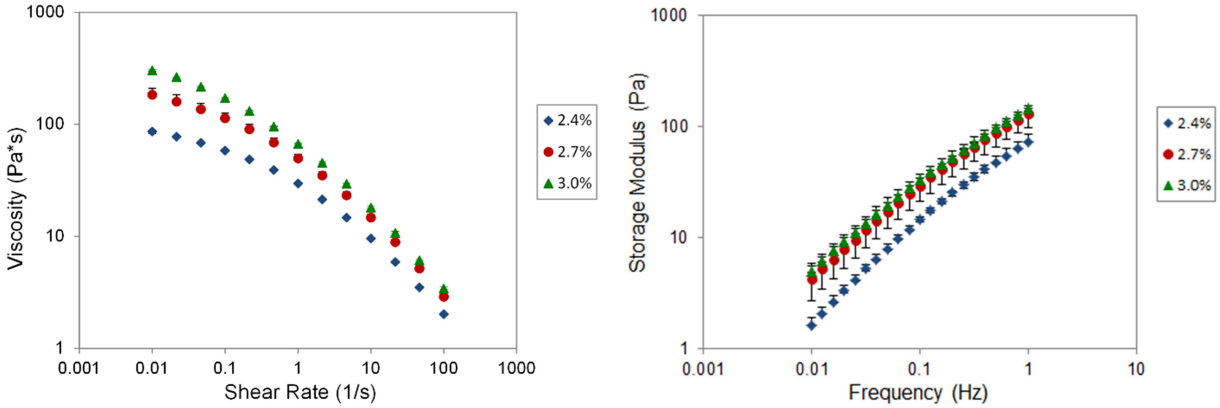

Figure 2.3a and 2.3b: Effects of Concentration of HEC (high MW). Example viscosity (2.3a) and viscoelasticity (2.3b) data for hydroxyethyl cellulose (HEC) with a molecular weight of 1,000,000. Data points indicate median ± max/min for replicates.

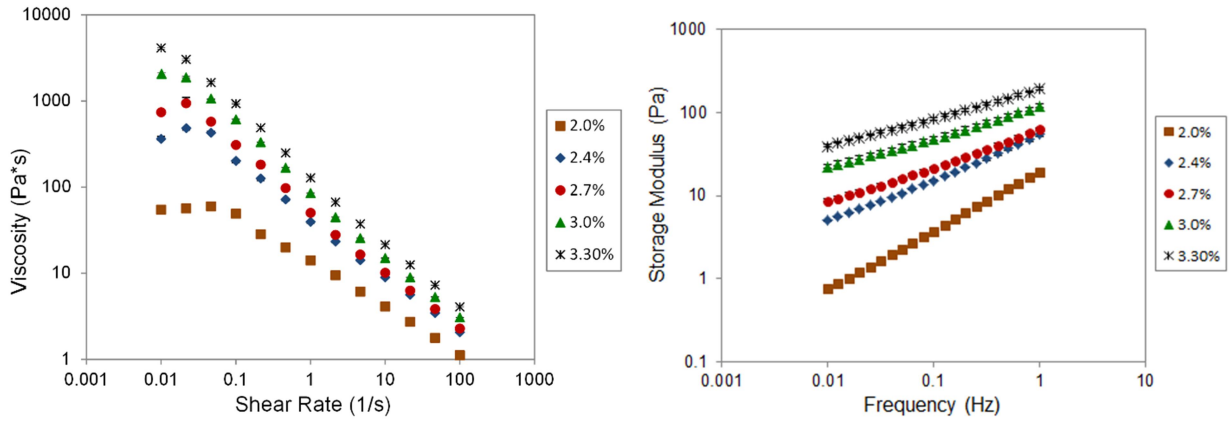

Figure 2.4a and 2.4b: Effects of Concentration of CMC (higher MW). Example viscosity (2.4a) and viscoelasticity (2.4b) data for carboxymethyl cellulose (CMC) with a molecular weight of 700,000. Data points indicate median ± max/min for replicates.

Additionally, substituent groups appear to moderate concentration effects. A concentration increase of 0.4% raises the viscosity at the lowest shear rate of the high molecular weight CMC by nearly an order of magnitude (Figure 2.4b). The same increase for either molecular weight of HEC would require a concentration increase of several percent. These differences in physical property variation with concentration between difference cellulose ethers with different molecular weights and substituent groups are explored in the following sections.

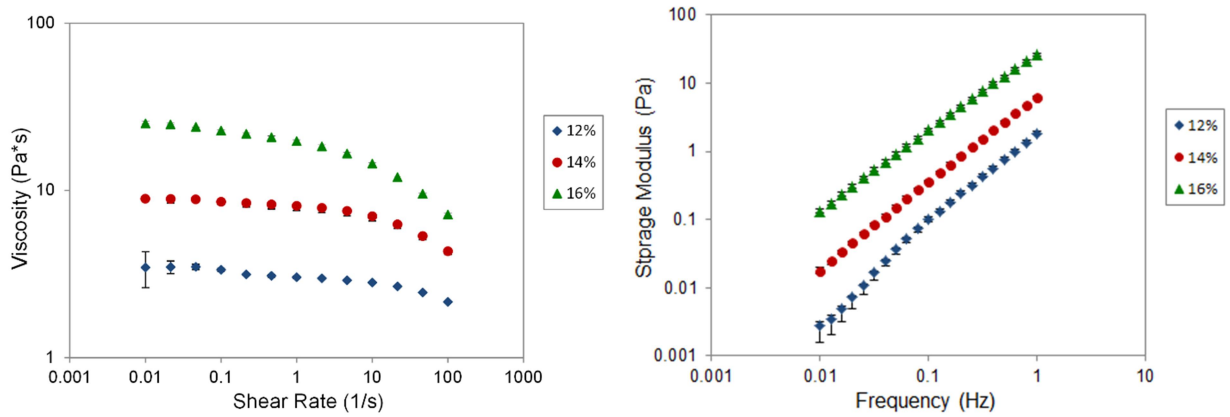

Figure 2.5a and 2.5b: Effects of Concentration of HEC (low MW). Example viscosity (2.5a) and viscoelasticity (2.5b) data for hydroxyethyl cellulose with a molecular weight of 90,000. Data points indicate median ± max/min for replicates.

2.3.2 Molecular Weight Effects

Figures 2.6 and 2.7 illustrate rheological property variation with molecular weight at constant solution concentration. In the previous section, Figures 2.3 through 2.5 indicated that the dependence of rheological properties on concentration was also highly dependent upon molecular weight, as expected. Furthermore, physical properties do not vary linearly with molecular weight for HECs or CMCs. For example, Figure 2.6a shows that the viscosity decrease is magnified as the MW of HEC is decreased. This decrease results in the viscosity at the lowest shear rate decreasing by nearly two orders of magnitude. The decrease for the CMC in Figure 2.7 is even more pronounced.

The HEC in Figure 2.6 indicates a high degree of nonlinearity in the variation of physical properties with molecular weight. The HEC data, shown in Figures 2.3, 2.5, and 2.6 collectively, indicate that the rheological properties have an increasing dependence on concentration as molecular weight decreases. In addition, there is a decreasing dependence on molecular weight as the concentration increases. Additional comparison of Figures 2.6 and 2.7 indicates that substituent groups also moderate molecular weight effects. The variation in properties between a lower and higher molecular weight is much greater for the CMC than the HEC. These variations between substituent groups are further explored in the next section.

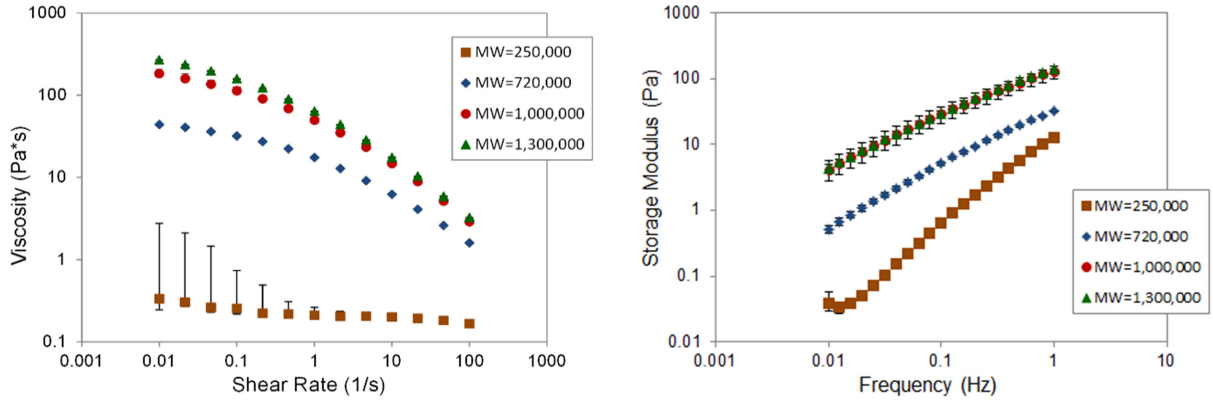

Figure 2.6a and 2.6b: Effects of Molecular Weight of HEC. Example viscosity (2.6a) and viscoelasticity (2.6b) data for hydroxyethyl cellulose at a concentration of 2.7% with a DS of 1.5 (the molecular weight of 720,000 hydroxyethyl cellulose has a DS of 1.0). Data points indicate median ± max/min for replicates.

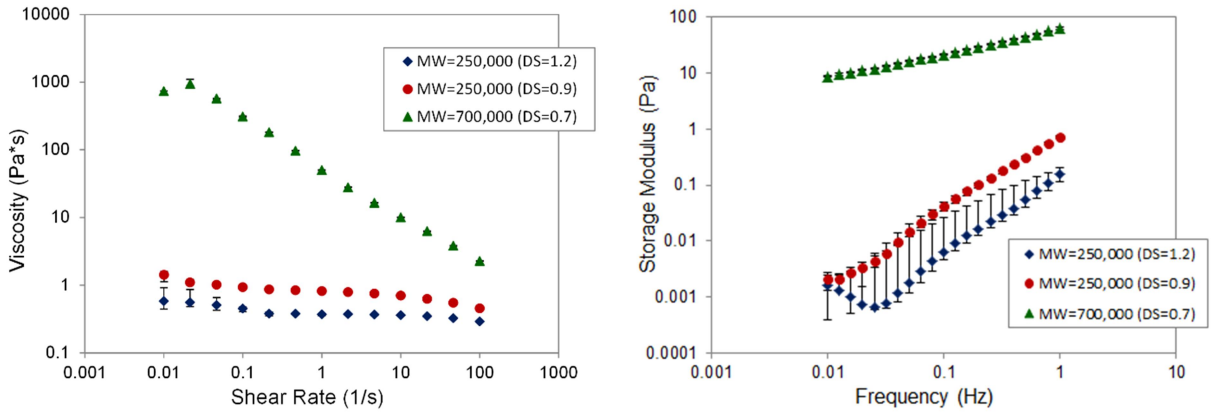

Figure 2.7a and 2.7b: Effects of Molecular Weight of CMC. Example viscosity (2.7a) and viscoelasticity (2.7b) data for carboxymethyl cellulose at a concentration of 2.7%. Data points indicate median ± max/min for replicates.

2.3.3 Substituent Effects

Figure 2.8 depicts rheological property variation due to changes in the substituent groups of cellulose ethers at approximately constant molecular weight. Confirming trends displayed in Figures 2.3 through 2.7, there are clear differences in physical properties with variation in substituent groups. Figure 2.8 shows that for the same molecular weight and concentration, the viscosity of a CMC is over an order of magnitude higher than the HEC at the lowest shear rates, and the storage modulus is approximately two orders of magnitude higher than that of HEC. A similar increase in viscosity and storage modulus can be observed when comparing Figure 2.6 (HEC 720,000) and Figure 2.7 (CMC 700,000).

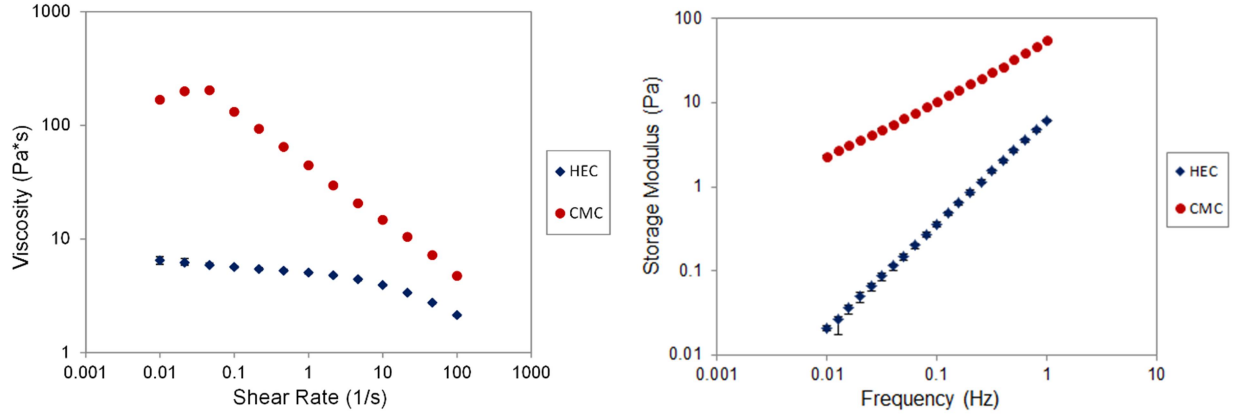

Figure 2.8a and 2.8b: Effects of Substituent Group. Example viscosity (2.8a) and viscoelasticity (2.8b) data for carboxymethyl cellulose (DS = 0.9) and hydroxyethyl cellulose (DS = 1.0), both with a molecular weight of 250,000 at a concentration of 6.0%. Data points indicate median ± max/min for replicates.

2.3.4 MS/DS Effects

The MS/DS for a cellulose ether indicates the number of side chain substitutions on average per glucose repeat unit. The carboxymethyl groups on CMCs do not have additional hydroxyl groups to facilitate longer side chains, so only a DS number is needed to describe this behavior. The hydroxyethyl groups on HECs do have an additional hydroxyl group which can further react, forming longer side chain substitutions. In a group contribution model, the MS is the important number to describe an HEC since is enumerates all the side groups present, not just the substitutions sites as described by the DS.

Figure 2.9 illustrates that the degree of substitution in addition to the type of substitution for CMCs also has a dramatic impact on physical properties. The increase in degree substitution from 0.9 to 1.2 caused the low shear-rate viscosity of the CMC to decreases by over an order of magnitude and the low-frequency storage modulus to decrease by over two orders of magnitude. These data, along with Figure 2.8, indicate that both the degree and type of substitution influence physical properties.

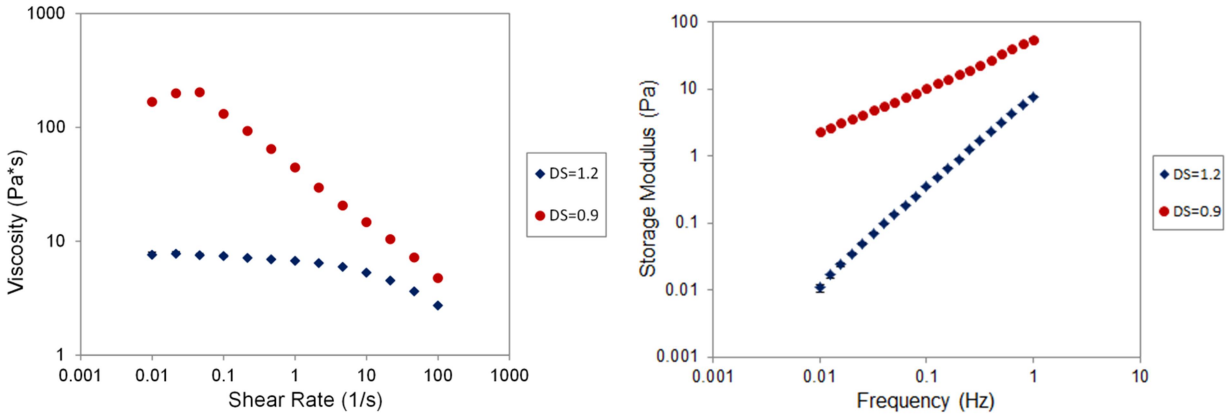

Figure 2.9a and 2.9b: Effects of DS/MS. Example of viscosity (2.9a) and viscoelasticity (2.9b) data for carboxymethyl cellulose DS = 0.9 and DS = 1.2 with a molecular weight of 250,000 at a concentration of 6.0%. (The DS = 0.9 data are the same data shown in Figure 2.8 for the CMCs. It is interesting to note that the DS = 1.2 CMC data here are similar to the HEC data in Fig 2.8.) Data points indicate median ± max/min for replicates.

2.4 Discussion

In this section, I describe the construction of the quantitative structure-property relationships (QSPRs), which are formed from an analysis of the rheological results and trends presented above. First, I discuss the rheological trends and the process for determining nonlinear and interaction terms in the QSPRs. Subsequently, I discuss the interpretation and limitations of the QSPRs.

2.4.1 Nonlinear and Interaction Terms in QSPRs

The preceding rheological results indicate that the physical properties of the cellulose ether solutions do not linearly depend on variations in structural properties. Figures 2.3 through 2.9 show that rheological properties vary nonlinearly with concentration or molecular weight, and that there are interactions between the dependence on concentration, molecular weight, and the degree/type of substitution. Thus, we expected that a QSPR formed from only linear correlations with structural properties would not perform well. Table II.IV shows the linear QSPR correlations with the best goodness of fit. The goodness of fit for the correlation of the shear-thinning index is fairly low (r^2 under 80%), and the correlations for the other three physical properties are unacceptably poor for the purposes of property prediction and molecular optimization.

Table II.IV: Linearly Regressed QSPRs for the Physical Properties[a] Correlated with the Structural Parameters[b].

Correlation	r^2 [c]
$\boldsymbol{m} = 2838 + 9.31\text{x}10^{-4}\,\mathbf{MW} + 7545\,\mathbf{C} - 317.6\,{}^{0}\chi + 51.6\,{}^{0}\chi^{V}$	0.3940
$\boldsymbol{n} = -1.255 - 6.23\text{x}10^{-7}\,\mathbf{MW} - 2.493\,\mathbf{C} + 0.3441\,{}^{0}\chi - 0.1977\,{}^{0}\chi^{V}$	0.7875
$\boldsymbol{G'} = 130.6 + 5.17\text{x}10^{-5}\,\mathbf{MW} + 303.2\,\mathbf{C} - 18.38\,{}^{0}\chi + 7.055\,{}^{0}\chi^{V}$	0.4569
$\boldsymbol{G''} = 36.08 + 5.474\text{x}10^{-5}\,\mathbf{MW} + 327.5\,\mathbf{C} - 0.4751\,{}^{0}\chi - 6.361\,{}^{0}\chi^{V}$	0.4863

[a] Rheology data from Table III.
[b] Structural parameters are molecular weight, concentration, and the two connectivity indices in Table II.
[c] r^2 is goodness of fit. These results reflect that a linear relationship with structural properties is not sufficient for predicting physical properties, and thus the nonlinear dependence and interaction of the structural properties need to be incorporated into the QSPRs.

The poor performance of the linear QSPRs in Table II.IV indicate that a linear correlation with structural properties is insufficient for predicting physical properties of these cellulose ether solutions. The linear QSPRs are deficient because they do not capture the nonlinear effects of concentration and molecular weight summarized in the preceding sections, and because they do not capture the interdependence between the structural properties (concentration and molecular weight). In addition, the zeroth-order connectivity indices do not completely capture the impact of the degree of substitution – they reflect substituent type, but not the location of nearest neighbors. In other words, treating the structural parameters as isolated variables does not adequately reflect how small changes in degree of substitution

can have large impacts on the molecular weight and concentration dependence of physical solution properties.

The previous rheological results provide insight into the construction of QSPRs that incorporate nonlinear and interaction terms. The next step was to use power relationships to explore single nonlinear relationships between each physical measurement and each structural property. For example, Figure 12.10 shows an example of a CMC consistency (*m*) varying with concentration with a 4.75 power. Similar trends to comparable powers were observed for regressions of shear-thinning, storage modulus, and loss modulus (plots not shown for brevity). However, the single nonlinear regressions illustrated the hazards of creating single regressions to correlate physical properties across all types of cellulose ethers, since the concentration effects on physical properties were more pronounced in CMCs compared to HECs. Similarly, the dependence on molecular weight was also not constant between cellulose ethers with different substituent groups. These nonlinear single regressions also indicated that consistency had a higher dependence upon concentration as compared to molecular weight.

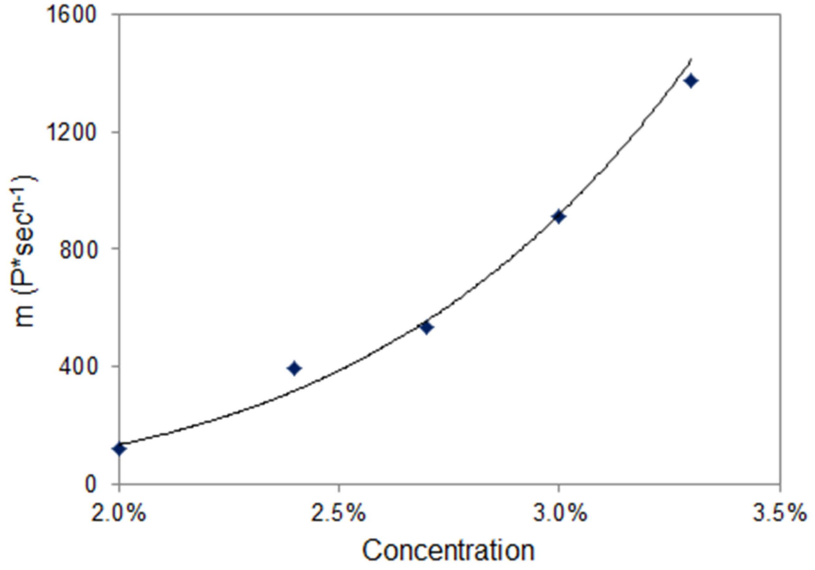

Figure 2.10: Example of a power relationship between a physical property (e.g., consistency) and a structural property (e.g., concentration). Consistency variation with concentration for carboxymethyl cellulose with a molecular weight of 700,000. These values are the consistency (*m*) from the same data presented in Figure 4a, and demonstrate an example of the nonlinear behavior of each physical parameter as a function of each molecular structure parameter (including concentration).

The analysis of such single nonlinear trends also highlights the interdependence between molecular weight and concentration, confirming existing literature sources (225, 226). The nonlinear trends indicate that as molecular weight decreased, the effects of concentration on rheological properties became more acute. This result emphasizes that molecular weight and concentration are interdependent, inverse properties that cannot be considered as separate variables when developing property-structure correlations. Similarly, an analysis of the nonlinear dependence on MS/DS reinforced the importance of the type and amount of substitution in determining rheological properties. Taken together, all the nonlinear behaviors reinforce the nonlinearity and interdependence of the four structural parameters (including concentration) to one another.

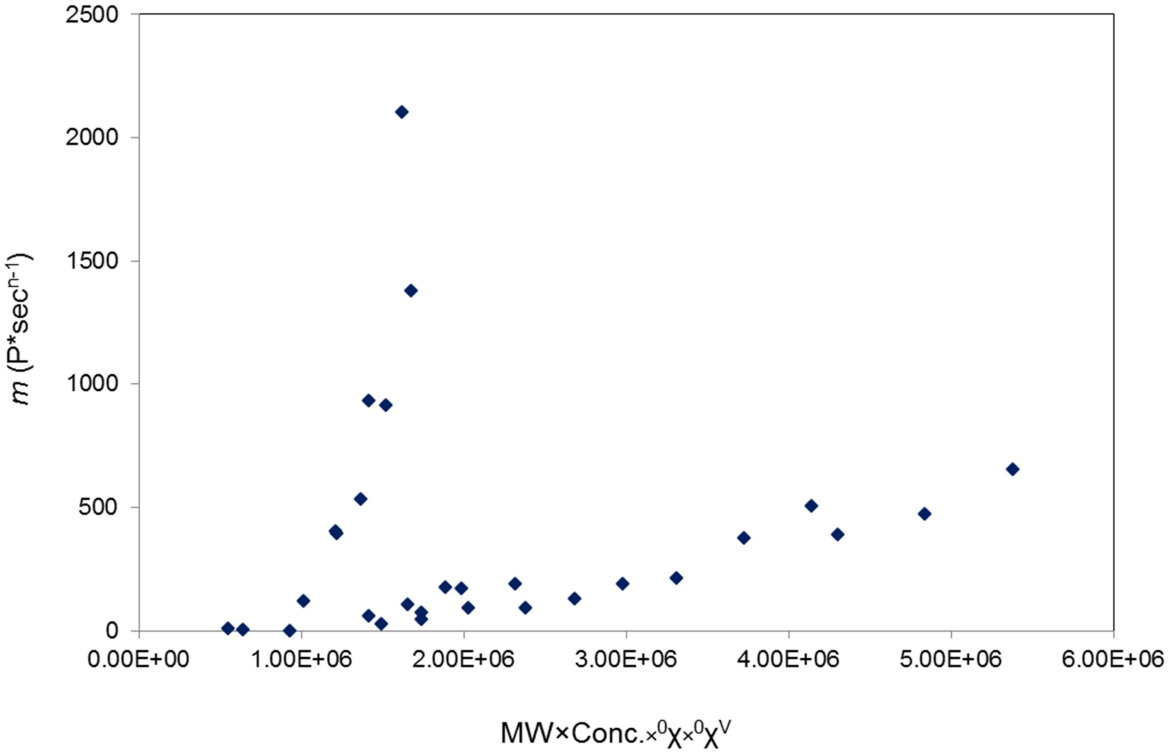

Figure 2.11: Example of two distinct nonlinear trends in a physical property as a function of a single, combined structural parameter. All consistency data plotted against the four structural parameters combined as a single combined parameter: $MW * Conc * {}^{0}\chi * {}^{0}\chi^{V}$. Two separate trends were evident. The steeper, or higher, trend contains data from the CMCs with a DS of 0.7 and 0.9 while the lower trend contains all the HECs and the CMC with a DS of 1.2.

To further explore the interdependence of the structural properties, Figure 2.11 shows the consistency data plotted against the structural variables multiplied together to generate a single combined

parameter. Figure 2.11 shows a strong nonlinear trend and reveals that the data are divided into two clearly demarcated trends. Both follow power regressions for the consistency based on the combined structural parameter but one trend has a much steeper slope than the other. The steeper, or higher, trend contains data from the CMCs with a DS of 0.7 and 0.9 while the lower trend contains all the HECs and the CMC with a DS of 1.2. Interestingly, the two distinct trends are also seen when the storage modulus, loss modulus, and shear-thinning index are plotted versus the single structural parameter (plots not shown for brevity). However, in the case of the shear-thinning index, the physical variation with the structural parameter was linear. The occurrence of the two distinct trends reflects how the zeroth-order connectivity indices do no fully capture the type and degree of substitution.

In summary, the preceding analysis suggests how the collective data can be grouped in a meaningful way when forming nonlinear QSPRs, and suggests the use of two separate sets of QSPRs. The shape of the plots indicates the final form of the QSPRs. For consistency, storage modulus, and loss modulus, the plots indicate power regression as the best functional form, while for shear-thinning index the best functional form was linear.

The final QSPRs, based on nonlinear and interactive terms, for the model building set are shown in Tables II.V and II.VI below. They were formed by separating the data into two sets, modeling all the physical properties except shear-thinning index using a power regression, and combining structural parameters into interaction terms. The power regression QSPRs for each physical property were generated by considering all possible combinations of single, double, triple, and quadruple structural parameters and selecting the correlation with the best r^2 values and q^2 values. The QSPR fits improved dramatically from the linear case in Table IV and all correlations have r^2 values well over 90%. The q^2 values are all over 80% and, excluding the shear-thinning values, are close to the r^2 values. The q^2 values were formed using leave-one-out cross-validation, and since the q^2 values are comparable to r^2 values, we can conclude the correlations are both accurate and useful for prediction.

This final predictive model is composed entirely of empirical relations between molecular structure and rheological properties. The model eschews mechanistic impute and does not consider the

causes of the observed behavior. However, the high r^2 and q^2 values for all the correlations indicates they are accurate for describing the observed behavior and predictive of rheological properties for other cellulose ether solutions. This methodology provides a framework for creating future predictive property models for compounds where information of mechanistic behavior is lacking.

Table II.V: Final QSPRs for Subset of Model Building Set Containing all HECs and the CMC with a DS of 1.2.

Correlation	r^2	q^2
$\boldsymbol{m} = -367.1 + 4.355\text{x}10^{-7}(\mathbf{MW*C})^2 + 52.37\ {}^0\chi - 32.22\ {}^0\chi^V$	0.94	0.93
$\boldsymbol{n} = 0.9291 - 3.862\text{x}10^{-7}\ \mathbf{MW} - 0.2903\ \mathbf{C} + 0.03714\ {}^0\chi - 0.04311\ {}^0\chi^V$	0.93	0.89
$\boldsymbol{G'} = 6.2952\text{x}10^{-26}(\mathbf{MW*C*}{}^0\chi)^{4.7471}$	0.96	0.95
$\boldsymbol{G''} = 1.3687\text{x}10^{-16}(\mathbf{MW*C*}{}^0\chi)^{3.1231}$	0.92	0.90

Table II.VI: Final QSPRs for Subset of Model Building Set Containing CMCs with a DS of 0.7 and 0.9.

Correlation	r^2	q^2
$\boldsymbol{m} = 1.7239\text{x}10^{-22}(\mathbf{MW*C*}{}^0\chi)^{4.6596}$	0.96	0.95
$\boldsymbol{n} = 1.583 - 1.338\text{x}10\text{-}6\ \mathbf{MW} - 1.154\ \mathbf{C}$	0.94	0.81
$\boldsymbol{G'} = 4.2682\text{x}10^{-34}(\mathbf{MW*C*}{}^0\chi)^{6.5881}$	0.99	0.99
$\boldsymbol{G''} = 3.2139\text{x}10^{-21}(\mathbf{MW*C*}{}^0\chi)^{4.1515}$	0.95	0.95

2.4.2 Interpretation of QSPRs

The final form of the correlations in Tables V and VI reveal interesting trends about how the structural parameters impact the physical properties and their relative importance. As previously stated, all correlations are modeled using power regression except for the shear-thinning index since this property was accurately described by a linear fit with the structural parameters as independent variables. Also, the consistency correlation for the data subset in Table II.V was modeled using a quadratic model since in this instance this improved upon the power fit. The power fits also indicate that consistency and loss modulus vary with the structural properties to a similar extent while the storage modulus has a steeper dependence on the interaction term in both sets of correlations. This behavior suggests that as the values of the structural properties increase, the elastic portion of the fluid increases to a greater extent compared to the viscous portion. Generally, as the molecular weights, concentrations, and degrees of substitution of the compounds increase, the fluid becomes increasingly elastic. As the combined structural parameter

increases, the ratio of the viscous portion of the fluid to the elastic portion shifts to favor the elastic portion.

When comparing the two tables, the connectivity indices are much more important in the QSPRs in Table II.V compared to Table II.VI. This is because Table II.V fits a larger range of data with more diverse structures while Table II.VI is purely CMCs with little variation in DS. In fact, only one connectivity index could be used to fit the data in Table II.VI because, for one type of cellulose ethers (either all HEC or all CMC), the connectivity indices are interrelated and no longer independent variables. Somewhat similarly, only one connectivity index was used in the QSPRs in Table II.V for storage and loss modulus. This was because the addition of the second index had little impact on the r^2 value and the concentration and molecular weight had much greater impacts on the overall accuracy of the fit.

The dominance of molecular weight and concentration on the physical properties can be seen in the correlations in Table II.VI. The shear-thinning index depends solely on these properties and the connectivity index in the other three correlations had a much smaller impact on accurate fit than the other two structural parameters. This grouping of correlations indicates that the type of cellulose ether and side chain structure is much more important when determining which set of correlations to use and has a lesser impact on the correlations themselves.

2.4.3 Limitations of QSPRs

The high accuracy and performance of the two QSPR sets allows these correlations to be useful for describing the physical properties of cellulose ethers with known structures and allows for optimization and design of cellulose ethers for specific applications. The samples in this study revealed one trend for all cellulose ethers with a DS above or equal to 1.0 and another trend for all cellulose ethers with a DS less than or equal to 0.9. Further research is needed to determine where the exact transition between the two trends occurs and if there is a value for the DS that acts as a threshold.

Further studies may explore techniques to quantify the effects of buffer concentration within the QSPRs, as well as the effect of the presence of an API. The current model building set incorporates cellulose ethers in aqueous solution with no buffers, preservatives, pH modifiers, or anti-HIV drugs.

However, final formulation of a microbicide delivery vehicle with the active agent may require buffers or other additives to ensure proper drug performance and reduce irritation with the contacting epithelial surfaces (200). Correlations may need to be modified to account for rheological property variations caused by such additives. This correction becomes complicated, however, if the effect of buffer concentration depends on substituent type. Published rheology data on similar CMC and HEC solutions suggest this is the case (206-208). For example, Andrews *et. al.* (206) conducted experiments with solutions using PBS at pH 7.2 instead of pure water at 20°C. The rheology results for the HECs in those studies (206, 207) are much higher than those in this study and the results for the CMC (206-208) are much lower than those seen in this study. The reduced temperature of those HEC experiments partially explains the increase in HEC properties. However, the increase may also be due to the presence of the PBS. This buffer may also be responsible for the drastic decrease in CMC properties (206-208) when compared to the pure water solution in our study. These differences in behavior may be attributable to the charged nature of the carboxymethyl substituent groups whereas all other cellulose ethers are nonionic. Such divergent responses to changing buffer concentration between the two types of cellulose ethers is a challenge for the development of rheological property-molecular structure correlations that can correct for buffer strength. This behavior may even necessitate separate corrected correlations for charged and uncharged cellulose ethers.

The rheological effect conferred by the API seems to be negligible in comparison to this buffer effect. Preliminary testing (199) of the tenofovir gel used in the CAPRISA 004 looked at the rheology of the final microbicide formulation as well as the universal placebo. That study showed very similar rheology for the two formulations, indicating the API has a small rheological impact. This is likely due to the fact that the large size of the cellulose ether polymers dwarves the size of most APIs and thus dominates the rheological behavior of the final microbicide formulation.

2.5 Conclusion

This study demonstrates that the rheological properties of cellulose ethers exhibit complex dependencies on molecular weight, concentration, and substituent group that cannot be adequately

described by linear regressions. In order to rationally design microbicide delivery vehicles of cellulose formulations, the patterns in rheological properties were analyzed and quantified to produce improved correlations and models. The new correlations emphasized the nonlinear dependence of rheological properties on molecular weight and concentration. The correlations showed the importance of the identity of the substituent group and type of cellulose ether over the amount of substitution of the functional groups. The amount of substitution did influence the overall form of the predictive model by clearly demarcating two sets of correlations with different trends, allowing for the generation of accurate and validated QSPRs. Future studies should consider cellulose ethers with a greater ranges of DS values to locate the exact threshold between 0.9 and 1.0 that separates the two QSPR sets.

The current set of correlations form a predictive model that can be used to select the appropriate cellulose ether product possessing optimal rheological properties for a variety of industrial and medical uses. This predictive model is used in the final study to select a cellulose ether with more ideal spreading behavior those in current products, such as the universal placebo and clinical trial formulations. Patient acceptability studies and mathematical models of spreading indicate the ideal rheological properties that correspond with effective microbicide spreading and user acceptance. The correlations in this study provide the exact molecular structure and concentration of a cellulose ether solution for use as that ideal delivery vehicle. A novel delivery vehicle with optimal properties is designed based solely on knowledge of the molecular structure and solution concentration. The template outlined above is utilized in the next two studies to generate additional correlations relating molecular structure of this polymer data set to biocompatibility and drug compatibility. The final study incorporates these diverse property correlations into a molecular design problem that identifies an optimal polymer structure that promotes ideal microbicide safety, efficacy, and acceptability.

Chapter 3

Quantitative Structure-Property Relationships for Inhibition of *Chlamydia trachomatis* and Biocompatibility of Cellulose Ether Vaginal Microbicide "Gels"

3.1 Introduction

To be both safe and effective, anti-HIV vaginal microbicides must possess a number of ideal physical, chemical, and biological properties. A microbicide must be retained in the vagina sufficiently long enough to deliver the active drug to its proper site of action so as to inactivate or otherwise block or halt HIV infection. Microbicides that offer short-term protection must be safe for repeated and extensive use. The formulations should not harm, disrupt, irritate, or promote an inflammatory response on the vaginal epithelium (190). These criteria apply to both the active drug that prevents infection and the delivery vehicle that carries the drug to the site of action.

The healthy cervicovaginal surface provides an efficient barrier against infections and diseases (227). Intact epithelial cells of the female genital tract prevent microbe diffusion and penetration into the body while cervical mucus traps and washes microbes out of the genital tract. This intact vaginal epithelium surface resists HIV infection when challenged. This is because epithelial cells lining the vagina and cervix do not possess target receptors susceptible to HIV binding, and thus HIV cannot enter and infect these cells. For a microbicide formulation to be safe for repeated and extended topical use it must preserve this environment. Additionally, vaginal microbicide formulations used to prevent HIV transmission must lack pro-inflammatory activities. Mucosal inflammation recruits activated CD4-positive cells, such as helper T-cells, macrophages, and dendritic cells, which serve as HIV host cells. This recruitment and activation facilitates viral replication and enhances HIV-1 penetration through epithelial tissues (228).

Several cytokines facilitate the activation of these recruitment pathways and thus their upregulation indicates the presence of inflammation. The presence of some of these pro-inflammatory cytokines indicates mucosal surface toxicity and associated inflammation (182). Of these, the cytokine interleukin-8 (IL-8) is produced by a variety of cells, including vaginal epithelial cells, and recruits neutrophil granulocytes, CD4+ T-cells, and macrophages (229). Some cytokines, such as IL-1α, IL-1β, IL-6, and IL-

8, stimulate HIV-1 replication in infected cells. IL-1α or IL-1β works synergistically with IL-6 to promote viral expression and replication in infected promonocyte cells (230). IL-8 promotes viral replication in both macrophages and T lymphocytes (231). Additionally, studies (232) of HIV-exposed seronegative commercial sex workers have indicated that those individuals with innate HIV immunity display lower levels of pro-inflammatory cytokines (IL)-1α, IL-6, and IL-8 compared to HIV negative controls. For these reasons up-regulation of these particular cytokines should be avoided when designing a novel microbicide formulation to prevent HIV infection. The present study measured increased production of IL-6 and IL-8 to access *in vitro* HIV recruitment associated inflammation. These two cytokines promote HIV infection by recruiting different host cells and thus represent different inflammation pathways.

While minimizing inflammation and recruitment of HIV-vulnerable immune cells, the vaginal epithelium must be preserved as a barrier to HIV penetration. Major causes of epithelial disruptions are STIs. Vaginal infections, particularly bacterial infections caused by *Chlamydia trachomatis*, cause vaginal lesions that are associated with higher rates of HIV infection when a patient is subsequently challenged by the virus (233). An active drug specifically designed to prevent HIV infection may not prevent other concurrent STIs. A delivery vehicle that non-specifically prevents such infections would further promote the body's innate defenses and aid overall microbicide efficacy.

There is a need for novel delivery vehicles that possess optimal biocompatibility and inhibition physical properties in next generation microbicides. The final study in Chapter 4 utilizes CMD as a methodology to achieve this desired optimization that considers these several different target properties at once for a range of candidate molecules. CMD can consider multiple physical properties with conflicting targets to produce many possible molecules quickly, which in turn accelerates the process of drug discovery.

The present study looks at the cytotoxicity, pro-inflammatory cytokine production, and *C. trachomatis* inhibition conferred by a set of compounds to determine differences in biocompatibility and inhibitory ability based on molecular structure. This is accomplished by measuring biological compatibility and inhibition of a model building set of compounds and creating correlations relating the

measured properties to structural data. These relationships are incorporated into an optimization problem in the final study to generate novel delivery vehicles with optimal physical properties.

3.2 Materials and Methods

3.2.1 Materials

3.2.1.1 Model Building Set: Cellulose Ethers

To conduct the experiments that generate the QSPR model for the optimization problem, a model building set of current delivery vehicles is required. The model building set in this study includes the eight cellulose ethers from the first study. The present model building set is expanded by adding two methyl celluloses (MCs) and five hydroxypropyl methyl celluloses (HPMCs). This creates a final model building set of 15 cellulose ethers possessing various side chain substitutions, degree of substitution, molar substitution, and molecular weight. They are shown in Table III.I below.

Cellulose ether based delivery vehicles have undergone little experimental evaluation. The HEC in the Universal Placebo has been extensively characterized (200), but biocompatibility data for similar cellulose ethers is lacking. When additional cellulose ethers are considered for evaluation, such as a MC, publications fail to report the type of MC and do not include the DS, the molecular weight, or product identification (234). Further, the evaluation of this MC focused on rheological properties and drug compatibility and neglected safety. Thus, much of the experimental data available in the literature on the relevant properties of cellulose ethers cannot be used in this current study because the corresponding molecular structure data necessary for correlations is unavailable.

Table III.I: 15 cellulose ethers evaluated for cytotoxic effects against vaginal cells. The average molecular weight, molar substitution, degree of substitution, product information, and label key are provided.

Label	Compound	MW	MS/DS	Source
Nat	Hydroxyethyl Cellulose	1,000,000	2.5/1.5	Natrosol 250 HX Pharm Hercules/Aqualon
HEC 1	Hydroxyethyl Cellulose	1,300,000	2.5/1.5	Sigma-Aldrich
HEC 2	Hydroxyethyl Cellulose	90,000	2.5/1.5	Sigma-Aldrich
HEC 3	Hydroxyethyl Cellulose	250,000	2.0/1.0	Sigma-Aldrich
HEC 4	Hydroxyethyl Cellulose	720,000	2.5/1.5	Sigma-Aldrich
CMC 4	Carboxymethyl Cellulose, sodium salt	250,000	-/0.9	Sigma-Aldrich
CMC 5	Carboxymethyl Cellulose, sodium salt	250,000	-/1.2	Sigma-Aldrich

CMC 7HF	Carboxymethyl Cellulose, sodium salt	700,000	-/0.7	Cellulose Gum 7HF Hercules/Aqualon
HPMC 7	Hydroxypropyl Methyl Cellulose	10,000	0.2-0.3/1.8-2.0	Sigma-Aldrich
HPMC 8	Hydroxypropyl Methyl Cellulose	86,000	0.2-0.3/1.8-2.0	Sigma-Aldrich
HPMC E	Hydroxypropyl Methyl Cellulose	86,000	0.23/1.9	Methocel E Dow Chemical
HPMC F	Hydroxypropyl Methyl Cellulose	86,000	0.13/1.8	Methocel F Dow Chemical
HPMC K	Hydroxypropyl Methyl Cellulose	86,000	0.21/1.4	Methocel K Dow Chemical
MC 6	Methylcellulose	40,000	-/1.6-1.9	Sigma-Aldrich
MC A	Methylcellulose	86,000	-/1.8	Methocel A Dow Chemical

3.2.1.2 Experimental Reagents and Equipment

The cytotoxic and inflammatory effects of 15 cellulose ethers were evaluated *in vitro* using a human immortalized vaginal (VK2/E6E7) epithelial cell line (235), generously provided by our colleague Dr. Miezan Ezoulin in Dr. BBC Youan's laboratory at UMKC. These cells were grown in keratinocyte serum-free medium (KSFM) (Life Technologies, Inc.) supplemented with 0.1 ng/ml human recombinant epidermal growth factor (EGF), 0.05 mg/ml bovine pituitary extract, and 44.1 mg/L calcium chloride (235). Cytotoxicity was assessed by adding cells to 96 well plates and, after a period of incubation described below, alamarBlue® (Life Technologies, Inc.) was added and absorbance at 570 and 600 nm was read using a spectrophotometer (PowerWave HT Microplate Spectrophotometer).

Cytokine concentration was determined using Human IL-6 and IL-8 ELISA Kits (BD OptEIA™, BD Biosciences) and a spectrophotometer reading absorbance at 450 nm, with a correction at 570 nm. Synthetic macrophage-activating lipopeptide-2 (MALP-2) (Enzo Life Sciences) at 50 nM was used as a pro-inflammatory control.

The inhibitory effects were evaluated using *C. trachomatis* lymphogranuloma venereum (LGV) serovar L2/434/Bu elementary bodes (EBs) purified from infected mouse fibroblast (L929) cells (236), generously provided by our colleague Dr. Scott Hefty. The fibroblast cell line (L929) was grown in RPMI 1640 culture medium (Mediatech, Inc.) supplemented with 5% fetal bovine serum (FBS) (Thermo Fisher Scientific) and 10 µg/mL gentamycin (MP Biomedicals) (237).

Information about the 15 cellulose ethers is presented in Table III.I above. The HEC known as Natrosol and the CMC known as Cellulose Gum 7HF were provided by Hercules/Aqualon. The MC known as Methocel A and the HPMCs known as Methocel E, F, and K were provided by Dow Chemical. All others were purchased from Sigma-Aldrich.

3.2.2 Methods

3.2.2.1 Cytotoxicity Assay

For the cytotoxicity assessment, VK2/E6E7 cells were added to 96 well plates at 75% of confluence (approximately $3x10^4$ cells per well) and given approximately 24 hours to adhere (235). At this point the media was removed and replaced with media containing either 0.25% of cellulose ether, or media containing no cellulose ether which served as the negative control. A concentration of 0.25% was chosen as this was determined to be the maximum concentration at which the solution viscosity would not negatively impact cell viability. The plates were incubated with the test compounds for 24 hours. After this time the test solutions were removed and fresh media was added containing 10% alamarBlue®. After an additional incubation period of 6-7 hours the absorbance was read on a spectrophotometer at 570 and 600 nm, adapted from (182).

Cytotoxicity was calculated as the inverse of viability of a sample compared to the control after 24 hours in VK2/E6E7 cells. All tests were performed in triplicate and the averages of those tests are reported, along with the standard deviation. A statistical analysis consisting of t-tests, which compare each cellulose ether to the negative control, and a one-way ANOVA, which compared the cellulose ethers to each other, was conducted using Windows Excel and p values <0.05 were considered significant.

3.2.2.2 Pro-inflammatory Soluble Cytokine Assays

For the inflammation assessment, VK2/E6E7 cells were added to 96 well plates at 75% of confluence (approximately $3x10^4$ cells per well) and given approximately 24 hours to adhere. At this point the media was removed and replaced with media containing 0.25% of cellulose ether and the plates were incubated for 24 hours. After this time the supernatants containing soluble mediators were collected. Concentrations of IL-6 and IL-8 were measured using ELISA Kits and a spectrophotometer reading

absorbance at 450 nm and correcting at 570 nm, adapted from (183). Concentrations were compared to a negative control of media with no compound and a positive control of MALP-2 (50 nM) (238). As was done for the cytotoxicity data, all tests were performed in triplicate and the averages of those tests are reported, along with the standard deviation. A statistical analysis consisting of t-tests, which compare each cellulose ether and MALP-2 to the negative control, and a one-way ANOVA, which compared the cellulose ethers to each other, was conducted using Windows Excel and p values <0.05 were considered significant.

3.2.2.3 Chlamydia trachomatis Inhibition Assay

For the inhibition assessment, infectious forms of *C. trachomatis* (L2/434/Bu) cells, known as EBs, were incubated with cellulose ether compounds at room temperature for 1 hour at a concentration of 0.25%. This mixture was added for a 2 hour pre-infection at room temperature to a monolayer of L929 mouse fibroblast cells plated the previous day. At this time the supernatant was removed, fresh media was added, and the L929 cells were incubated for an additional 24 hours. At the end of this time the cells were fixed with methanol, stained, and analyzed. The level of infection inhibition was determined relative to a buffer control containing no compounds and Polymyxin B serving as a positive inhibition control, from (184). All tests were performed in triplicate and the averages of those tests are reported, along with the standard deviation. The experiments were graciously performed by collaborator Dr. Ichie Osaka in Dr. Scott Hefty's laboratory as per the author's instructions.

3.2.2.4 QSPR Generation

The biocompatibility and inhibition data were incorporated into a set of Quantitative Structure-Property Relationships, or QSPRs. These QSPRs relate physical properties to molecular topology of the cellulose ethers. In the present study the relevant physical properties are percent cytotoxicity, IL-6 and IL-8 concentration, and percent inhibition of *C. trachomatis*. The molecular topology of the cellulose compounds is represented by molecular structural descriptors. These descriptors include the average molecular weight and two zeroth-order connectivity indices used and described in the previous study. The connectivity indices were calculated using the same equations and method as described in the previous

study of rheological properties. Those equations generate a pair of connectivity indices for each cellulose ether polymer with a unique MS/DS. The results for the expanded model building set are shown in Table III.II below.

Table II: Calculated Connectivity Indices for Unique Cellulose Ether Solutions[a,b]

Cellulose Ether	MS	DS	$^0\chi$	$^0\chi^V$
HEC	2.5	1.5	13.35	10.33
HEC	2.0	1.0	12.29	9.41
CMC	NA	.7	10.14	7.14
CMC	NA	.9	10.74	7.53
CMC	NA	1.2	11.64	8.11
HPMC	0.2-0.3	1.8-2.0	10.14	8.27
HPMC	0.23	1.9	10.08	8.21
HPMC	0.13	1.8	9.71	7.85
HPMC	0.21	1.4	9.32	7.68
MC	NA	1.6-1.9	9.29	7.45
MC	NA	1.8	9.32	7.50

[a] Calculations of connectivity indices were based on MS/DS values for an average glucose repeat unit.
[b] The two connectivity indices ($^0\chi$ and $^0\chi^V$) are defined in Equations 2.2 and 2.3.

To generate the QSPRs two biological measurements (cytotoxicity and inhibition of *C. trachomatis*) were correlated with up to three structural properties (average molecular weight and the two connectivity indices above). Pro-inflammatory cytokine production, measured as the production of IL-6 and IL-8, were omitted from the QSPR model for reasons described below. The final correlations were produced using R statistical software (224), and evaluated for accuracy using r^2 and predictive quality using q^2 as described in the previous rheological study. Linear and nonlinear dependence on the three structural properties, as well as interaction terms between the structural properties, were considered when generating QSPRs. The QSPRs with the best goodness of fit and cross-validation performance were identified from these possible correlations with the three structural descriptors.

3.3 Results

In this section, the biocompatibility results and trends are presented. The effects of molecular weight, substituent type, and MS/DS are presented, and the following Discussion section will illustrate the construction of a QSPR model using these trends.

3.3.1 VK2/E6E7 Cytotoxicity Assay Reveals Structure Dependent Response

VK2/E6E7 cells were incubated with cellulose ether compounds for 24 hours before their viability was assessed using an alamarBlue® assay. Several replicates of this experiment were carried out and Figure 3.1 below shows a representative data set. Cellulose ether derivatives from commercial sources, such as the ones listed in Table III.I, are considered "generally recognized as safe" (GRAS) chemicals by the FDA. However, as Figure 3.1 shows, variable viability was observed across the model building set and several compounds produced moderate cytotoxic effects in excess of 20%. These effects were statistically significant ($p < 0.05$) compared to the negative control for all compounds except HPMC E and MC 6.

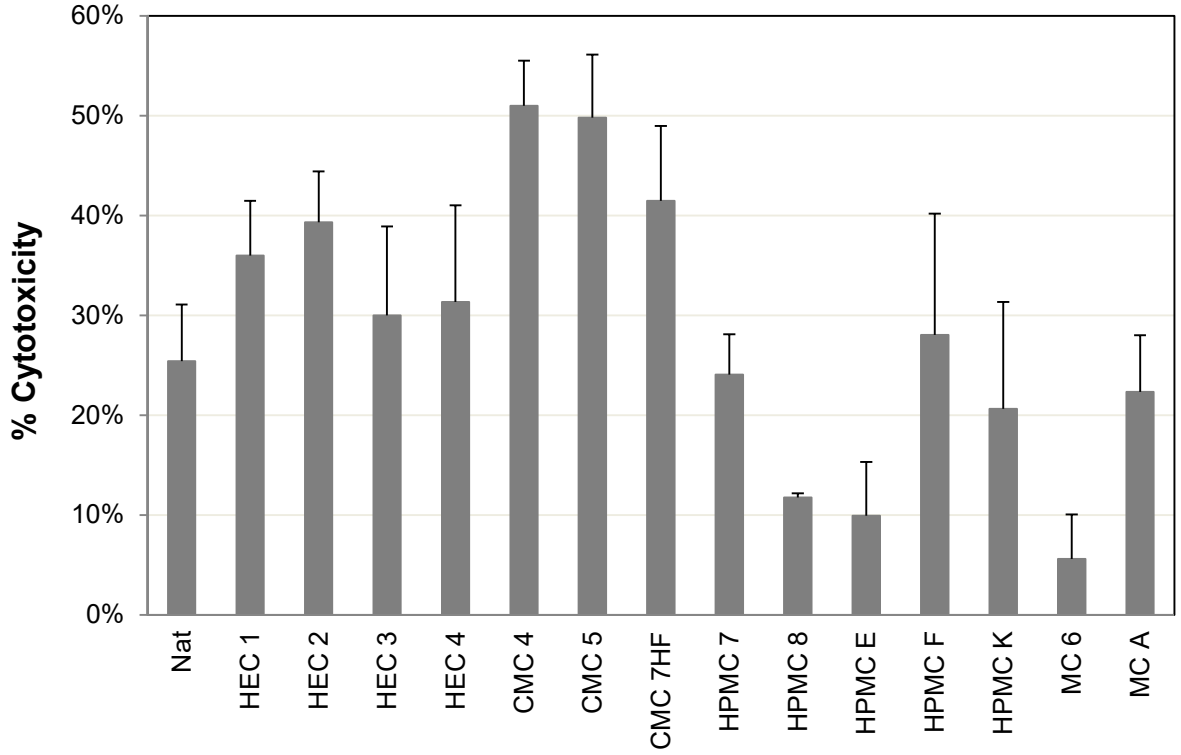

Figure 3.1: Cytotoxic response induced by cellulose ethers. Cytotoxicity was calculated as the inverse of viability of a sample compared to the control after 24 hours in vaginal (VK2/E6E7) cell lines. Bars represent means of triplicate experiments and error bars represent standard deviation. All compounds had p values < 0.05 compared to the negative control, with the exception of HPMC E and MC 6. ANOVA results are described in the text.

While most of the compounds produced a significant cytotoxic effect compared to the control after 24 hours, the response each compound produced varied. The cytotoxic response depends on

molecular structure. In particular, the type of side chain substitution appears to be the dominant molecular effect causing differential toxicity. The CMCs consistently have the highest cytotoxicity. HECs have an intermediate, though still pronounced cytotoxicity. Lastly, the MCs and HPMCs have more variable cytotoxic levels, though collectively they are lower still than the HECs. This indicates that the charge character or polarity of the polymer molecules might have an impact on the epithelial cells. CMCs are ionized salts, the side chains of HECs are non-charged polar groups, the side chains of HPMCs are non-charged slightly polar groups, though to a far lesser degree than HECs, and the side chains of MCs are non-charged non-polar groups. Figure 3.1 suggests that as a cellulose ether becomes less charged and less polar, moving from CMC to HEC to HPMC or MC, cytotoxicity decreases.

In addition to the t-tests performed to evaluate the statistical significance of each cellulose ether compared to the control, a one-way ANOVA was performed to assess the statistical significance of the 15 cellulose ethers compared to each other. The results were somewhat less pronounced than the t-tests comparing the compounds to the control. Even so, several cellulose ethers displayed statistical significance compared to each other with $p < 0.05$. MC 6 was significantly lower than all the CMCs, all the HECs except Nat, and HPMC F. HPMC E was significantly lower than all the CMCs and all the HECs except Nat and HEC 3. HPMC 8 was significantly lower than all the CMCs and HECs 1 and 2. Finally, Nat, MC A, and HPMCs 7, F, and K were significantly lower than CMCs 4 and 5. These results consistently indicate that a difference of approximately 25% indicates that the cellulose ethers are significantly different from each other.

The results of replicate assays were variable such that the numerical value of the cytotoxic effect produced by each compound changed. Compounds with low cytotoxicity, such as the HPMCs and MCs, in some replicates might exhibit no or even negative cytotoxicity in other replicates. Compounds with moderate cytotoxic effects, such as the HECs, might exhibit low cytotoxicity in other replicates that did not prove statistical significance. However, the overall trends were preserved between replicates. CMCs always exhibited the highest cytotoxicity to statistical significance. HPMCs and MCs exhibited the lowest cytotoxic levels and were often not cytotoxic or exhibited very marginal effects. HECs exhibited

moderate cytotoxic effects between the two other types of cellulose ethers. Some replicates indicated a pronounced moderate level of cytotoxicity above 20% and some replicates were lower than this threshold, suggesting these compounds produce marginal toxic effects. These marginal effects might be acceptable for many drug formulations but may cause adverse effects in a topical formulation designed for repeated and prolonged use. Thus it would be desirable to minimize these effects in a final formulation.

3.3.2 Cytokine Assays Reveal Negligible Pro-inflammatory Response

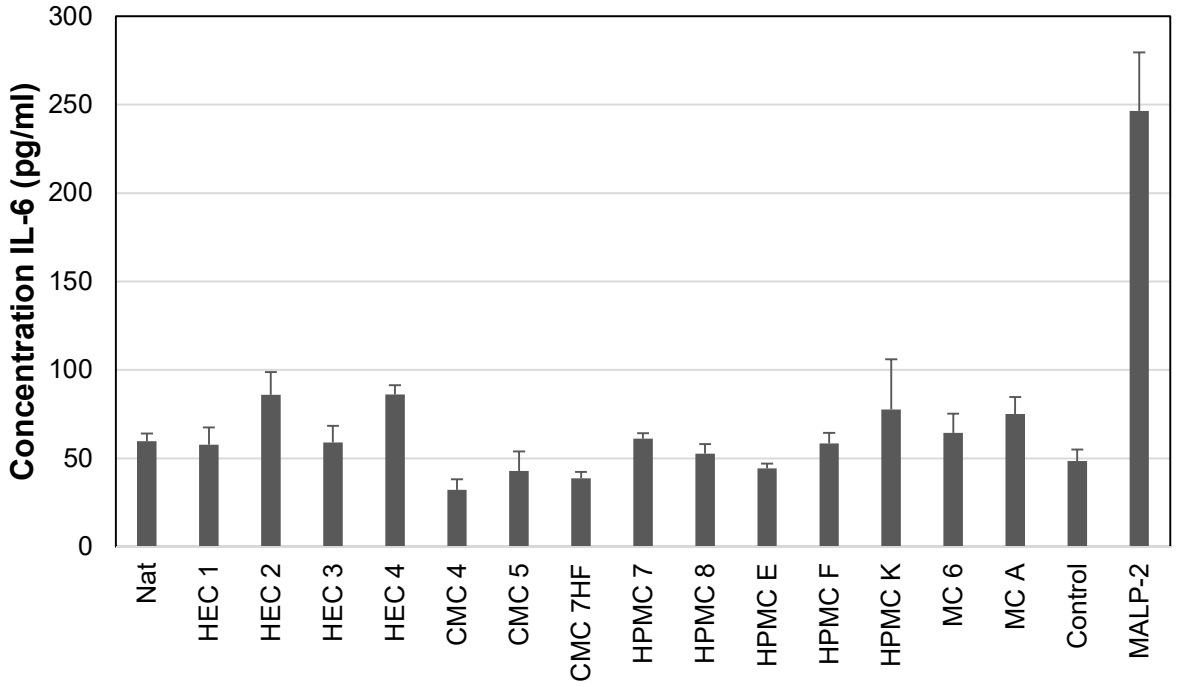

Figure 3.2: IL-6 production induced by cellulose ethers. Pro-inflammatory response induced by cellulose ethers indicated by production of IL-6 after 24 h exposure in vaginal (VK2/E6E7) cell line. Triplicate replication with standard deviation error bars. Bars represent means.

Initially the cellulose ether compounds were not expected to produce a significant pro-inflammatory response. This assumption was made for similar reasons to the initial assumption about cytotoxic effects. The wide variety of pharmaceutical applications cellulose ethers are currently used for would indicate an absence of harm. The slight cytotoxic effects produced by some of the tested compounds in the previous section revised this estimation. For this reason the pro-inflammatory effects of the cellulose ethers were evaluated by measuring production of IL-6 and IL-8 using ELISA kits. Several experimental replicates were performed and Figures 3.2 and 3.3 show a representative data set for IL-6

and IL-8 production, respectively. There were no experimentally consistent, statistically significant increases in production of IL-6 or IL-8 compared to the negative control of media caused by any of the 15 cellulose ethers.

The IL-6 data displayed in the representative replicate in Figure 3.2 does exhibit a slight, statistically significant increase in production compared to the negative control for HECs 2 and 4. However, such trends are absent from other data replications where the negative control is slightly higher. These marginal, inconsistent changes to IL-6 production caused by the cellulose ethers indicate these compounds have little impact on IL-6 upregulation. These marginal fluctuations become especially trivial when compared to the dramatic, almost 10-fold increase in IL-6 conferred by the positive control, MALP-2, which stimulates cytokine production in VK2 cells. The lack of consistent statistical significance between experimental replications precludes the construction of a QSPR relating IL-6 production to cellulose ether molecular structure. This subsequently prevents the use of IL-6 production as a physical property in the final design optimization problem.

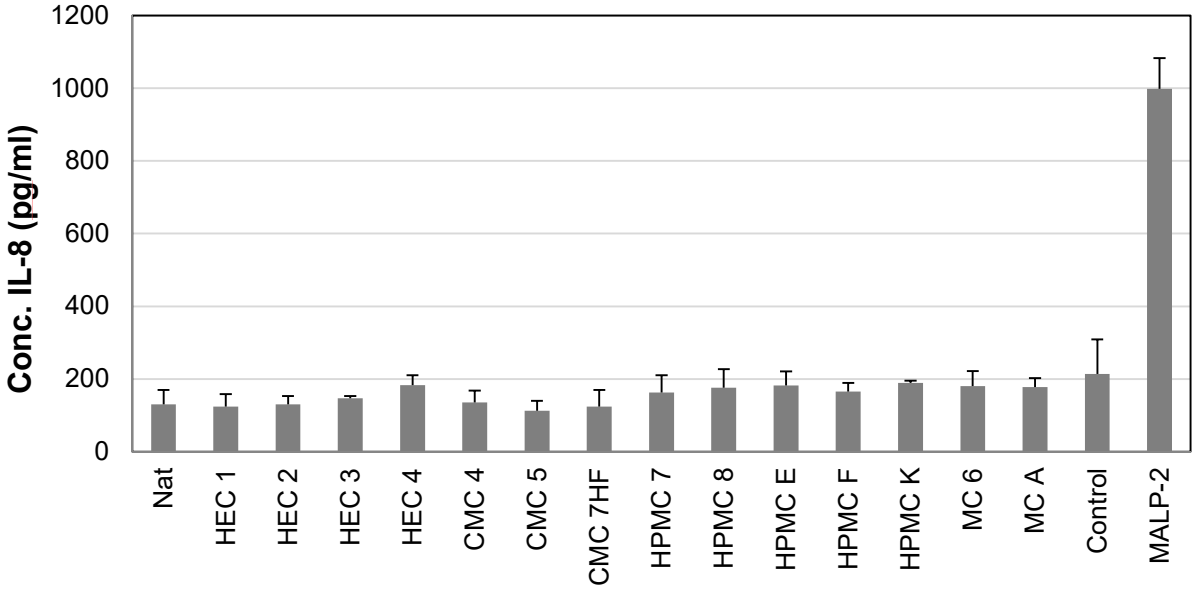

Figure 3.3: IL-8 production induced by cellulose ethers. Pro-inflammatory response induced by cellulose ethers indicated by production of IL-8 after 24 h exposure in vaginal (VK2/E6E7) cell line. Triplicate replication with standard deviation error bars. Bars represent means.

The IL-8 data displayed in Figure 3.3 does not display any statistically significant increase in production compared to the negative control for any of the cellulose ether compounds. This can be seen

even more clearly than in the case for the IL-6 data since the IL-8 production of the negative control for the replicate shown is either equal to or greater than the compounds. For the IL-8 data MALP-2 produced an approximately 5-fold increase in production compared to the negative control, further reinforcing the lack of upregulation conferred by the compounds. Just as with the IL-6 data, the lack of statistically significant upregulation of IL-8 compared to the negative control along with the lack of variability between the different cellulose ether compounds precludes the construction of a QSPR relating IL-8 production to molecular structure. Fortunately for clinical use, both data sets indicate cellulose ethers do not produce unfavorable cytokine responses. Unfortunately for this study these data cannot be used in a final optimization problem.

3.3.3 *C. trachomatis* Assay Reveals Variable Inhibition Response

L929 cells were incubated with a mixture of EBs and each of the 15 cellulose ethers for two hours and then for another 24 hours post-exposure to allow the *C. trachomatis* infection to grow before being stained with methanol and enumerated. These results are shown in Figure 3.4 below. The purpose of this study was to see if any cellulose ether compounds provided a non-specific barrier to *C.* trachomatis infection and, if so, did the degree of inhibition have any relation to molecular structure. Figure 3.4 indicates that several of the compounds exhibited moderate inhibition of *C. trachomatis* in excess of 30% and a few had over 50% inhibition. Further, the large variability between the 15 compounds indicates differences in degree of inhibition due to molecular structure.

The data in Figure 3.4 reveal trends when considered in groupings due to substituent type. Nat and HEC 1 had the highest degree of inhibition (over 50%) while HEC 2 has the lowest inhibition. Interestingly, Nat and HEC 1 are the HECs with the highest molecular weight while HEC 2 has the lowest molecular. Considering the HECs in isolation, there is a very strong dependence of degree of inhibition on molecular weight. From highest to lowest molecular weight, the HECs are ordered as HEC 1 > Nat > HEC 4 > HEC 3 > HEC 2. This is very similar to the order of highest to lowest inhibition for the HECs: Nat > HEC 1 > HEC 4 > HEC 3 > HEC2.

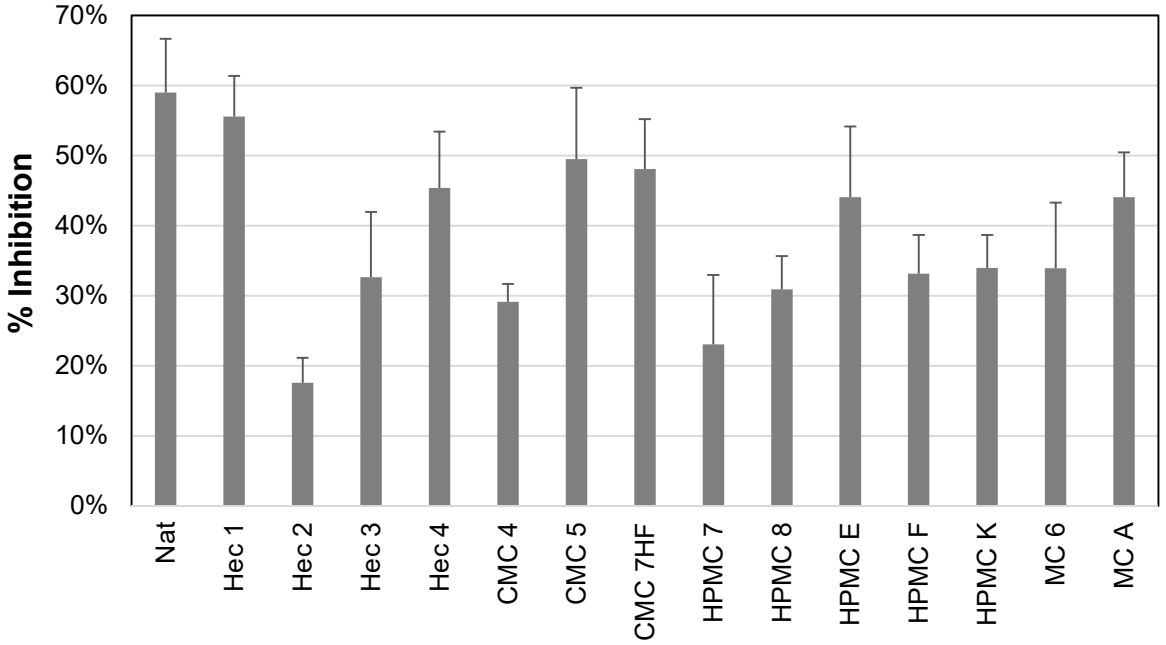

Figure 3.4: Inhibition of *C. trachomatis* induced by cellulose ethers. Inhibition was calculated as the inverse of infection compared to control after 2 hour exposure. Bars represent means of triplicate experiments and error bars represent standard deviation.

The trends for the data for the HPMCs and MCs are similar to those for the HECs, though less pronounced. HPMCs 8, E, F, and K have the same molecular weight and similar MS/DS structure. Thus they would be expected to exhibit similar physical properties. This is mostly true for the inhibition data, although HPMC E is somewhat higher than the others, even though its structure is almost the same as HPMC 8. Fortunately, the molecular weight trend for the HECs does continue for these data. HPMC 7 has a lower molecular weight than the other HPMCs and also has a slightly lower degree of inhibition. Similarly, MC 6 has a much lower molecular weight than MC A and a slightly lower degree of inhibition as well. The consistency of this trend of inhibition correlating with average molecular weight suggests a possible QSPR to describe these data, as discussed in the next section.

One interesting trend that is not readily apparent from Figure 3.4 is that HPMCs and MCs appear to have a higher inhibitory ability compared to the HECs and the CMCs. At first look at Figure 3.4, the high molecular weight HECs and CMCs had the highest degree of inhibition while the HPMCs and MCs were in the middle of the present data set. However, all the HPMCs and MCs tested had much lower molecular weights compared to these high molecular weight HECs and CMCs. The highest molecular

weight HPMCs and MCs (HPMCs 8, E, F, K and MC A) had an average molecular weight of 86,000. This is comparable to HEC 2, which had a molecular weight of 90,000. At around the same molecular weight some of the HPMCs and MCs had double the inhibition conferred by an HEC. Since the rest of the data indicates an increase in inhibition with an increase in molecular weight, this suggests that HPMCs and MCs with molecular weights comparable to Nat and HEC 1 would have even higher degrees of inhibition than displayed in Figure 3.4. These trends relating inhibition to molecular structure, particularly molecular weight and substituent group type suggest that this data set will be useful for the generation of a QSPR predictive model that can be incorporated into a later optimization problem to design novel compounds with non-specific inhibitory effects.

3.4 Discussion

The following section will expand upon the trends discussed in the above results section in order to construct quantitative structure-property relationships (QSPRs). These will form a predictive model that will be incorporated into a design problem formulation in future work. The preceding results sections began to identify trends in these data relating biological properties to molecular structure. Unfortunately the limited variation and negligible difference from the negative control in the pro-inflammatory results, represented in this study as IL-6 and IL-8 production, prevent any further analysis of these data or incorporation into any sort of predictive model. Fortunately, both the cytotoxicity and *C. trachomatis* inhibition data displayed more statistically significant variations between compounds and their negative controls. Further, there seemed to be variation in observed data correlating with variation in molecular structure. This allows for the possible construction of a predictive model incorporating these two properties. However, further analysis will be described in the following sections before constructing such a model.

3.4.1 Exploration of Trends and Generation of Cytotoxicity QSPR

The QSPR analysis begins by considering the cytotoxicity data in Figure 3.1. These data seem to indicate a logical progress correlating cytotoxicity to molecular structure. In particular substituent group effects appear to be particularly strong. As described above, the CMCs have the highest cytotoxicity, the

HECs are intermediate, and the MCs/HPMCs have the lowest cytotoxicity. This overall progression seems somewhat linear, so a linear correlation using all 15 compound cytotoxicity points was attempted. The molecular descriptors included average molecular weight and two connectivity indices to indicate substituent type as well as MS/DS. The resulting correlating was fair, but not particularly accurate, with an r^2 value of 0.79. To improve upon this figure, further analysis was performed.

Since the cytotoxicity trend seemed to depend upon substituent group, each type of cellulose ether was isolated for further analysis. Examining the trends by substituent type revealed that effects of substituent type dwarfed all other molecular descriptors. The HECs have similar MS/DS values but widely varying molecular weight. However, there was no clear relation between the molecular weight of these compounds and cytotoxicity. Nat and HEC 1 are the highest molecular weight HECs, while HEC 2 and HEC 3 have the lowest molecular weights. Yet HEC 1 and HEC 2 have similar cytotoxicity values, at the high end of the HEC data, and Nat and HEC 3 have similar, lower values. This mismatch between cytotoxicity and molecular weight continues for the other types of compounds. The CMCs indicate that increasing molecular weight might decrease cytotoxicity while the MCs indicate the opposite. CMC 7HF has a higher molecular weight than CMCs 4 and 5, which have slightly higher cytotoxicity. Conversely, MC A has a higher molecular weight than MC 6 and a higher cytotoxicity. The HPMCs are also erratic with respect to molecular weight. HPMC 8, E, F, and K all have the same molecular weight, but HPMC 8 and E have very low cytotoxicity and HPMC F and K are about twice as high. HPMC 7 has a much lower molecular weight than the other four yet is comparable in cytotoxicity to HPMC F and K. For these reasons cytotoxicity cannot be correlated with molecular weight in any meaningful way. This lack of relationship hinders the accuracy of a QSPR using the three previously mentioned molecular descriptors and all 15 cytotoxicity data points.

To overcome this limitation, data was averaged to achieve the final QSPR form for the cytotoxicity data. Since cytotoxicity depended heavily on substituent group but not on molecular weight or MS/DS variations, each type of cellulose ether was grouped together in the final QSPR. A zero-order connectivity index, ${}^{0}\chi$, was used to identity the type of cellulose ether. For the HECs the five cytotoxicity

values were averaged as were the five corresponding $^0\chi$ values. This was repeated for the CMCs, HPMCs, and MCs, resulting in four cytotoxicity values and four indices. A further correction value was required to generate the final QSPR. The CMCs have intermediate $^0\chi$ values but the highest cytotoxicity values. Several scalar corrections were evaluated and a scalar of 1.5 multiplied by the average $^0\chi$ value of the CMCs resulted in a correlation with the best r^2 value. This correction was necessary because the CMCs are actually sodium salts and the ionized sodium in their structures is not taken into account in the calculation of the connectivity indices. It appears in the case of cytotoxicity this attribute of the molecular structure is important.

The final correlation is shown in Table III.III below and the predictive model is illustrated in Figure 3.5. The QSPR fit is improved dramatically by grouping substituent type together, raising the r^2 from 0.79 to essentially 1 (0.997). The q^2 value is also extremely high (0.99), indicating that the QSPR is highly useful for predicting average $^0\chi$ and thus for identifying the proper substituent group. This QSPR can be incorporated into a future optimization problem formulation.

Table III.III: Final QSPR for Cytotoxicity Data.

Correlation	r^2	q^2
cyto = 0.04676 $^0\chi$ – 0.2871	0.997	0.99

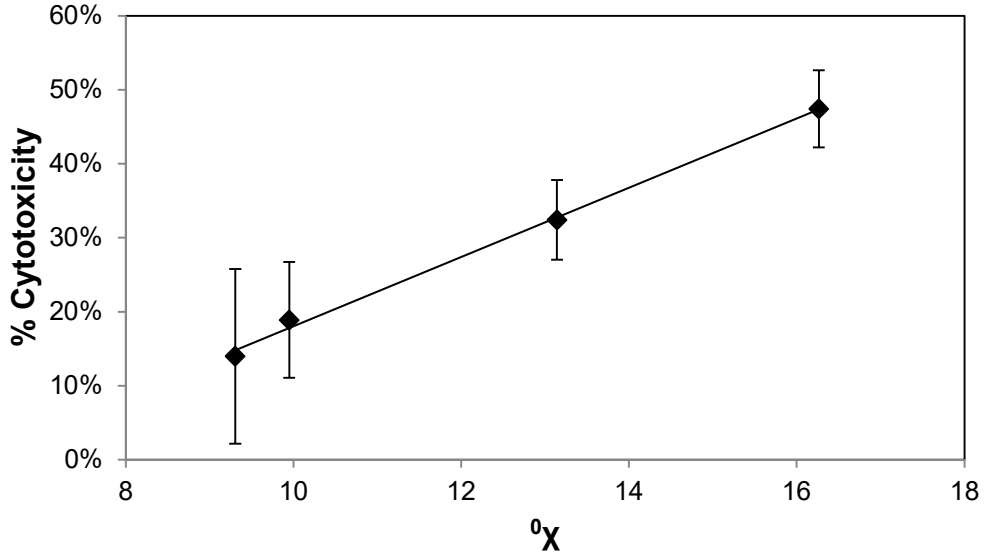

Figure 3.5: QSPR fitting cytotoxicity data to substituent type. $^{0}\chi$ from least to greatest is MC, HPMC, HEC, and CMC.

3.4.2 Exploration of Trends and Generation of *C. trachomatis* Inhibition QSPR

Creating a QSPR using the *C. trachomatis* inhibition data from Figure 3.4 requires more thorough analysis than of the cytotoxicity data in the previous section. The larger degree of variability in the data compared to the cytotoxicity data makes cursory identification of trends difficult. For instance, contrary to the cytotoxicity data, the inhibition data shows large variability within the same substituent type. Further, within substituent type there does appear to be correlation between degree of inhibition and molecular weight. The inhibition conferred by the HECs is highest for high molecular weight HECs and lowest for low molecular weight HECs. This pattern is repeated for the HPMCs, the MCs, and some (but not all) of the CMCs. After this trend was identified, a linear correlation relating *C. trachomatis* inhibition to molecular weight and the two connectivity indices was attempted. The resulting QSPR had an r^2 of 0.65, much too low for use in a predictive model. Other correlation forms, such as power, exponential, or logarithmic did not provide a substantial improvement to the accuracy of the QSPR.

Since a single QSPR did not seem to fit the entire data set well, the data was analyzed separately by substituent group to elucidate any further trends and to determine if a subset of the data could be incorporated into a more limited, but more accurate QSPR. In particular the HEC data had a strong dependence upon molecular weight. A linear correlation relating just these five inhibition data points to molecular weight had a fair r^2 value (0.88). However, a power-law correlation relating HEC inhibition to molecular weight had a very high r^2 value (0.97). This correlation was highly accurate and could be used in a predictive model. Further, the power was raised to a decimal less than one, contrary to the positive powers displayed in the rheology QSPR model in the previous paper. This indicates that for the HEC and CMC substituent groups at a fixed concentration there is an upper limit of inhibition after which further molecular weight increases have little impact.

The other data in the other three substituent groups was analyzed to see if it would fit in this correlation. This analysis identified CMCs 4 and 7HF, but not CMC 5, as having behavior remarkably

similar to the HECs and thus this data was used to generate a QSPR relating molecular weight to *C. trachomatis* inhibition. Incorporating either connectivity index into this equation in any relation actually lowered the r^2 value and thus these descriptors were omitted. This QSPR is shown as A in Table III.IV and Figure 3.6 below. Once again, the very high r^2 and q^2 values indicate that this QSPR is both accurate and predictive and thus useful in a predictive model for a future optimization problem.

The remaining data was then analyzed to determine if all the data could be incorporated into a predictive model with a separate QSPR. This remaining data consisted of all the HPMCs, all the MCs, and the CMC with DS = 1.2. Luckily, this remaining data did seem to correlate with molecular structure. In particular this data exhibited a very similar dependence upon molecular weight as the HEC and CMC subset, with degree of inhibition rising with increased molecular weight. The form of the correlation was also similar to the QSPR for the HECs and CMCs as a linear correlation was fair, but a power-law dependence raised to a decimal power was better. However, even with a smaller subset of data the accuracy was lower than useful ($r^2 = 0.71$). This low accuracy was due to the HPMCs. These compounds had very similar MS/DS values and fairly similar degrees of inhibition. In addition, four of these compounds, HPMC 8, E, F, and K, had the same average molecular weight. Thus there was little variation in molecular structure and degree of inhibition to differential these data. When correlated with HPMC 7, MC 6, MC A, and CMC 5, the other four HPMCs grouped around one point on the graph. With half the data at one point, this skewed the results of the correlation, putting extra emphasis on this point and lowering the overall accuracy (calculated as r^2) of the correlation. For this reason the HPMCs with the same molecular weight were averaged as was done for the cytotoxicity data. The two connectivity indices and degree of inhibition were averaged for these four points to give a single, average HPMC with molecular weight of 86,000.This resulted in a data set consisting of five points: CMC 5, MC 6, MC A, HPMC 7, and an average HPMC with a molecular weight of 86,000.

The final correlation for this half of the data is shown as B in Table III.IV and Figure 3.7 below. The analysis described in the previous paragraphs resulted in a QSPR with dramatically improved accuracy and predictive power, raising r^2 to 0.95 and q^2 to 0.94, very near the values for the QSPR for the HEC and

other CMC data. The power of the correlation is lower, indicating that the upper limit of inhibition conferred by HPMCs and MCs is generally lower than that of the HECs and CMCs. Similar to that previous QSPR, this QSPR depends heavily on molecular weight. In addition, this subset of the data did display some variation with the connectivity indices. In particular, as the indices increased the inhibition tended to decrease. Thus this QSPR depends upon the combined parameter of molecular weight divided by connectivity indices multiplied together.

Table III.IV: Final QSPRs for Inhibition of *C. trachomatis* Data. QSPR A contains all the HEC data as well as CMCs with DS = 0.7 and 0.9. QSPR B contains all the MC and HPMC data as well as CMC with DS = 1.2. The HPMC with Molecular Weight = 86,000 were averaged.

Correlation	r^2	q^2
A: inh = $0.001169(\mathbf{MW})^{0.4489}$	0.97	0.95
B: inh = $0.07089(\mathbf{MW}/({}^{0}\chi * {}^{0}\chi^{V}))^{0.2454}$	0.95	0.94

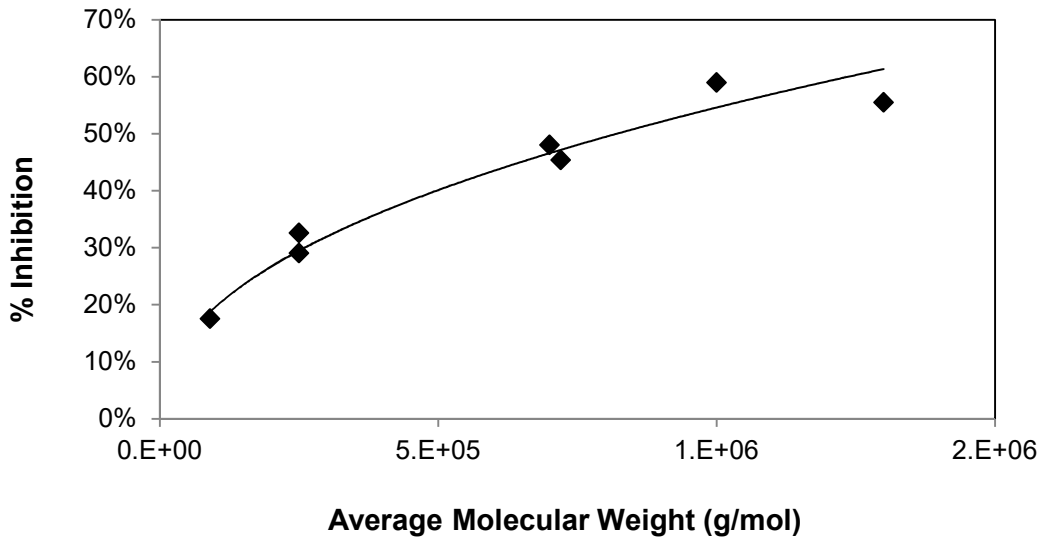

Figure 3.6: QSPR fitting HECs and CMCs DS = 0.7 and 0.9 to molecular weight.

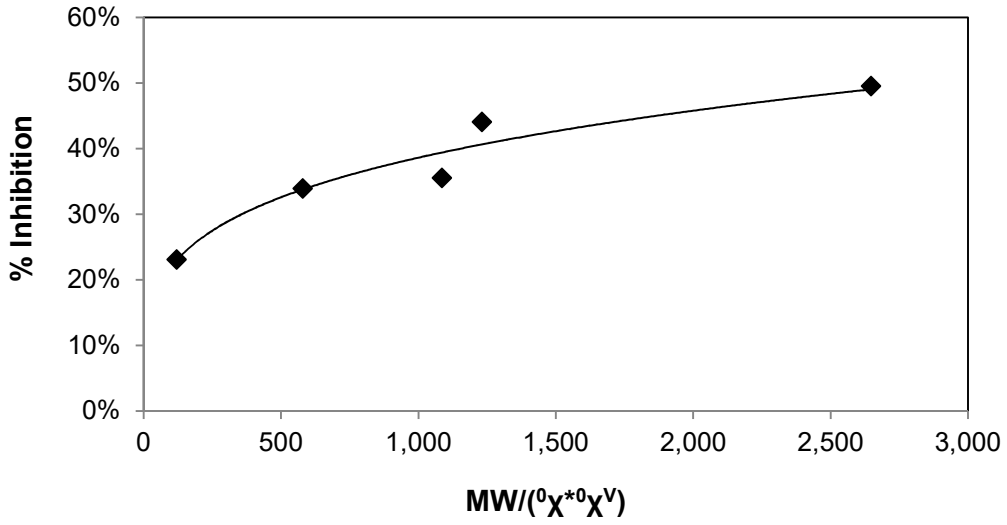

Figure 3.7: QSPR fitting MCs, HPMCs, and CMC (DS = 1.2) to molecular weight divided by multiple of connectivity indices. HPMCs with molecular weight = 86,000 are averaged.

3.4.3 Interpretation of QSPR Model

The preceding three QSPRs form a model to predict cytotoxicity and inhibition of *C. trachomatis* infection based on molecular structure descriptors. This predictive model is intended as a purely empirical model devoid of mechanistic impute. These models are not intended to indicate the causes of the observed behavior. Such a methodology allows for the creation of predictive property models for compounds where structural data exists but information on mechanistic behavior is lacking. The high r^2 and q^2 for all QSPRs in the current predictive model indicate that they both accurately predict the current observed behavior and are predictive of the behavior other cellulose ether compounds.

In addition to providing a valid empirical model, the current predictive model does give some indication of possible biological mechanisms for the observed behavior. The inhibition of *C. trachomatis* is highly correlated with molecular weight. As the molecular weight increases, so does the degree of inhibition. Previous work has shown that molecular weight is highly correlated with viscosity. Thus the inhibition might be due to viscosity effects. The increasingly viscous cellulose ether solutions may non-specifically inhibit the diffusion of the EBs and in that manner prevent infection. A low cellulose ether concentration of 0.25% was selected to try to minimize this impact. At this concentration all the solutions

were Newtonian with a viscosity approaching that of water. However, some small variations might remain and influence inhibition behavior.

Conversely, cytotoxicity has no dependence upon molecular weight, but does correlate highly with substituent type. This indicates that increasing viscosity is not impacting the health of the cells, but the type of cellulose ether does. This QSPR indicates that cytotoxicity increases from MCs to HPMCs to HECs to CMCs. Interestingly, this trend is from least to most polar substituent. MCs have non-polar methyl groups surround the cellulose core. HPMCs have mostly methyl groups with a few polar hydroxypropyl groups facing the solution. HECs have all polar hydroxyethyl groups covering the exterior. Finally, CMCs create a charged solution of ionized sodium and carboxymethyl groups. This trend indicates that the negatively charged and highly polar cellulose ether compounds irritate or otherwise harm the cells while the non-polar MCs are less hazardous. This trend is consistent with expectations since ionic compounds create hyperosmolar solutions, which are thought to increase toxic effects on cells (239). This might also explain the failure of cellulose sulfate as a vaginal microbicide since cellulose sulfate is ionic in solution and might produce marginal cytotoxic effects (113). These competing phenomena allow for a robust optimization problem formulation in which different molecular characteristics can be prioritized to create a novel, ideal delivery vehicle with minimal cytotoxicity and maximal inhibition of *C. trachomatis*.

There are limitations to the present study that will influence the final optimization study. The averaging done to generate some of the QSPRs will limit the accuracy of the predictive model. In particular, the cytotoxicity QSPR can be used to predict which substituent type has a certain range of cytotoxicity, but not necessarily the exact cytotoxicity for each unique MS/DS for each predicted compound. Since the HPMC data had to be averaged for the inhibition QSPR, this correlation predicts molecular weight and that a compound should be a HPMC, but not necessarily the MS/DS of that HPMC. Finally, the experimental error was not reflected in the final predictive model, which only considered the correlation error. Optimization problems using similar methodologies, such as Roughton *et al.* (177),

propagated such error through the final correlations to indicate a range of predicted structures that are statistically similar.

3.5 Conclusions

This study demonstrates that some biological properties of cellulose ethers exhibit dependency upon molecular structure. These dependencies correlate with different aspects of molecular structure, such as substituent group and molecular weight, and exhibit different correlation forms, such as linear and power regressions. Not all of the data was successfully correlated with the connectivity index method for quantifying molecular structure, but enough data did generate accurate and predictive QSPRs useful for a predictive model of biocompatibility and inhibition. Future studies should incorporate cellulose ether compounds with a greater range of MS/DS values to explore if these values have any impact on cytotoxicity and to resolve more clearly the demarcation between the two inhibition QSPRs.

This set of QSPRs form an accurate predictive model that can be used to select other cellulose ether compounds with optimal cytotoxicity for a variety of topical medical applications and optimal inhibition of *C. trachomatis* for vaginal and anal formulations. This predictive model can be used to select a cellulose ether compound with lower cytotoxicity and higher or lower inhibition of *C. trachomatis* than in current products. Designing for lower inhibition will allow for the production of a true universal placebo formulation that does not confer unevaluated protection against *C. trachomatis*, which will non-specifically prevent HIV infection. It will also prevent the production of a universal placebo formulation with slight cytotoxicity which could produce unintended harm in patients and thus skew the results of clinical trials. Additionally, this model can be used to produce a microbicide formulation with increased non-specific inhibition of *C. trachomatis* infection which in turn could boost inhibition of HIV conferred by the microbicide.

The correlations detailed above can produce novel cellulose ether molecular structure for these disparate uses. This allows for the design of an ideal placebo and ideal microbicide using only knowledge of molecular structure. This methodology was successfully completed in a previous study of rheology and in this current study of biocompatibility. This predictive model will be is expanded in the next study to

generate additional correlations relating molecular structure of this model building set to drug compatibility, in particular drug loading and release. The final study incorporates all these diverse property correlations, including the biocompatibility and inhibition correlations detailed above, the rheological correlations in the previous study, and the drug compatibility correlations created in the next study, into a molecular design problem. This design problem formulation is solved to identify optimal cellulose ether structures that generate ideal patient safety, drug efficacy, and user acceptability.

Chapter 4

Quantitative Structure-Property Relationships for Drug Solubility and Release and Computational Molecular Design of Cellulose Ether Vaginal Microbicide "Gels"

4.1 Introduction

To provide efficacy against HIV, vaginal microbicides must possess a number of optimal physical, chemical, and biological properties. The microbicide must be retained at the site of action sufficiently long enough to deliver the API at the proper dosage to block, halt, or inactivate HIV. The delivery vehicle must solubilize a sufficient concentration of the API and then release the proper dose to the proper site in the body depending on the API's method of action.

First generation APIs, including surfactants, detergents, and vaginal defense enhancers, tended to non-specifically inhibit HIV infection by disrupting the viral envelope, capsid, or lipid membrane (23). This class of microbicides has been largely abandoned after a clinical trial of nonoxynol-9 displayed a 50% increase in HIV infection in the heavy-use treatment group compared to the placebo group (87). The next class, polyanions, non-specifically blocks HIV infection by binding to the viral envelope. This class too has also fallen out of favor after the largely unexplained failures of large scale clinical trials such as PRO 2000 (104) and cellulose sulfate (112). The newest class of microbicides consists of antiretroviral (ARV) agents. ARVs may prevent HIV infection by preventing viral entry into host cells, preventing viral DNA integration into host DNA, or preventing virion assembly and maturation. A subclass of ARVs is reverse transcriptase inhibitors (RTIs). RTIs inhibit virial replication by preventing reverse transcription of viral RNA into DNA. This class of drugs is especially promising for microbicide development because it includes tenofovir. A clinical trial of CAPRISA 004 (128), a 1% tenofovir gel, reduced HIV 39% overall in the treatment arm compared to the placebo, and 54% in individuals with high adherence. For this reason tenofovir was chosen as a model API for the current study.

The specific mechanism of action of tenofovir requires a delivery vehicle with optimal solubility and release behavior. Drug solubility limits the size of the dose that can be delivered while release limits the dose that reaches the target cells and tissues. These, in turn, limit the overall efficacy of the API. Low

aqueous drug solubility presents a major obstacle to formulation design since the drug must be delivered through aqueous biological fluids, such as human vaginal fluid. Even hydrophilic drugs, such as tenofovir may exhibit different degrees of aqueous solubility depending upon the hydrophilic and ionic behavior of the formulation. Conversely, high solubility can be a hindrance to release. Drugs that are highly soluble in formulation may resist diffusing out of that formulation if they are less soluble in the release medium. In the case of tenofovir, it is imperative that the microbicide release the API out of formulation so it can reach the target cells and enter their cytoplasm where it can have activity against the HIV reverse transcriptase enzyme. This class of API must be highly soluble in the microbicide formulation and easily released to be effective against HIV infection. A high concentration gradient is required to release a substantial amount of tenofovir to not only reach the target cells but penetrate within them. The proper delivery vehicle formulation is necessary to achieve this optimal action.

The present study aims to improve microbicide development by providing a framework to develop next generation delivery systems with improved properties. This study looks at the solubility of tenofovir in and release of tenofovir from a set of formulation compounds to determine differences in drug compatibility based on the molecular structure of formulation components. There is a need for novel delivery vehicles that possess optimal release profiles as the next generation of microbicides is generated with APIs that have ever more specific activity against HIV. A computational framework is desired to create these novel DDSs with a range of optimal properties, including drug compatibility, biocompatibility and inhibition, and rheology. Computational molecular design (CMD) provides one such computation framework.

CMD (157) is an optimization methodology that generates products with optimal behavior by relating that behavior empirically to physical or chemical properties. In turn, these properties are related empirically to molecular structure. Novel products are proposed by incorporating these empirical relations into an optimization problem formulation and then solving the problem to generate structures that correspond to ideal properties and behavior. This methodology is achieved by the following steps. First, a set of compounds, known as a model building set, with known molecular structures are selected. The

relevant physical or chemical properties of these compounds are then measured. At the same time structural descriptors, which numerically describe the molecular structure, are calculated for the compounds. These measured data and calculated structural descriptors are then incorporated into QSPRs. These QSPRs are integrated into an optimization problem formulation along with a number of structural feasibility constraints to ensure chemically possible molecules are generated. This problem is solved to generate several novel molecular structures that possess the target physical properties that correspond to the desired behavior. CMD is an advantageous methodology because multiple properties and behaviors with conflicting optimal targets can be considered within one problem. This problem can be solved quickly multiple times to produce many candidate molecules and thus accelerate the timeline of discovery by minimizing the need for high-throughput screening. This final study aims to demonstrate the feasibility of such a methodology when applied to vaginal microbicide delivery.

This study demonstrates the completion of a CMD problem to generate candidate structures for ideal novel vaginal microbicide delivery vehicles. The present study first measures tenofovir solubility and release in a model building set of compounds to determine how molecular structure of a delivery vehicle impacts API activity. These data are then correlated with molecular descriptors to create a predictive model. This predictive model, along with the rheological, biocompatibility, and inhibition predictive models from previous studies, is incorporated into an optimization problem formulation. This optimization problem is then solved to generate several candidate novel delivery vehicle structures with optimal drug compatibility with tenofovir, optimal rheological properties, and optimal biocapability.

4.2 Materials and Methods

4.2.1 Materials

4.2.1.1 Model Building Set: Cellulose Ethers

To conduct the experiments that generate the QSPR model for the optimization problem, a model building set of current delivery vehicles is required. This current study used the same 15 cellulose ethers used in the biocompatibility and inhibitions studies and displayed in Table III.I.

As mentioned in the previous two chapters, cellulose ethers have undergone little experimental evaluation. The release of tenofovir from the HEC used in the CAPRISA 004 formulation (199) has been evaluated as well as permeation of HIV through the same HEC and a MC (234). However, data on drug solubility and drug release are lacking for the wider range of cellulose ethers evaluated in this present study. Further, when excipients are evaluated for their impact on drug solubility and release, other types of compounds are considered and cellulose ethers are largely ignored (196). Thus, the experimental data necessary for the completion of this present study is absent from literature for the current model building set of cellulose ethers.

4.2.1.2 Experimental Reagents and Equipment

Model drug tenofovir was graciously provided by Gilead Sciences, Inc. Acetonitrile was purchased from Fisher Scientific. Triethylamine and phosphoric acid (85%) were purchased from Sigma-Aldrich. All water used in the study was Milli Q water purified in a Millipore water purification system (Millipore Corporation). The HEC known as Natrosol and the CMC known as Cellulose Gum 7HF were generously provided by Hercules/Aqualon. The MC known as Methocel A and the HPMCs E, F, and K were generously provided by Dow Chemical. All other cellulose ethers were purchased from Sigma-Aldrich.

Both the solubility and release studies were performed in a thermostatically controlled, benchtop CO_2 incubator with a built in shaker (New Brunswick™ S41i, Eppendorf). The release study was performed using Spectra/Por cellulose ester membrane dialysis bags (Spectra/Por Float-A-Lyzer G2, MWCO 3.5-5 kDa) from Spectrum Laboratories, Inc. The concentration of tenofovir in both studies was measured using an HPLC system (Shimadzu Corporation) consisting of an LC-20AB solvent delivery system, a DGU-20A3R degassing unit, a CBM-20A system controller, a CTO-20AV column oven, and a SPD-20A UV-VIS detector. A Kromasil™ C18 column (150 x 4.6 mm, 5 µm) was used for the separation and the data was processed using LabSolutions software.

4.2.2 Methods

4.2.2.1 Solubility

The solubility, method adapted from (196), of tenofovir in cellulose ether solutions was found by adding an excess of tenofovir powder (over 15 mg) to an aqueous sample of cellulose ether solution (1 mL). This shaker incubation method was selected as it was performed in several studies, including preclinical evaluation of CAPRISA 004 (199). All 15 sample solutions contained 0.675% of cellulose ether. Initially solubility testing was attempted at a concentration of 2.7%, modeled on the universal placebo concentration. However, at this concentration several solutions were too viscous to allow substantial diffusion of tenofovir powder and thus artificially lowered the overall solubility. For this reason the concentration of cellulose ether was diluted by a factor of four. These solutions were incubated for 24 h (37 °C and 200 rpm) to allow the sample to reach equilibrium. After this time the samples were centrifuged (21,000 *g*, 2 min) to remove any undissolved tenofovir powder. The samples were then diluted by a factor of 100 and the concentration of tenofovir was found using the HPLC system described below. Triplicate HPLC readings for each sample were measured.

4.2.2.2 Release

The release, method adapted from (197), of tenofovir from cellulose ether solutions was found by creating 1 mL solutions of all 15 sample compounds containing 0.675% cellulose ether and 1% tenofovir to mirror the solubility study. This method was specifically chosen to isolate the differences in initial release from solutions caused by different cellulose ethers. A solution containing 1% tenofovir was selected as this was the concentration in the CAPRISA 004 study (199). 1 mL samples of these cellulose ether and tenofovir solutions were placed inside sealed membrane dialysis bags. These dialysis bags were then submerged in 20 mL of release medium (Milli Q water). The samples were incubated for 6 h at 37 °C and agitated at 60 rpm to allow the tenofovir to release from the solution, through the semi-permeable membrane, and into the release media. After this time the dialysis bags containing the cellulose ether solutions were removed from the release media. The release media were vortexed thoroughly to homogenize the concentration of tenofovir, and the released concentration was found using the HPLC system described below. Triplicate HPLC readings for each sample were measured.

4.2.2.3 HPLC Calibration

Concentrations of tenofovir in solution were measured using reverse phase HPLC with UV detection, method adapted from (240). The injection volume was maintained at 10 µL and all sample measurements were performed in triplicate. The mobile phase was water (pH 5.1) and acetonitrile (35:65 *v/v*) at a flow rate of 1 mL/min. The aqueous phase, water (pH 5.1), was prepared by adding 1 mL of trimethylamine to 1000 mL of water and adjusting the final pH using phosphoric acid (85%). Trimethylamine and phosphoric acid were added to the water to minimize peak tailing. Tenofovir was detected by UV absorbance measurement at 259 nm at ambient conditions (25 °C). Ten solutions containing different levels of tenofovir concentrations were selected to construct the calibration curve. The calibration curve was linear over the concentration range of 100 µg/mL to 2 µg/mL (Figure 4.1 below).

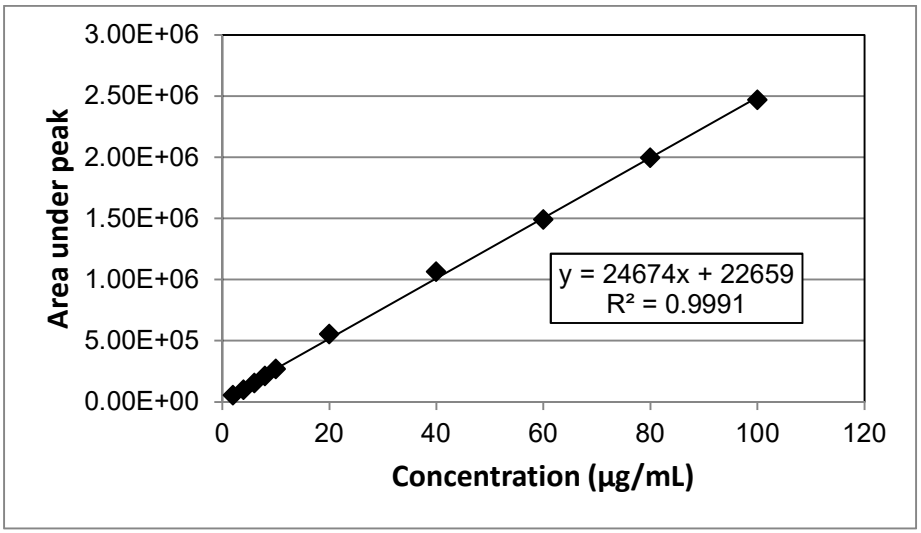

Figure 4.1: Calibration curve for calculation of concentration of tenofovir in solution using HPLC method. Each point represents the mean of triplicate measurements.

4.2.2.4 QSPR Generation

The solubility and release data were incorporated into a set of QSPRs (158). These QSPRs relate physical properties to the molecular topology of the cellulose ethers. In the present study the relevant physical properties are solubility concentration of tenofovir and mass of tenofovir released. The molecular topology of the cellulose compounds is represented by molecular structural descriptors. These descriptors include the average molecular weight and two zeroth-order connectivity indices described in the previous

two studies. The final correlations were produced using R statistical software (224), and evaluated for accuracy using r^2 and predictive quality using q^2 as described in Chapter 2. Linear and nonlinear dependence on the three structural properties, as well as interaction terms between the structural properties, were considered when generating QSPRs. The QSPRs with the best goodness of fit and cross-validation performance were identified from these possible correlations with the three structural descriptors.

4.2.2.5 Optimization Problem Formulation and Solution

The above described QSPRs were integrated along with QSPRs from previous rheology and biocompatibility studies into a predictive model. This predictive model was incorporated with the structural descriptors previously described into an optimization problem formulation. The current problem takes the form of a mixed-integer nonlinear program (MINLP) (241). This form arises because the selection structural side groups require integer decision variables, and some of the predictive QSPRs take nonlinear forms. The objective function of the problem formulation seeks to minimize the differences between the ideal target property values and the property values predicted by the QSPRs, as shown in Equation 4.1 below. This objective function depends upon the QSPR model as well as several structural feasibility constraints. In the current problem these constraints include a limiting molecular weight range, a limiting concentration range, and a limitation on the number of side chain substitutions to no more than three per glucose unit (except for HEC molecules, which can have longer side chain lengths).

$$\min z = \sum_i \frac{1}{P_i^{scale}} \left| P_i^{predicted} - P_i^{target} \right| \qquad \text{Equation 4.1}$$

where z is the objective function, $P_i^{predicted}$ is the property predicted by the QSPR, P_i^{target} is the ideal target property, and P_i^{scale} is a scalar to ensure that properties with very different values (e.g. consistency and shear-thinning) are scaled to the same values so one property does not dominate the optimization solution.

The above problem was solved using the deterministic solver DICOPT in the optimization software GAMS (242). This methodology has been used to solve CMD problems in the past (243, 244). Since the problem form is MINLP, there are many locally optimal solutions that are not necessarily the

global optimum. Solution of the optimization problem will result in one of these local optima. This means the most ideal structure will not necessarily be generated. However, the problem can be solved multiple times to generate many locally optimal solutions. This behavior is advantageous, however, because not all feasibility constraints are included in the problem formulation. Some, such as synthesis feasibility, may disqualify solution structures. The generation of multiple molecular structures helps ensure that an experimentally feasible molecule will be designed.

4.3 Results

In this section, the drug solubility and drug release results and trends are presented. The effects of molecular weight, substituent type, and MS/DS are presented. The section concludes with a presentation of the QSPRs generated from the correlation of these data with molecular structure.

4.3.1 Solubility

The solubility of tenofovir in all 15 cellulose ether solutions is shown in Figure 4.2 below. Further, a one-way ANOVA was performed to assess statistical differences between the cellulose ethers, with $p < 0.05$ considered significant. These data do indicate some differences in tenofovir solubility in aqueous solution due to cellulose ether molecular structure. The HECs have fairly constant solubility (approximately 2.7 mg/mL). The CMCs have markedly increased solubility (approximately 3.5 to 4.2 mg/mL) compared to the HECs. This indicates that charged CMC salts facilitate solubility of the hydrophilic tenofovir over polar, uncharged HECs. Further, the solubility increase proffered by the CMCs does seem to depend upon substitution effects since the solubility of tenofovir increases as the DS increases from 0.7 to 0.9 to 1.2. Both the HECs and CMCs do indicate a slight dependence upon molecular weight as there is a general trend among both substituent types that as molecular weight increases, solubility decreases.

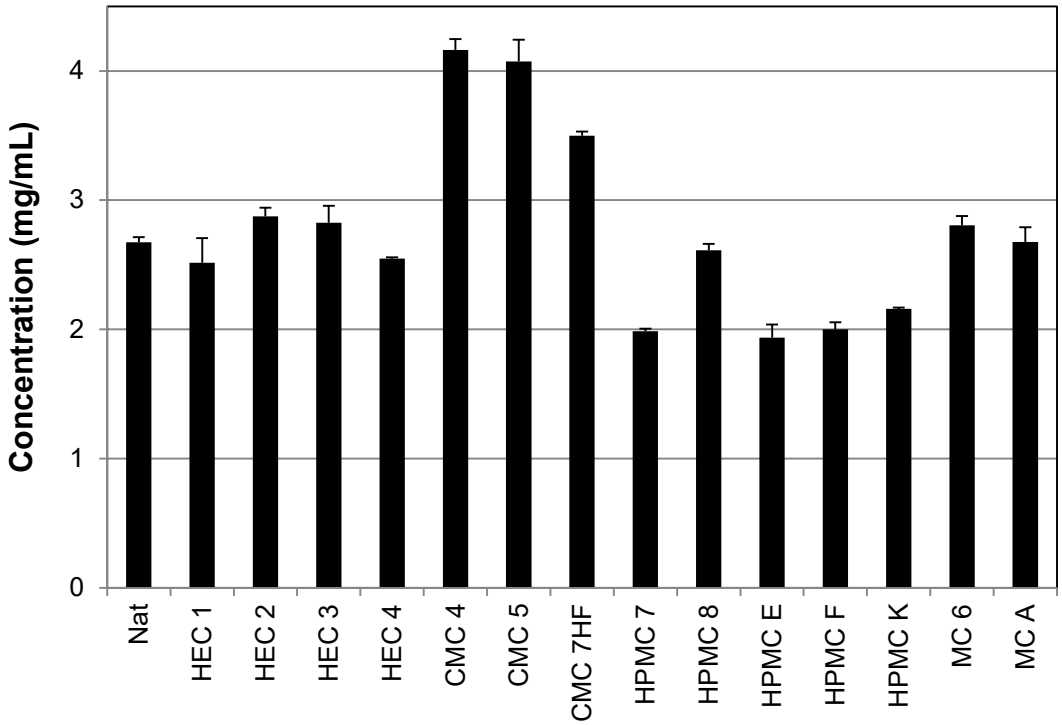

Figure 4.2: Solubility of tenofovir in 0.675% cellulose ether solutions. Bars represent means of triplicate measurements and error bars represent standard deviations.

The molecular structure effects are less clear for the MCs and HPMCs. The MCs have similar solubility compared to the HECs and exhibit just a slight decrease as the molecular weight increases from 40,000 to 86,000. Conversely, the HPMCs display a decrease in solubility (approximately 1.9 to 2.6 mg/mL) compared to the other cellulose ethers. These data are fairly consistent except for HPMC 8, which has a much higher solubility than the other HPMCs, and is comparable to the MCs and HECs. This is unexplained since HPMC 8 has a molecular structure identical to HPMC 7, though at a higher molecular weight, and a molecular structure very similar to HPMC E, which has the same molecular weight. In general, the cellulose ethers do reveal some differences in tenofovir solubility due to molecular structure. This difference appears to be primarily due to substituent type. The HPMCs on average have the lowest solubility, the MCs and HECs have similar, intermediate solubility, and the CMCs have the highest solubility, which increases as DS increases.

The results of the ANOVA reinforce these differences and trends. The CMCs had solubility that was significantly higher than all other compounds, and CMCs 4 and 5 were significantly higher than CMC 7HF. All the HECs and both MCs were significantly higher than HPMCs 7, E, F, and K (although not HPMC 8). Additionally, high solubility HECs 2 and 3 were significantly higher than low solubility HECs 1 and 4.

4.3.2 Release

The release of tenofovir from all 15 cellulose ether solutions is shown in Figure 4.3 below. Further, a one-way ANOVA was performed to assess statistical differences between the cellulose ethers, with $p < 0.05$ considered significant. These data do indicated some differences in amount of tenofovir released based on molecular structure, though the trends are quite different from those observed for the solubility. Conversely to the solubility data, which tended to decrease with molecular weight with the exception of the HPMCs, the release data does not appear to depend upon molecular weight. The HECs and MCs indicate a general trend of decreasing release with increasing molecular weight, while the CMCs and HPMCs have the opposite trend. There is no compelling reason for why this might be so, since in previous studies the HECs and CMCs tend to exhibit similarities in behavior while the HPMCs and MCs tend to be paired.

The results of the ANOVA reinforce these differences and trends. HPMC E had significantly higher release than all other compounds. The other HPMCs (with the exception of HPMC 7, which was significantly lower than all compounds) had significantly release than all the HECs, CMCs 4 and 5, and MC A. CMC 7HF and MC 6 had the same statistical significance as the HPMCs. CMCs 4 and 5 had significantly higher release than all the HECs, and MC A had higher release than all the HECs except HEC 3. Further, HECs 1 thru 4 had significantly higher release than Nat.

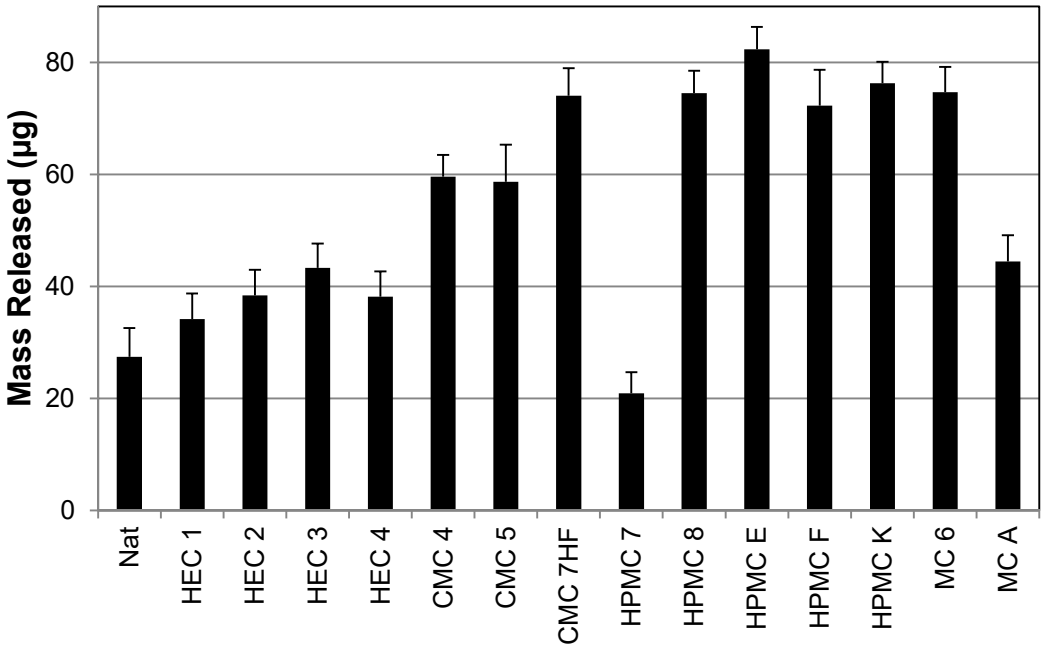

Figure 4.3: Release of tenofovir from cellulose ether solutions. Bars represent means of triplicate measurements and error bars represent standard deviations.

Once again, type of substituent group appears to be the most important structural factor influencing amount of tenofovir released. The HECs release the least tenofovir, while on average the CMCs release an intermediate amount, and the HPMCs and MCs release the most. There are a few exceptions to this trend, HPMC 7 and MC A. These data will be discussed more fully in the next section. There appears to be no compelling reason as to why they are substantially lower than the other HPMCs and MCs. MC A has the same molecular structure as MC 6 and the same molecular weight as HPMCs 8, E, F, and K. HPMC 7 has the same structure as HPMC 8 at a lower molecular weight. Although, as already pointed out, such a decrease in molecular weight did not impact any of the other compounds to such an extent. Overall, the data indicate a progression from least to most amount of tenofovir released as the substituent type changes from HEC to CMC to HPMC and MC. This trend becomes even clearer if the outlier points are disregarded.

4.3.3 QSPRs

The generation of QSPRs using the drug compatibility data began by considering the solubility data in Figure 4.2. These data did suggest several trends that imply a correlation between tenofovir

solubility and molecular structure. Type of substituent group seems to be the dominate effect. There is a large difference in solubility based on substituent group with CMCs displaying the highest solubility, HECs and MCs displaying a similar moderate solubility, and HPMCs displaying the lowest solubility. There also appears to be a slight inverse dependence of solubility on molecular weight. After the identification of these trends, a correlation was attempted.

Since there did not appear to be a clear power, exponential, or logarithmic dependence of tenofovir solubility on any of the molecular descriptors, a linear correlation was attempted. The descriptors included molecular weight and the two connectivity indices. The resulting correlation was fair, with and r^2 value of about 0.86. However, the correlation appeared to be skewed due to a clustering of data around similar solubility values. In particular, HPMCs 8, E, F, and K have the same molecular weight, similar connectivity indices values, and similar solubility values. For this reason the HPMCs with the same molecular weight were averaged, generating an average solubility and average connectivity indices. The data were then correlated again with one point replacing the four HPMC points. This improved the r^2 value to 0.92. This final correlation, labeled **s**, is shown in Table IV.I below, and the predictive model is illustrated in Figure 4.4. The q^2 value of 0.86 is fair, though not as high as for some of the previous correlations. This may be because three unique descriptors are used to describe solubility, rather than one combined parameter as seen in some previous QSPRs. A lower q^2 may imply some degree of correlation over-fit, but removing any of the descriptors did not improve this value. Still, this correlation is adequate for incorporation into the overall predictive model of the optimization problem.

The final correlation in the predictive model is generated from the tenofovir release data in Figure 4.3. Similar to the solubility data, these data did suggest trends relating amount of tenofovir released to the molecular structure of the cellulose ether. However, these trends appeared to depend solely on the identity of the substituent type. There was no consistent trend relating molecular weight to drug release. Instead, drug release increased as substituent type changed from HEC to CMC and finally to HPMC and MC. Given this progress, a correlation was attempted.

As always, a linear correlation was attempted first with the molecular weight and two connectivity indices serving as molecular descriptors. The resulting correlation was quite poor, with an r^2 value of 0.43. When the data was analyzed with this trend line the reason for this poor r^2 became apparent. As discussed in the section above, HPMC 7 and MC A appear to be exceptions from the major observed trends. This was even more apparent when the correlation was fit over the data. The rest of the data fit the trend line quite well while these two points were much too low. As already mentioned, there does not appear to be a compelling reason for why these points are so much lower. MC A is similar in structure to MC 6 and in molecular weight to HPMC 8, E, F, and K. all five of these compounds have similar release values. MC A is expected to have a value similar to these other five but is substantially lower. Further, HPMC 7 is much lower than the other HPMCs even though the structure is similar. In this case the molecular weight is much lower; however MC 6 has a low molecular weight and yet does not have a substantial decrease in amount of tenofovir release. For these reasons, these points were excluded from the final correlation. Further, MC 6 was excluded from the final correlation since there was no compelling reason why a high molecular weight MC has a low release value and a low molecular weight MC has a high release value. Thus the final correlation can only predict the structure of HECs, CMCs, and HPMCs with a molecular weight of 86,000 and above.

The final correlation relating cellulose ether molecular structure to tenofovir release, labeled **r**, is shown in Table IV.I below and Figure 4.5. By eliminating the two exceptions to trends, the r^2 value was increased to 0.94, a quite dramatic improvement. It should be noted that the final correlation depends solely upon ${}^0\chi$. The molecular weight and ${}^0\chi^V$ values did slightly improve the r^2 value, however when cross-validation was performed the q^2 value decreased when either of these descriptors was added to the correlation. This implies the correlation is over-fit with these values and is more robust with only one molecular descriptor. The improved q^2 value implies that a slightly less accurate correlation is much more predictive.

This last correlation will be incorporated with the solubility correlation and the QSPRs from previous studies to form an overall predictive model. In the Discussion section this predictive model will

be incorporated into an optimization problem formulation to design a microbicide formulation compound with ideal rheology, cytotoxicity, inhibition of *C. trachomatis*, solubility of tenofovir, and release of tenofovir.

Table IV.I: Final QSPRs for Solubility and Release Data. For **s** the HPMCs with molecular weight = 86,000 were averaged. For **r** the MCs and HPMC 7 were excluded.

Correlation	r^2	q^2
$\mathbf{s} = 3.109 - 2.901*10^{-7}\,\mathbf{MW} + 1.117\,{}^{0}\chi - 1.471\,{}^{0}\chi^{V}$	0.92	0.86
$\mathbf{r} = 193.6 - 11.93\,{}^{0}\chi$	0.94	0.92

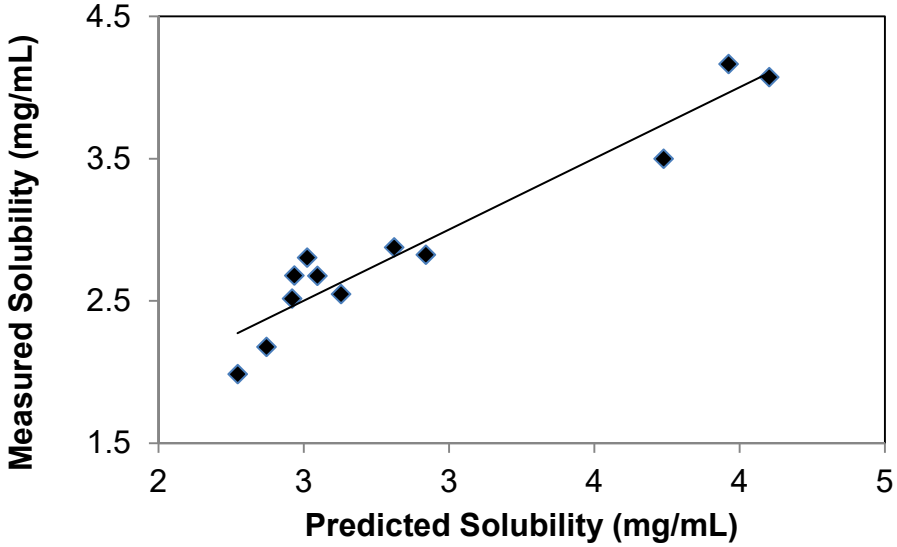

Figure 4.4: QSPR fitting solubility data to molecular structure.

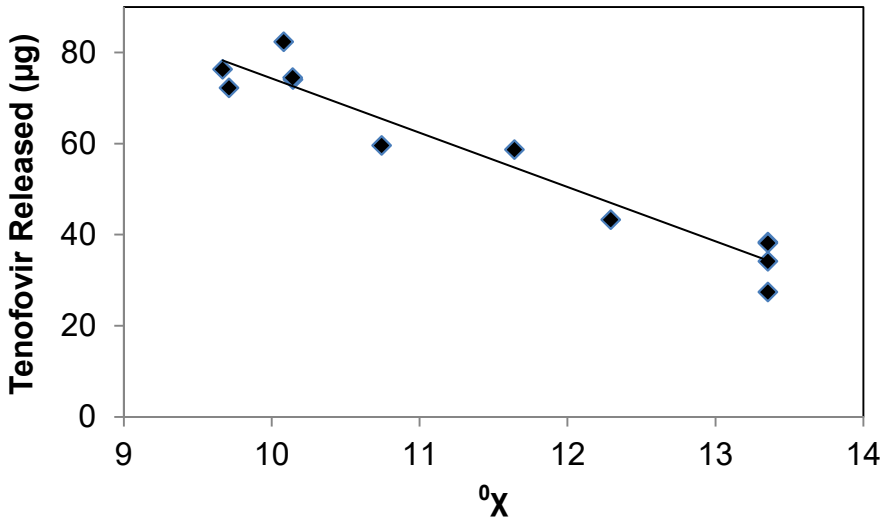

Figure 4.5: QSPR fitting release data to ${}^{0}\chi$.

4.4 Discussion

In this section the formulation and solution of the optimization problem are discussed. The final predictive model from the present and previous studies is summarized, including limitations to the QSPRs. This is incorporated into an optimization problem formulation, along with a set of structural constraints. Target properties are selected and the problem is solved to generate proposed novel candidate delivery vehicles structures.

4.4.1 Optimization Problem Formulation

The successful completion of the solubility and release studies generated a set of QSPRs to describe tenofovir compatibility behavior. These QSPRs join previously generated correlations from Chapter 2 describing rheological properties and correlations from Chapter 3 describing biocompatibility and inhibition of *C. trachomatis* to form the final predictive model for the optimization problem. This model is shown in Table IV.II below. There are three QSPRs that describe consistency (m), roughly divided by substituent group. There are two QSPRs that describe shear-thinning (n), again roughly divided by substituent group. A robust correlation with an acceptably high r^2 and q^2 value could not be generated using these connectivity indices to describe n for MCs and HPMCs. A single QSPR describes cytotoxicity, with the correlation relating average substituent group to average cytotoxicity. Two QSPRs describe inhibition of *C. trachomatis*, once again roughly divided by substituent group type. Finally, one QSPR each describes solubility of tenofovir in cellulose ether solution and release of tenofovir from solution. The release correlation excludes MCs and the low molecular weight HPMC since these data were not consistent with the trends established by the rest of the cellulose ethers as summarized in Sections 4.3.2 and 4.3.3. It should be noted there is an additional correlation describing the consistency behavior of MCs and HPMCs, which was not included in the previous rheology results in Chapter 2. That chapter focused on HECs and CMCs because they exhibited consistent, reproducible rheology results for all measured properties. Conversely, MCs and HPMCs did not have reproducible values for storage and loss modulus. Only their viscosity data was reproducible. For that reason these data were excluded from the detailed discussion of trends in Chapter 2 but the resulting correlation is included here.

Table IV.II: Final Predictive Model for Optimization Problem.

Correlation	r^2	q^2	Applicability
$\boldsymbol{m} = -367.1 + 4.355\text{x}10^{-7}(\mathbf{MW*C})^2 + 52.37\ {}^0\chi - 32.22\ {}^0\chi^V$	0.94	0.93	HECs & CMC 5
$\boldsymbol{m} = 1.7239\text{x}10^{-22}(\mathbf{MW*C*}{}^0\chi)^{4.6596}$	0.96	0.95	CMC 4 & 7HF
$\boldsymbol{m} = 2.126 - 2.796\text{x}10^{16}\ \mathbf{MW}^{-2.9} + 1.366\text{x}10^{6}\ \mathbf{C}^{2.4}$	0.99	0.92	HPMCs & MCs
$\boldsymbol{n} = 0.9291 - 3.862\text{x}10^{-7}\ \mathbf{MW} - 0.2903\ \mathbf{C} + 0.03714\ {}^0\chi - 0.04311\ {}^0\chi^V$	0.93	0.89	HECs & CMC 5
$\boldsymbol{n} = 1.583 - 1.338\text{x}10\text{-}6\ \mathbf{MW} - 1.154\ \mathbf{C}$	0.94	0.81	CMC 4 & 7HF
$\mathbf{cyto} = 0.04676\ {}^0\chi - 0.2871$	0.997	0.99	All*
$\mathbf{inh} = 0.001169(\mathbf{MW})^{0.4489}$	0.97	0.95	HECs & CMC 4, 7HF
$\mathbf{inh} = 0.07089(\mathbf{MW}/({}^0\chi*{}^0\chi^V))^{0.2454}$	0.95	0.94	MCs, HPMCs**, CMC 5
$\mathbf{s} = 3.109 - 2.901*10^{-7}\ \mathbf{MW} + 1.117\ {}^0\chi - 1.471\ {}^0\chi^V$	0.92	0.86	All**
$\mathbf{r} = 193.6 - 11.93\ {}^0\chi$	0.94	0.92	HECs, CMCs, HPMCs***

*QSPR was formed by averaging by substituent group. Thus the cytotoxicity values and ${}^0\chi$ values were averaged for HECs, CMCs, HPMCs, and MCs, resulting in a correlation with four average points.
**QSPR was formed by averaging HPMCs at MW=86,000. There were four such compounds that clustered around one point and sometimes skewed trends. Thus the ${}^0\chi$ values, ${}^0\chi^V$ values, and experimental data were averaged to generated one combined HPMC with MW=86,000.
***QSPR excludes MCs and HPMC 7.
****$\boldsymbol{m}$ = consistency, $\boldsymbol{n}$ = shear-thinning index, **cyto** = cytotoxicity, **inh** = inhibition of *C. trachomatis*, **s** = solubility, **r** = release

After the generation of the predictive model, the next step is to identify target values for all the physical properties measured. From Equation 4.1, the goal of the optimization problem is to minimize the difference between these target property values and property values predicted by the QSPRs. Table IV.III below shows these target values based on different patient groups and treatment arms. The target values for consistency and shear-thinning were taken from concurrent thin film flow experiments provided by a colleague in Dr. Sarah Kieweg's laboratory, Sunil Karri (245). Those computational models simulated thin film flow between elastic surfaces, analogous to the flow of a viscoelastic fluid in the human vagina. A parametric study was then performed on those results to identify the rheological properties that corresponded to ideal spreading behavior. For this current study two sets of target rheological properties were selected from those simulation results, corresponding to two ideal spreading behavior cases. In those simulations, an average vaginal length of 15 cm was assumed, along with a fluid application time of 100 sec. Further, women were grouped into different patient cases based on vaginal tissue elasticity. In particular, vaginal childbirth greatly reduces this elasticity (246). Nulliparous women, women who have never given birth, were assumed to have a vaginal elasticity of 50 kPa (247), while multiparous women,

women who had multiple vaginal births, were assumed to have a vaginal elasticity of 10 kPa (248). The corresponding target values for consistency and shear-thinning are in Table IV.III.

The other target properties are separated between microbicide and placebo formulations. All cases should strive to minimize cytotoxicity as close to 0% as possible. However, inhibition of *C. trachomatis* varies between microbicide and placebo. The delivery vehicle for the microbicide should ideally also non-specifically inhibit *C. trachomatis* infection, as close to 100% as possible. Conversely, the delivery vehicle placebo, which contains no API, should not inhibit HIV infection or any other STI. Thus the delivery vehicle placebo should have an inhibition rate as close to 0% as possible. Finally, for the microbicide delivery vehicle the solubility and release of tenofovir should be maximized. A value of 100 µg was chosen as the release target since this value was well above all the values observed experimentally in the above solubility study. A value of 1 mg/mL was chosen for the solubility because this was the solubility of the 1% tenofovir gel used in the partly successful CAPRISA 004 study (128). This solubility value was a minimum requirement and all solubility values predicted above that value were considered acceptable.

In all there were four different treatment cases. These corresponded to two treatment arms: microbicide formulation or placebo, and two patient cases: nulliparous or multiparous. Thus the four treatment cases are nulliparous microbicide, nulliparous placebo, multiparous microbicide, and multiparous placebo.

Table IV.III: Target Values for Optimization Problem.

Physical Property	Target Value	Comment
Consistency (*m*)	250-300 (275)*	Nulliparous Case
Consistency (*m*)	50-100 (75)*	Multiparous Case
Shear-thinning (*n*)	0.4-0.5 (0.45)*	Nulliparous Case
Shear-thinning (*n*)	0.9-1.0 (0.95)*	Multiparous Case
Cytotoxicity	0%	All Cases
Inhibition *C. trachomatis*	100%	Microbicide
Inhibition *C. trachomatis*	0%	Placebo
Tenofovir Solubility	Maximize (≥ 1 mg/mL)	Microbicide
Tenofovir Release	Maximize (100 µg)	Microbicide

*Values obtained from (245).

Finally, the above QSPRs and their corresponding target properties were incorporated into an optimization problem formulation. To complete the optimization problem, a number of structural feasibility constraints were included. The structural parameters include average molecular weight, solution concentration, type of substituent group, and amount of substitution. The limitations imposed upon these parameters are shown in Table IV.IV below. The molecular weight of the cellulose ethers depends upon the chain length of the cellulose raw material, and has an upper limit. The molecular weight was constrained within and slightly above the range of the model building set. The concentration range roughly represents the range used in the rheology studies. The type of substituent group is limited to the four that appear in the correlations. Finally, the amount of substitution was limited based on the type of substituent group. A cellulose strand with 10 glucose repeat units, corresponding to a total of 30 substitution sites, was used to model the substituent effects. Since carboxymethyl and methyl groups do not form side chains, the maximum number of substitutions for these groups was 30, while hydroxyethyl and hydroxypropyl, which can form side chains, have no upper limit. Additionally, a lower limit to side chain substitutions was established. This is because cellulose is insoluble in water, but becomes soluble at some threshold. This threshold (249) is different for each substituent type based on polarity and ionic nature, as shown in Table IV.IV below. With these values determined and incorporated into the problem formulation, the optimization problem can finally be solved to generate novel molecular structures.

Table IV.IV: Structural Feasibility Constraints.

Structural Property	Limiting Range
Average Molecular Weight	0-2,000,000 g/mol
Concentration	0.001-20%
Type of Substitution	Hydroxyethyl (or) Carboxymethyl (or) Methyl (and/or) Hydroxypropyl
Number of Substitutions: HEC	≥ 5
Number of Substitutions: CMC	$30 \geq CMC \geq 4$
Number of Substitutions: MC	$30 \geq MC \geq 12$
Number of Substitutions: HPMC	≥ 1

4.4.2 Optimization Problem Solution

The optimization problem was formulated to minimize Equation 4.1. It was subject to the QSPRs that form the property prediction model in Table IV.II, the target property values in Table IV.III, and the structural feasibility constraints in Table IV.IV. This problem takes the form of a mixed-integer nonlinear program (MINLP). This is because the property prediction model has both linear and non-linear QSPRs and the number of possible substituent groups of each type is an integer. This problem was written in GAMS software and solved using the DICOPT solver. Further, the code was separated into five different problem formulations based on type of substituent group, one for HECs, MCs, and HPMCs, and two for CMCs. This method is similar to one employed by Harper and Gani (250) who stipulated that for a MINLP problem in which the number of binary integers is small and can be enumerated, that a NLP problem can be solved for each set of binary variable values. The separation performed of the MINLP based on substituent type in this current dissertation lowers the integer decisions in the problem solution from two to one, allowing for more robust deterministic solution of the simplified MINLP problem.

Each of these problem formulations had a single QSPR from Table IV.II for each of consistency, shear-thinning, cytotoxicity, *C. trachomatis* inhibition, and tenofovir release for a total of five correlations. The appropriate QSPR for each property was selected to correspond to the substituent type of the problem formulation and was subject to the structural feasibility constraints unique to that substituent type. For example, the HEC problem formulation was subject to the first consistency, shear-thinning, and *C. trachomatis* inhibition QSPRs in Table IV as well as the overall cytotoxicity and release QSPRs. The number of substituent groups for the HECs was limited to ≥ 5.

This formulation scheme was repeated for the MCs and HPMCs and done twice for the CMCs since the data for these cellulose ether types are divided among two sets of QSPRs, with one predictive model for DS$\leq$0.9 and one predictive model for DS$\geq$1.2. The separation was carried out to allow for the generation of candidate molecular structures for each substituent type. Preliminary observations of the data gathered in the rheology, biocompatibility, and drug compatibility studies indicated that the HPMCs and MCs might dominate the solution space, since these compounds had lower cytotoxicity and higher release than the HECs and CMCs on average. Thus the separation of the problem formulation was carried

out to ensure the generation of candidate molecular structures for HECs, CMCs, HPMCs, and MCs for comparison purposes to verify if the assumption about the above trends in physical properties was indeed true.

The optimization problem formulations were solved multiple times for each substituent type. The best molecular candidates for each substituent type as well as the four possible treatment cases are reported in Table IV.V below. For this current optimization problem, the best structures are defined as those structures that have *m* and *n* values within the target ranges, solubility values above 1 mg/mL, and the lowest cytotoxicity values. Further, if the candidate structure is for the microbicide formulation it has the highest release and the highest *C. trachomatis* inhibition values. If the candidate molecule is for the placebo then it has the lowest *C. trachomatis* inhibition value. Structures that possessed values outside of the consistency and shear-thinning range presented in Table IV.III were rejected. Further, solubility was not included as a parameter in the optimization problem formulation. This was because solubility had a somewhat inverse relationship with release in that release increased as amount of substitution decreased while solubility tended to decrease. Release was deemed the more important property of the two. Thus solubility was used as a post-optimization check, and candidate structures with a predicted solubility ≤ 1 mg/mL were rejected.

Table IV.V: Candidate Molecular Structures for Novel Delivery Vehicles.

Delivery Vehicle for Nulliparous Microbicide					
Property	**HEC**	**CMC (≤0.9)**	**CMC (≥1.2)**	**HPMC**	**MC**
MW	1,486,000	868,000	1,572,000	1,000,000	1,000,000
c	1.92%	1.91%	1.58%	2.87%	2.87%
$^{0}\chi$	9.11	9.25	11.64	9.20	8.90
$^{0}\chi^{V}$	6.68	6.55	8.11	7.19	6.92
DS or MS	0.5 (MS)	0.4 (DS)	1.2 (DS)	0.1/1.2	1.2 (DS)
m	250	250	250	275	275
n	0.4	0.4	0.4	-	-
% inh	68.9%	54.1%	77.0%	75.2%	76.5%
% cyto	13.9%	36.1%	52.9%	14.3%	12.9%
r	84.9 µg	83.3 µg	54.7 µg	83.9 µg	-
s	3.03 mg/mL	3.55 mg/mL	3.72 mg/mL	2.51 mg/mL	2.58 mg/mL

Delivery Vehicle for Nulliparous Placebo					
Property	**HEC**	**CMC (≤0.9)**	**CMC (≥1.2)**	**HPMC**	**MC**

MW	1,223,000	791,000	1,309,000	13,700	13,700
c	2.49%	2.18%	2.07%	20%	20%
$^{0}\chi$	9.11	9.25	11.64	9.20	8.90
$^{0}\chi^{V}$	6.68	6.55	8.11	7.19	6.92
DS or MS	0.5 (MS)	0.4 (DS)	1.2 (DS)	0.1/1.2	1.2 (DS)
m	300	300	300	275	275
n	0.5	0.4	0.5	-	-
% inh	63.2%	51.9%	73.6%	26.2%	26.7%
% cyto	13.9%	36.1%	52.9%	14.3%	12.9%

Delivery Vehicle for Multiparous Microbicide					
Property	**HEC**	**CMC (≤0.9)**	**CMC (≥1.2)**	**HPMC**	**MC**
MW	110,000	490,000	251,000	1,000,000	1,000,000
c	12.9%	2.39%	5.00%	1.66%	1.66%
$^{0}\chi$	11.87	9.25	11.64	9.20	8.90
$^{0}\chi^{V}$	9.05	6.55	8.11	7.19	6.92
DS or MS	1.8 (MS)	0.4 (DS)	1.2 (DS)	0.1/1.2	1.2 (DS)
m	50	50	50	75	75
n	0.9	0.9	0.9	-	-
% inh	21.4%	41.9%	49.1%	75.2%	76.5%
% cyto	26.8%	36.1%	52.9%	14.3%	12.9%
r	52.0 µg	83.3 µg	54.7 µg	83.9 µg	-
s	3.02 mg/mL	3.66 mg/mL	4.10 mg/mL	2.51 mg/mL	2.58 mg/mL

Delivery Vehicle for Multiparous Placebo					
Property	**HEC**	**CMC (≤0.9)**	**CMC (≥1.2)**	**HPMC**	**MC**
MW	97,000	407,000	63,000	14,000	14,000
c	14.6%	3.35%	20%	20%	20%
$^{0}\chi$	11.87	9.25	11.64	9.20	8.90
$^{0}\chi^{V}$	9.05	6.55	8.11	7.19	6.92
DS or MS	1.8 (MS)	0.4 (DS)	1.2 (DS)	0.1/1.2	1.2 (DS)
m	50	100	50	75	75
n	0.9	1.0	0.9	-	-
% inh	20.2%	38.5%	30.8%	26.2%	26.7%
% cyto	26.8%	36.1%	52.9%	14.3%	12.9%

These candidate molecular structures reveal many intriguing trends that lead to suggestions for next generation delivery vehicles for both microbicides and their corresponding placebos. The physical properties had differing degrees of dependency on different molecular descriptors, facilitating a robust optimization. Both cytotoxicity and tenofovir release depended solely on substituent group, with cytotoxicity decreasing and release increasing with decreased substitution. Luckily, decreasing cytotoxicity while simultaneously increasing release were both target properties, so decreasing amount of

substitution synergistically improved these predicted properties. For this reason, all the candidate molecular structures (except HEC for the multiparous group) have the minimum degree of substitution allowed for each substituent type. These optimization results suggest that the most ideal microbicide delivery vehicles have the minimum allowable MS/DS values for solubility in the acidic microbicide formulation.

With both cytotoxicity and release influencing amount of substitution, molecular weight and concentration were the main descriptors varied to optimize consistency, shear-thinning, and *C. trachomatis* inhibition. Inhibition depended mainly, or for some substituent groups solely, on molecular weight. Thus in the constrained optimization problems, those that had QSPRs for both consistency and shear-thinning, the goal became to optimize molecular weight while keeping the rheological properties within their suggested ranges. Consistency increased with both molecular weight and concentration, while shear-thinning decreased as these parameters increased. These antagonist effects limited the acceptable range of concentration and molecular weight for the HECs and CMCs. For this reason the range of *C. trachomatis* was limited for these compounds. Conversely, since a predictive shear-thinning QSPR could not be generated, the MCs and HPMCs were unbound. Thus, to maximize inhibition for the microbicide delivery vehicle the molecular weight can be maximized to the limit of the allowable range while the concentration is lowered to maintain consistency at the proper value. To minimize inhibition for the placebo, the molecular weight can be lowered to the limit of the allowable range while the concentration is raised its limit. Based on this optimization behavior, the molecular weight of the MCs and HPMCs was restricted to 1,000,000 g/mol to allow for a more straight-forward comparison with the HEC and CMC candidate structures.

Analyzing all the candidate structures for all four treatment cases allows for recommendations to be made for next generation delivery vehicles. In particular, HPMCs appear to be the best candidates. These cellulose ethers exhibit low cytotoxicity and high release. Further, *C. trachomatis* inhibition of HPMCs can be varied by a large amount to create a microbicide with high inhibition and a placebo with low inhibition. This flexibility is allowed partly due to the inability to create a predictive QSPR

describing shear-thinning behavior. However, a parametric study performed by a colleague in Dr. Sarah Kieweg's laboratory, Dr. Md Rajib Anwar (251) of a spreading simulation similar to the one used to generated target consistency and shear-thinning values indicated that consistency is much more important than shear-thinning. That study indicated that shear-thinning can vary over most of the range between 0 and 1.0 without having much of an impact on spreading behavior. However, it should be noted that a Herschel-Bulkley fluid with a yield stress was used in that study instead of the power-law fluids used throughout this dissertation. Thus, shear-thinning might be negligible compared to consistency and yield stress in a Herschel-Bulkley fluid but shear-thinning might not be negligible compared to just consistency in a power-law fluid. Even with this limitation, the HEC and CMC optimization problems were repeated with the shear-thinning eliminated as a constraint. As in the case of the MCs and HPMCs, this allowed these problems to become unbound and percent inhibition could vary over a much greater range while consistency was maintained at its target value. Even with this much greater degree of freedom for all the cellulose ethers, HPMCs continued to have candidate structures with more ideal properties than the other substituent types.

As discussed above, CMCs are not recommended for use as either a microbicide or placebo formulation because of their higher cytotoxicity compared to the other substituent types. The lowest allowable CMC degree of substitution (DS=0.4) has a predicted cytotoxicity of 36%. This is not a high value, but the microbicide formulation ideally will be used with every sexual encounter, possibility multiple times per day, for years. A chronic low level cytotoxicity could irritate the vaginal epithelium, cause micro-abrasions, and facilitate entry of HIV and other STIs. This harm would invalidate any benefit of the formulation conferred by the API. Further, because CMCs 4 and 7HF have a steeper dependence upon molecular weight than the other cellulose ethers, the maximum allowable molecular weight to maintain the target consistency is lower, which in turn lowers *C. trachomatis* infection. CMC 5 does have a lower dependence upon molecular weight, allowing for larger molecular weight CMCs with much higher percent inhibition. However, these CMCs have a much higher DS and thus a much higher

cytotoxicity. This is an undesirable tradeoff, and thus CMCs should be avoided as vaginal delivery vehicles in favor of other cellulose ethers.

The removal of CMCs from consideration leaves the HECs, HPMCs, and MCs. The MCs are also removed from further consideration. Although MCs have slightly better *C. trachomatis* inhibition and solubility than comparable HPMCs, they do not exhibit predictable release behavior and thus cannot be optimized for with as high a degree of certainty as the other cellulose ethers. This leaves the HECs and HPMCs. Reviewing the nulliparous microbicide case in Table VII indicates that HECs and HPMCs have very similar ideal properties. For a similar range of consistency and shear-thinning values, HECs and HPMCs have very similar values of cytotoxicity, *C. trachomatis* inhibition, and release. Further, HECs have slightly higher tenofovir solubility. When HEC optimization is unconstrained by shear-thinning, the ideal properties for the other three treatment cases become very similar between the HECs and HPMCs. However, a closer inspection will reveal HECs have similar ideal properties to HPMCs because the optimization allowed them a greater range of molecular descriptors. Only by lowering the HECs to the theoretical limit of their solubility (MS=0.5) did the cytotoxicity, inhibition, and release values reach those of the HPMCs. The multiparous HEC with an MS closer to that observed in the model building set (MS=1.8) had much lower inhibition and release, and slightly higher cytotoxicity, when compared to the multiparous HPMC. Further, for the nulliparous case, the HEC only had comparable properties to the HPMC because the molecular weight was allowed to vary over a greater range. At a comparable molecular weight an HPMC has an inhibition of *C. trachomatis* approximately 20% higher than an HEC. Based on the predictive capability of the QSPR model and the cytotoxicity, HECs and HPMCs are preferable to MCs and CMCs. While both HECs and HPMCs are applicable as microbicide and placebo formulations, HPMCs are slightly more favorable.

4.5 Conclusions

The completion of this final study indicates the successful completion of a computational molecular design problem. This study successfully measure solubility and release of tenofovir in a model building set of cellulose ether compounds. These property data were successfully correlated with

molecular structure descriptors to create a predictive QSPR model that related the molecular structure of most cellulose ethers to drug compatibility. This predictive model was successfully combined with the predictive models from previous studies. Thus an overall predictive model was created that related molecular structure to rheology, biocompatibility, and drug compatibility. This overall predictive model was successfully integrated into an optimization problem formulation. Target properties were successfully identified based on the observations in the present studies and concurrent thin film flow studies. Structural feasibility constraints were obtained from literature sources and experimental observations from this and previous studies. These target properties and structural constraints were incorporated along with the QSPRs to generate the final optimization problem formulation. Finally, this optimization problem was solved in GAMS several times to create novel candidate microbicide and placebo structures for different groups of women.

The optimization problem was solved to generate many feasible molecular structures to serve as vaginal delivery vehicles. These candidates have predicted properties for a wide range of applicable microbicide properties. Many of the predicted structures have improved behavior compared to the currently used "Universal Placebo." In addition, the segregation and solution of the optimization problem by substituent type revealed several trends to inform future microbicide development. Minimizing MS/DS to the limit of solubility generally results in lower cytotoxicity and higher drug release. Increasing molecular weight increases *C. trachomatis* infection. One cellulose ether with a unique MS/DS can be selected for each treatment case. A high molecular weight can be selected for the raw material. The molecular weight can then be shortened to service both nulliparous and multiparous women. The molecular weight can be further shortened and the cellulose ether concentration can be increased to create a placebo with similar properties to the microbicide delivery vehicle except with lower *C. trachomatis* infection. The CMCs should be avoided for their higher cytotoxicity compared to the other cellulose ether types. HECs, HPMCs, and MCs are all acceptable delivery vehicles. However, MCs have less predictable behavior, and at comparable molecular weight and degree of substitution, HPMCs have more ideal

properties compared to HECs. Thus HPMCs are recommended for further evaluation and incorporation as delivery vehicles into next generation microbicides.

The success completion of this study serves to validate the use of computational molecular design to rationally design vaginal microbicide delivery vehicles. The techniques outline in this and the previous studies can be expanded. More physical properties, such as mucoadhesion can be considered to create an ever more robust optimization problem formulation. This allows for the generation of candidate microbicides with even more specific activity. This methodology can be used to design compatibility with other APIs or other tissue systems, such as rectal microbicides. Other cell cytotoxicities, drug solubility and release profiles, and non-specific inhibition of STIs can be correlated with molecular structure and incorporated into the present optimization problem formulation. This methodology can be repeated for a new model building set for a new class of delivery vehicles for vaginal, rectal, or dermal delivery. Finally, this CMD methodology can be expanded to other pharmaceutical fields to rationally design delivery vehicles and drugs for a wide array of purposes. By repeated solution of similar optimization problem formulations, properties that limit molecular structure can be identified, as was done in the present case. Critical molecular structure descriptor values can be identified. Additionally, the properties identified in the predictive model can be weighted differently to evaluate which are more important to ideal performance than others. These methods combined with high-throughput screening could lead to more streamlined and improved drug and formulation discover in the field of vaginal microbicides as well as other pharmaceutical fields.

Chapter 5

Discussions and Conclusions

There remains a pressing need for female-controlled prevention tools to protect against HIV/AIDS. Topical microbicides with "gel" delivery vehicles have undergone the most extensive characterization and clinical evaluations. They have also been responsible for some of the most significant failures in the field of microbicide clinical trials, whether by failing to prove efficacy or by causing outright harm. This indicates a need to establish a methodology to rationally design delivery vehicles with better understood and more ideal properties. An ideal microbicide must be safe to use, effective against HIV, and acceptable to the patient. A number of large scale clinical trials have failed to prove efficacy against HIV by failing to exhibit one or more of these characteristics. Thus these characteristics should be evaluated at the pre-clinical stages and next generation delivery vehicles should be designed to encompass all these properties. The present study considered several properties relating to these three necessary characteristics. Safety was described by *in vitro* cytotoxicity and inflammation. Efficacy was described by solubility of the microbicide, release of the microbicide, and non-specific inhibition of *C. trachomatis*. Patient acceptability was related to rheological properties. CMD was used to design candidate delivery vehicles that considered each of these properties when creating novel structures. The culmination of this entire study, including the rheology study in chapter 2, the biocompatibility and inhibition study in chapter 3, and the solubility and release study as well as optimization solution in chapter 4, represents the successful application of the CMD methodology to the field of topical vaginal microbicide "gels."

5.1 Discussion of Rheological Study

The study of rheological properties in chapter 2 sought to describe the rheology of a variety of delivery vehicles, restricted to cellulose ethers for the entirety of the whole study. Previous studies had looked a rheology of one or a few cellulose ethers, but none had compared such a large number of these compounds to each other. This study successfully measured the rheology of individual cellulose ethers at various concentrations. The data revealed intriguing trends relating these measured properties to

molecular weight, concentration, and substituent effects. Further, these trends provided insight that allowed for the successful generation of a set of nonlinear QSPRs that accurately predicted rheological behavior based on molecular structure. The completion of this first study was highly encouraging for the completion of the subsequent studies in that differences in physical properties were observed based on differences in identity of cellulose ether, and further that these differences could be numerically described.

Although the first rheology study was successful in both creating a predictive model describing rheological properties based on molecular structure and providing a framework for the other studies in chapters 3 and 4, analysis of this data did present several limitations. The first that must be mentioned is that rheology data for the HPMCs and MCs evaluated in the biocompatibility, inhibition, and drug compatibility studies are not presented in chapter 2. This is because no consistent storage and loss modulus data for the HPMCs and MCs could be measured. These data are obtained by performing oscillatory frequency sweeps at a constant stress in the linear viscoelastic regime over a range of frequencies. However, for the range of stresses measured by the instrumentation, the HPMCs and MCs did not exhibit a linear regime. Instead, these data took on a sigmoidal shape. Without a linear regime the results of these frequency sweeps varied widely depending on the stress chosen. For this reason the HPMC and MC rheology data were not presented in chapter 2 and the correlations for G' and G'' were excluded from the final optimization problem formulation in chapter 4. Further, concurrent thin film flow studies did not suggest ideal target values of G' or G'' to optimize for, providing another reason to exclude these correlations from the final optimization problem formulation. Thus the final QSPR model in chapter 4 cannot predict elastic behavior of cellulose ether solutions.

Another major limitation found in the rheology study in chapter 2 is that no single QSPR could be generated to a high degree of accuracy or predictive capability to describe all the cellulose ether solutions measured. The final rheological predictive model had to be divided into three correlations for consistency and two for shear-thinning according to side chain substituent type. Further, no correlation could be generated to describe the shear-thinning behavior of HPMCs and MCs according to their molecular

structure. Although this segregation of data represents a major limitation in the rheology study in chapter 2, it does reveal an interesting trend in rheological properties of cellulose ethers based on substituent type.

The rheological properties of all cellulose ether solutions increase nonlinearly to some power with molecular weight and concentration. However the steepness of this nonlinear variation differs greatly between HECs, CMCs, and HPMCs/MCs. The study in chapter 2 showed two distinct trends separating the HEC and CMC consistency data. The CMCs (excluding CMC 5) have a much steeper dependence upon molecular and concentration compared to the HECs. This means they have much higher consistency values at similar molecular weights and concentrations compared to the HECs. Although not shown, the HPMCs and MCs exhibit a trend separate from both the HEC and CMC trends. This HPMC/MC trends is even steeper than the other two trends, indicating an even greater consistency at comparable molecular weights and concentrations. The exception to these general trends is CMC 5, which exhibits rheology comparable to HECs instead of CMCs. This indicates there might yet be another factor besides identity of substituent type, molecular weight, and concentration of cellulose ether solutions that influences their rheology.

The need to segregate rheology data in order to create an accurate predictive model indicates the present molecular descriptors might not be wholly appropriate for the present optimization problem formulation. Future work should consider other molecular descriptors to describe the side chain substitutions to see if these more accurately describe differences in rheological properties based on molecular structure.

Even with these limitations, the successful completion of the rheology study provides useful data, trends, and a predictive model. This predictive model was incorporated into the final optimization study in chapter 4 to design candidate microbicides and placebos with target consistency and shear-thinning correlated with applicability to different patient populations. These data and this predictive model can be useful to many diverse pharmaceutical fields and industrial industries. The type of cellulose ether can be selected based on the desired range of rheological properties and the molecular weight and concentration can be varied to produce solutions with precisely desired consistency and shear-thinning behavior.

5.2 Discussion of Biocompatibility and Inhibition Study

The study of *in vitro* biocompatibility and inhibition in chapter 3 sought to describe the cytotoxicity, inflammation production, and *C. trachomatis* inhibition conferred by the set of cellulose ethers. Once again, previous studies had considered one or a few of these properties for microbicide APIs and one or a few delivery vehicles. However, extensive safety data for cellulose ethers was lacking, chiefly because as excipient compounds they are assumed biologically inert. This study successfully measured these properties for 15 cellulose ethers at constant concentration and the data revealed interesting trends that challenged this long held assumption. Further some of these data were incorporated into a set of QSPRs that predicted degree of cytotoxicity and inhibition of *C. trachomatis* based on identity or the molecular weight of the cellulose ether.

Although not all of the biocompatibility data exhibited enough variation to incorporate into a QSPR, the completion of this study was perhaps even more successful than the previous rheology study. Prior to completion of that study different cellulose ethers were known to have different rheological properties. However, cellulose ethers were assumed to have the same negligible biocompatibility and inhibition properties. Luckily for clinical applications this assumption proved true for inflammatory cytokine production. However, the cytotoxicity study indicated that some cellulose ethers, in particular the ionic CMCs, might cause some harm to native tissues. Further, the inhibition study indicated that different cellulose ethers confer different non-specific inhibition of *C. trachomatis* infection, highly correlated with increased molecular weight, which in turn is highly correlated with consistency.

The above described cytotoxicity and inhibition data were successfully incorporated into a set of accurate and predictive QSPRs that describe these properties based on molecular structure. These QSPRs were successfully integrated into a predictive model in the final optimization study in chapter 4 to generate candidate delivery vehicles with predicted cytotoxicity and inhibition. However, similar to the rheology study in chapter 2, these QSPRs had a number of limitations.

The first major limitation pertains to the cytotoxicity QSPR. The measured cytotoxicity data displayed no consistent variation due to changes in molecular weight or alterations in the MS/DS. The

only consistent difference exhibited by these data correlated with identity of substituent group. CMCs were more cytotoxic than HECs, which, on average, were more cytotoxic than HPMCs and MCs. The lack of correlation with molecular weight or MS/DS produced correlations with poor fit when all the data were considered separately. A highly predictive correlation could only be generated when the data based on substituent type were averaged. Thus cytotoxicities of the CMCs, HECs, HPMCs, and MCs were averaged and their molecular structure was represented by an average connectivity index to indicate each type of substituent group. This allowed for a correlation that could accurately predict the type of substituent for a given candidate cellulose ether, but not the required molecular weight or MS/DS or that cellulose ether.

Further, statistical analysis of the cytotoxicity data revealed that with the large standard deviations exhibited in the data, only differences of about 25% were statistically significant. This informs interpretation of the optimization problem. Candidate structures with cytotoxicity up to 25% are not statistically significantly different from zero cytotoxicity. Candidate structures with cytotoxicity values within 25% of each other are not statistically significantly different from each other. Thus only high cytotoxicity values, such as the 40-50% conferred by CMCs, are significant to the design of a novel candidate structures.

A second major limitation is the groupings required to generate a predictive QSPR model to describe *C. trachomatis* inhibition. These data could not be described in a single, accurate QSPR. Rather two QSPRs, one for all the HECs and CMCs 4 and 7HF and one for all the HPMCs, MCs, and CMC5, had to be generated. Further, while all the data was used for the HEC/CMC QSPR, for the remaining QSPR most of the HPMC data had to be averaged. This was because there were four HPMCs with the same molecular weight and similar connectivity indices values, comprising the only molecular descriptors available for generate of the QSPR. The cluster of four data points around one point skewed the correlation and lowered the accuracy. For this reason these points were averaged. This creates a correlation that can accurately predict the molecular weight and identity of a novel cellulose ether structure. However, it cannot accurately predict the exact MS/DS of a generated HPMC. The correlation

can indicate that the novel structure should be a HPMC, but not what the MS/DS should be. This adds an additional limitation to the scope of the optimization problem solutions.

Both cytotoxicity and inhibition are vital when designing a delivery vehicle and placebo for HIV microbicides. A harmful delivery vehicle could increase clinical trial failure by disrupting the vaginal epithelium and promoting viral penetration, invalidating any positive benefit conferred by the API. Conversely, a delivery vehicle that non-specifically inhibits *C. trachomatis*, an STI that once obtained significantly increases a patient's risk of HIV infection when exposed, could boost the efficacy of a microbicide, or cause clinical trial failure if the placebo is more effective against *C. trachomatis* than the microbicide delivery vehicle. These results provide promising trends that provide insights that future studies should expand upon. The marginal cytotoxic and inhibitory effects described in the study in chapter 3 might explain some of the resent clinical trial failures, such as cellulose sulfate, which used ionic cellulose as the API and exhibited harm in some clinical trial, and PRO 2000, which used a different delivery vehicle in the microbicide formulation and placebo.

5.3 Discussion of Solubility and Release Study

The study of drug compatibility properties in chapter 4 sought to describe the solubility of tenofovir in and release of tenofovir from the model building set of 15 cellulose ethers. Previous studies would consider the solubility and release of one or a few drugs in one or a few excipients. Extensive data of these properties was lacking for cellulose ethers. Most studies would select an API and delivery vehicle, measure the solubility and release, and report these values without trying to maximize either property. Such tactics are acceptable for water soluble drugs such as tenofovir, but prove challenging for other APIs with less hydrophilic behavior. This study provides a framework to assess these properties that can be expanded to other, more challenging APIs. This study successfully measured solubility and release for tenofovir in cellulose ethers at constant concentration. Once again, as seen in the previous studies in Chapters 2 and 3, these data provided interesting trends relating these properties to molecular structure. These data were successfully incorporated into a set of QSPRs that predicted solubility based on all molecular descriptors and release based on substituent type. These QSPRs served as the final portion of

the predictive model that was incorporated into the optimization problem formulation in the final study and solved to generate candidate delivery vehicles.

Both solubility and release were successfully correlated with molecular structure. Although this behavior had not been explicitly described in previous studies, some trends could be assumed based on molecular structure. In particular, more hydrophilic compounds such as CMCS and HECs were assumed to confer increased solubility to hydrophilic tenofovir compared to more hydrophobic HPMCs and MCs. In a related manner, the release behavior was assumed to be exactly the opposite of the solubility behavior as the hydrophilic compounds would resist releasing the hydrophilic API while the hydrophobic compounds would facilitate this process. The experimental results somewhat supported these hypotheses. In particular the CMC solubility was much higher than all the other compounds. The HECs were higher than most HPMCs, but were unexpectedly comparable to the MCs. In contrast, the release was the highest for the HPMCs (except HPMC 7). The HPMCs were higher than the CMCs (comparable to CMC 7HF) and the CMCs were higher than the HECs. This is not a complete inverse of the solubility as predicted. While the HPMCs had the lowest solubility and highest release, the CMCs had the highest solubility and intermediate, not the lowest, release.

The solubility and release data were successfully incorporated into accurate and predictive QSPRs that complemented predictive models from the studies in Chapters 2 and 3. However, once again these QSPRs had a number of significant limitations. All the data points were used to generate a linear correlation describing solubility data. Similar to the inhibition QSPR, the four HPMCs with the same molecular weight and similar MS/DS values had to be averaged to overcome the clustering at one point in the graph that lowered r^2. This solubility correlation can accurately predict molecular weight and substituent type. For HECs, CMCs, and MCs this correlation can accurately predict MS/DS as well. Due to the average for HPMCs, this correlation can only indicate that a candidate cellulose ether should be a HPMC and not what the exact MS/DS should be. This limitation restricts predictive capability of the final optimization problem solution.

A final major limitation pertains to the release QSPR. To generate an accurate and predictive QSPR using this data, some data points had to be omitted. In particular HPMC 7 and MC A were appreciably lower than the other HPMCs and MC. There was no structural basis for this behavior. Thus to ensure the generation of a robust QSPR these points were omitted from the final correlation. MC 6 was also omitted because there was no compelling reason to include this MC if the other was excluded. This resulted in a final release correlation that could accurately predict the MS/DS of HECs, CMCs, and HPMCs with a molecular weight of 86,000 and greater. However, this correlation could not predict HPMCs with a lower molecular weight and could not predict MCs at all. This created the major limitation that MCs could not be designed to have optimal release.

5.4 Discussion of Optimization Study

The final study in chapter 4 sought to incorporate all the QSPRs from the previous rheology, biocompatibility, inhibition, and drug compatibly studies into a final predictive QSPR model. This predictive model was incorporated, along with some structural feasibility constraints, into an optimization problem formulation and then successfully solved to generate novel cellulose ether candidate structures with ideal physical properties. By varying molecular weight, type of substituent group, MS/DS, and concentration, the above physical properties could be designed to have improved or even ideal target properties. The successful completion of this study validates the use of CMD methodology to rationally design next generation microbicide delivery vehicles.

The optimization problem was solved for four different treatment groups, including two different groups of women that required different rheological properties, and the microbicide delivery vehicle and placebo which require maximizing and minimizing inhibition, respectively. In all cases the optimization problem sought to minimize degree of substitution since doing so maximized both release and minimized cytotoxicity. With these two physical properties restricting the connectivity indices, target rheological properties were achieved by altering molecular weight and concentration.

By solving the optimization problem uniquely for each type of substituent group, interesting trends in the solution space were observed. In particular, CMCs were not ideal since they exhibited

significantly higher cytotoxicity than the other substituent group types. Attempting to minimize this cytotoxicity by reducing DS resulted in decreased tenofovir release compared to the other substituent group types, which was not ideal. MCs were also not ideal since the lack of their integration into the release QSPR restricted the predictive ability of the optimization solution. MCs could be designed for low cytotoxicity and inhibition which might make them desirable for placebo formulations. HECs and HPMCs both generated favorable delivery vehicle structures with comparable high release, high inhibition, and low cytotoxicity. One intriguing trend suggested that HPMCs were actually the most favorable delivery vehicles. At comparable molecular weights HPMCs higher inhibition of *C. trachomatis* compared to HECs. This implies for HPMCs that the DS could be lowered to the limit of cellulose ether solubility and the molecular weight could be maximized to maximize inhibition while the solution concentration is altered to maintain optimal rheological properties.

Another interesting trend was observed when comparing the nulliparous and multiparous candidate structures. These patient cases had the same target values for all physical properties except rheology. Specifically, multiparous structures had lower consistency and higher shear-thinning indices compared to nulliparous structures. Observing the nulliparous and multiparous microbicide cases reveals the impact changing viscosity has on the other physical properties. These viscosity parameters depend heavily on molecular weight and concentration. Cytotoxicity and release depend mainly on substituent type and MS/DS and are thus very similar for both the nulliparous and multiparous cases. However, inhibition of *C. trachomatis* depends heavily on molecular weight and thus changes a great deal with changing consistency. Thus formulations with higher consistency have higher *C. trachomatis* inhibition. This could be a useful correlation to exploit, especially if consistency and shear-thinning indices could be adjusted while maintaining similar spreading behavior. Thus a microbicide formulation could be developed with a higher consistency to have higher inhibition of *C. trachomatis*. Conversely, a placebo formulation could have a lower consistency to have lower inhibition of *C. trachomatis* while maintaining similar spreading behavior to the microbicide formulation.

This optimization problem does have number of limitations that limit its predictive capability. The restrictions on the QSPRS generated in Chapters 2, 3, and 4 apply and limit how accurately some types of cellulose ethers can be predicted. In particular, several correlations predict that a cellulose ether should be a HPMC but do not predict its exact MS/DS since these correlations were generated using average HPMC values with average connectivity indices. As discussed above, a major limitation is that the release behavior of MCs cannot be predicted and thus these cellulose ethers cannot be fully evaluated for the prediction of a delivery vehicle, although they can accurately predict a placebo.

As described in Chapter 3, the cytotoxicity correlation is only an average for each substituent group. This correlation can predict cytotoxicity based on the identity of the cellulose ether but cannot be used to design for specific MS/DS. This correlation instructs the optimization problem to minimize cytotoxicity by minimizing a connectivity index and thus minimizing MS/DS. However, this correlation does not accurately correlate to MS/DS. Thus the predicted structures in Chapter 4 with low cytotoxicity due to low MS/DS might in reality have slightly higher cytotoxicity values.

A final major limit is due to the fact that the shear-thinning correlations could be generated from the HEC and CMC data, but not the HPMC and MC data. This is of particular concern because when solving the optimization problem the antagonistic molecular weight and concentration behavior of the consistency and shear-thinning correlations provided bounds to the HEC and CMC data. These compounds could not maximize or minimize their molecular weights or MS/DS to the limits of feasibility and maintain consistency and shear-thinning values within the recommended range. This placed limitations on the possible HEC and CMC candidate structures that were not placed upon the HPMCs and MCs.

Even with the above limitations, the successful solution of the optimization problem formulation did generate candidate molecular structures with more ideal properties than those exhibited by the model building set, including the “universal placebo.” This allows for the rational design of new cellulose ethers to create improved delivery vehicles and a better placebo. If the shear-thinning requirement can be relaxed, the current optimization problem suggested a high molecular weight HPMC with low

concentration and low MS/DS would serve as an optimal delivery vehicle for both nulliparous and multiparous women. An HPMC with the same MS/DS but low molecular weight and high concentration would serve as an optimal placebo in both cases. If this requirement is not relaxed, then HPMCs and MCs must be excluded from the design space. This leaves CMCs and HECs. CMCs have unfavorable cytotoxicity, so only HECs can be considered when designing an optimal delivery vehicle, as is used in the "universal placebo." Even so, the current predictive model and optimization problem formulation can identify the molecular weight, MS, and concentration of an ideal HEC delivery vehicle. That ideal delivery vehicle will improve upon the HECs currently in use in microbicide formulations.

6.0 References

1. Fauci AS. 25 years of HIV. Nature. 2008;453(7193):289-90.
2. World Health Organization. World Health Report 1999: Making a Difference. Geneva, Switzerland: WHO; 1999.
3. Joint United Nations Programme on HIV/AIDS (UNAIDS). How AIDS changed everything. Geneva, Switzerland: UNAIDS. 2015.
4. Glynn JR, Caraël M, Auvert B, Kahindo M, Chege J, Musonda R, et al. Why do young women have a much higher prevalence of HIV than young men? A study in Kisumu, Kenya and Ndola, Zambia. AIDS. 2001;15:S51-S60.
5. Simbayi L, Shisana O, Rehle T, Onoya D, Jooste S, Zungu N, et al. South African national HIV prevalence, incidence and behaviour survey, 2012. Pretoria: Human Sciences Research Council. 2014.
6. Joint United Nations Programme on HIV/AIDS (UNAIDS). Global Report: UNAIDS Report on the Global AIDS Epidemic 2013. Geneva, Switzerland: UNAIDS. 2013.
7. Dellar RC, Dlamini S, Karim QA. Adolescent girls and young women: key populations for HIV epidemic control. Journal International AIDS Society. 2015;18(Suppl 1):19408.
8. Siegfried N, Muller M, Deeks JJ, Volmink J. Male circumcision for prevention of heterosexual acquisition of HIV in men. Cochrane Database System Review. 2009;2.
9. Wodak A, Cooney A, WHO. Effectiveness of sterile needle and syringe programming in reducing HIV/AIDS among injecting drug users. Geneva, Switzerland: WHO. 2004.
10. MacArthur GJ, Minozzi S, Martin N, Vickerman P, Deren S, Bruneau J, et al. Opiate substitution treatment and HIV transmission in people who inject drugs: systematic review and meta-analysis. 2012.
11. Cohen MS, Chen YQ, McCauley M, Gamble T, Hosseinipour MC, Kumarasamy N, et al. Prevention of HIV-1 infection with early antiretroviral therapy. New England Journal of Medicine. 2011;365(6):493-505.
12. Weller S, Davis K. Condom effectiveness in reducing heterosexual HIV transmission. Cochrane Database System Review 2002;1(1).
13. Adetunji J, Meekers D. Consistency in condom use in the context of HIV/AIDS in Zimbabwe. Journal of Biosocial Science. 2001;33(01):121-38.
14. Campbell JC, Baty M, Ghandour RM, Stockman JK, Francisco L, Wagman J. The intersection of intimate partner violence against women and HIV/AIDS: a review. International Journal of Injury Control and Safety Promotion. 2008;15(4):221-31.
15. Mmari K, Sabherwal S. A review of risk and protective factors for adolescent sexual and reproductive health in developing countries: an update. Journal of Adolescent Health. 2013;53(5):562-72.
16. Shannon K, Strathdee SA, Goldenberg SM, Duff P, Mwangi P, Rusakova M, et al. Global epidemiology of HIV among female sex workers: influence of structural determinants. The Lancet. 2015;385(9962):55-71.
17. Zembe YZ, Townsend L, Thorson A, Silberschmidt M, Ekstrom AM. Intimate partner violence, relationship power inequity and the role of sexual and social risk factors in the production of violence among young women who have multiple sexual partners in a peri-urban setting in South Africa. PloS One. 2015;10(11):e0139430.
18. Ochieng-Ooko V, Ochieng D, Sidle JE, Holdsworth M, Wools-Kaloustian K, Siika AM, et al. Influence of gender on loss to follow-up in a large HIV treatment programme in western Kenya. Bulletin of the World Health Organization. 2010;88(9):681-8.
19. das Neves J, Sarmento B. Drug Delivery and Development of Anti-HIV Microbicides: CRC Press; 2014.
20. Abdool Karim Q, Baxter C, Abdool Karim S. Microbicides and their potential as a catalyst for multipurpose sexual and reproductive health technologies. BJOG: An International Journal of Obstetrics & Gynaecology. 2014;121(s5):53-61.
21. Ariën KK, Jespers V, Vanham G. HIV sexual transmission and microbicides. Reviews in Medical Virology. 2011;21(2):110-33.

22. Stone A. Microbicides: a new approach to preventing HIV and other sexually transmitted infections. Nature Reviews Drug Discovery. 2002;1(12):977-85.
23. Lederman MM, Offord RE, Hartley O. Microbicides and other topical strategies to prevent vaginal transmission of HIV. Nature Reviews Immunology. 2006;6(5):371-82.
24. McGowan I. Rectal microbicides: can we make them and will people use them? AIDS and Behavior. 2011;15(1):66-71.
25. Friend DR, Clark JT, Kiser PF, Clark MR. Multipurpose prevention technologies: Products in development. Antiviral Research. 2013;100:S39-S47.
26. Spreen WR, Margolis DA, Pottage Jr JC. Long-acting injectable antiretrovirals for HIV treatment and prevention. Current Opinion in HIV and AIDS. 2013;8(6):565-71.
27. Andrews CD, Yueh YL, Spreen WR, Bernard LS, Boente-Carrera M, Rodriguez K, et al. A long-acting integrase inhibitor protects female macaques from repeated high-dose intravaginal SHIV challenge. Science Translational Medicine. 2015;7(270):270ra4-ra4.
28. McGowan I, Siegel A, Duffill K, Shetler C, Dezzutti C, Richardson-Harman N, et al. A phase 1 open label safety, acceptability, pharmacokinetic, and pharmacodynamic study of intramuscular TMC278 LA (the MWRI-01 Study). AIDS Research and Human Retroviruses. 2014;30(S1):A71-A.
29. Amiji MM, Vyas TK, Shah LK. Role of nanotechnology in HIV/AIDS treatment: potential to overcome the viral reservoir challenge. Discovery Medicine. 2009;6(34):157-62.
30. Baert L, van‘t Klooster G, Dries W, François M, Wouters A, Basstanie E, et al. Development of a long-acting injectable formulation with nanoparticles of rilpivirine (TMC278) for HIV treatment. European Journal of Pharmaceutics and Biopharmaceutics. 2009;72(3):502-8.
31. Winner B, Peipert JF, Zhao Q, Buckel C, Madden T, Allsworth JE, et al. Effectiveness of long-acting reversible contraception. New England Journal of Medicine. 2012;366(21):1998-2007.
32. Shoupe D, Mishell DR. Norplant: subdermal implant system for long-term contraception. American Journal of Obstetrics and Gynecology. 1989;160(5):1286-92.
33. Gunawardana M, Remedios-Chan M, Miller CS, Fanter R, Yang F, Marzinke MA, et al. Pharmacokinetics of Long-acting Tenofovir Alafenamide (GS-7340) Subdermal Implant for HIV Prophylaxis. Antimicrobial Agents and Chemotherapy. 2015:AAC. 00656-15.
34. Major I, Boyd P, Kilbourne-Brook M, Saxon G, Cohen J, Malcolm RK. A modified SILCS contraceptive diaphragm for long-term controlled release of the HIV microbicide dapivirine. Contraception. 2013;88(1):58-66.
35. Zaveri T, Hayes JE, Ziegler GR. Release of tenofovir from carrageenan-based vaginal suppositories. Pharmaceutics. 2014;6(3):366-77.
36. D'Cruz OJ, Samuel P, Waurzyniak B, Uckun FM. Development and evaluation of a thermoreversible ovule formulation of stampidine, a novel nonspermicidal broad-spectrum anti-human immunodeficiency virus microbicide. Biology of Reproduction. 2003;69(6):1843-51.
37. Malcolm RK, Fetherston SM, McCoy CF, Boyd P, Major I. Vaginal rings for delivery of HIV microbicides. International Journal of Women's Health. 2012;4:595-605.
38. Ahrendt H-J, Nisand I, Bastianelli C, Gómez MA, Gemzell-Danielsson K, Urdl W, et al. Efficacy, acceptability and tolerability of the combined contraceptive ring, NuvaRing, compared with an oral contraceptive containing 30 µg of ethinyl estradiol and 3 mg of drospirenone. Contraception. 2006;74(6):451-7.
39. Chen J, Wu S, Shao W, Zou M, Hu J, Cong J, et al. The comparative trial of TCu 380A IUD and progesterone-releasing vaginal ring used by lactating women. Contraception. 1998;57(6):371-9.
40. Brache V, Alvarez-Sanchez F, Faundes A, Jackanicz T, Mishell DR, Lähteenmäki P. Progestin-only contraceptive rings. Steroids. 2000;65(10):687-91.
41. Henriksson L, Stjernquist M, Boquist L, Cedergren I, Selinus I. A one-year multicenter study of efficacy and safety of a continuous, low-dose, estradiol-releasing vaginal ring (Estring) in postmenopausal women with symptoms and signs of urogenital aging. American Journal of Obstetrics and Gynecology. 1996;174(1):85-92.

42. Speroff L. Efficacy and tolerability of a novel estradiol vaginal ring for relief of menopausal symptoms. Obstetrics & Gynecology. 2003;102(4):823-34.
43. Malcolm RK, Edwards K-L, Kiser P, Romano J, Smith TJ. Advances in microbicide vaginal rings. Antiviral Research. 2010;88:S30-S9.
44. Malcolm RK, Boyd PJ, McCoy CF, Murphy DJ. Microbicide vaginal rings: Technological challenges and clinical development. Advanced Drug Delivery Reviews. 2016.
45. Fetherston S, McCoy C, Murphy D, Boyd P, Brimer A, Holt J, et al. Formulation Development of a Combination Silicone Elastomer Ring for Vaginal Delivery of Dapivirine and Levonorgestrel. AIDS Research and Human Retroviruses. 2014;30(S1):A138-A.
46. Clark MR, Johnson TJ, Mccabe RT, Clark JT, Tuitupou A, Elgendy H, et al. A hot-melt extruded intravaginal ring for the sustained delivery of the antiretroviral microbicide UC781. Journal of Pharmaceutical Sciences. 2012;101(2):576-87.
47. Chen BA, Panther L, Marzinke MA, Hendrix CW, Hoesley CJ, Van Der Straten A, et al. Phase 1 safety, pharmacokinetics, and pharmacodynamics of dapivirine and maraviroc vaginal rings: a double-blind randomized trial. Journal of Acquired Immune Deficiency Syndromes. 2015;70(3):242-9.
48. Devlin B, Nuttall J, Wilder S, Woodsong C, Rosenberg Z. Development of dapivirine vaginal ring for HIV prevention. Antiviral Research. 2013;100:S3-S8.
49. Baeten JM, Palanee-Phillips T, Brown ER, Schwartz K, Soto-Torres LE, Govender V, et al. Use of a vaginal ring containing dapivirine for HIV-1 prevention in women. New England Journal of Medicine. 2016.
50. Karim SSA, Karim QA. Antiretroviral prophylaxis: a defining moment for HIV prevention. The Lancet. 2011;378(9809):e23.
51. Smith DK, Thigpen MC, Nesheim SR, Lampe M, Paxton L, Samandari T. Interim guidance for clinicians considering the use of preexposure prophylaxis for the prevention of HIV infection in heterosexually active adults.Morbidity and Mortality Weekly Report. 2012;61(31):586-9.
52. Grant RM, Lama JR, Anderson PL, McMahan V, Liu AY, Vargas L, et al. Preexposure chemoprophylaxis for HIV prevention in men who have sex with men. New England Journal of Medicine. 2010;363(27):2587-99.
53. Baeten J, Celum C, editors. Antiretroviral pre-exposure prophylaxis for HIV-1 prevention among heterosexual African men and women: the Partners PrEP Study. 6th IAS Conference on HIV Pathogenesis, Treatment and Prevention; 2011: IAS Rome.
54. Kibengo FM, Ruzagira E, Katende D, Bwanika AN, Bahemuka U, Haberer JE, et al. Safety, adherence and acceptability of intermittent tenofovir/emtricitabine as HIV pre-exposure prophylaxis (PrEP) among HIV-uninfected Ugandan volunteers living in HIV-serodiscordant relationships: a randomized, clinical trial. PLoS One. 2013;8(9):e74314.
55. Mantell JE, Myer L, Carballo-Dieguez A, Stein Z, Ramjee G, Morar NS, et al. Microbicide acceptability research: current approaches and future directions. Social Science & Medicine. 2005;60(2):319-30.
56. Morris GC, Wiggins RC, Woodhall SC, Bland JM, Taylor CR, Jespers V, et al. MABGEL 1: First Phase 1 Trial of the Anti-HIV-1 Monoclonal Antibodies 2F5, 4E10 and 2G12 as a Vaginal Microbicide. PloS One. 2014;9(12):e116153.
57. Grammen C, Ariën KK, Venkatraj M, Joossens J, Van der Veken P, Heeres J, et al. Development and in vitro evaluation of a vaginal microbicide gel formulation for UAMC01398, a novel diaryltriazine NNRTI against HIV-1. Antiviral Research. 2014;101:113-21.
58. Feldblum PJ, Adeiga A, Bakare R, Wevill S, Lendvay A, Obadaki F, et al. SAVVY vaginal gel (C31G) for prevention of HIV infection: a randomized controlled trial in Nigeria. PloS One. 2008;3(1):e1474.
59. Rupp R, Rosenthal SL, Stanberry LR. VivaGel™(SPL7013 Gel): A candidate dendrimer–microbicide for the prevention of HIV and HSV infection. International Journal of Nanomedicine. 2007;2(4):561.

60. Nel AM, Coplan P, van de Wijgert JH, Kapiga SH, von Mollendorf C, Geubbels E, et al. Safety, tolerability, and systemic absorption of dapivirine vaginal microbicide gel in healthy, HIV-negative women. AIDS. 2009;23(12):1531-8.
61. Veazey RS, Ketas TJ, Dufour J, Moroney-Rasmussen T, Green LC, Klasse P, et al. Protection of rhesus macaques from vaginal infection by vaginally delivered maraviroc, an inhibitor of HIV-1 entry via the CCR5 co-receptor. Journal of Infectious Diseases. 2010;202(5):739-44.
62. Das Neves J, Bahia M. Gels as vaginal drug delivery systems. International Journal of Pharmaceutics. 2006;318(1):1-14.
63. Manson KH, Wyand MS, Miller C, Neurath AR. Effect of a cellulose acetate phthalate topical cream on vaginal transmission of simian immunodeficiency virus in rhesus monkeys. Antimicrobial Agents and Chemotherapy. 2000;44(11):3199-202.
64. Zhang W, Hu M, Shi Y, Gong T, Dezzutti CS, Moncla B, et al. Vaginal Microbicide Film Combinations of Two Reverse Transcriptase Inhibitors, EFdA and CSIC, for the Prevention of HIV-1 Sexual Transmission. Pharmaceutical Research. 2015:1-13.
65. Akil A, Agashe H, Dezzutti CS, Moncla BJ, Hillier SL, Devlin B, et al. Formulation and Characterization of Polymeric Films Containing Combinations of Antiretrovirals (ARVs) for HIV Prevention. Pharmaceutical Research. 2015;32(2):458-68.
66. Akil A, Parniak MA, Dezzutti CS, Moncla BJ, Cost MR, Li M, et al. Development and characterization of a vaginal film containing dapivirine, a non-nucleoside reverse transcriptase inhibitor (NNRTI), for prevention of HIV-1 sexual transmission. Drug Delivery and Translational Research. 2011;1(3):209-22.
67. Ham AS, Rohan LC, Boczar A, Yang L, Buckheit KW, Buckheit Jr RW. Vaginal film drug delivery of the pyrimidinedione IQP-0528 for the prevention of HIV infection. Pharmaceutical Research. 2012;29(7):1897-907.
68. Sassi A, Cost M, Cole A, Cole A, Patton D, Gupta P, et al. Formulation development of retrocyclin 1 analog RC-101 as an anti-HIV vaginal microbicide product. Antimicrobial Agents and Chemotherapy. 2011;55(5):2282-9.
69. Huang C, Soenen SJ, van Gulck E, Vanham G, Rejman J, Van Calenbergh S, et al. Electrospun cellulose acetate phthalate fibers for semen induced anti-HIV vaginal drug delivery. Biomaterials. 2012;33(3):962-9.
70. Nel AM, Mitchnick LB, Risha P, Muungo LTM, Norick PM. Acceptability of vaginal film, soft-gel capsule, and tablet as potential microbicide delivery methods among African women. Journal of Women's Health. 2011;20(8):1207-14.
71. Pereira LE, Clark MR, Friend DR, Garber DA, McNicholl JM, Hendry RM, et al. Pharmacokinetic and safety analyses of tenofovir and tenofovir-emtricitabine vaginal tablets in pigtailed macaques. Antimicrobial Agents and Chemotherapy. 2014;58(5):2665-74.
72. Joshi S, Dutta S, Kumar B, Katti U, Kulkarni S, Risbud A, et al. Expanded safety study of Praneem polyherbal vaginal tablet among HIV-uninfected women in Pune, India: a phase II clinical trial report. Sexually Transmitted Infections. 2008;84(5):343-7.
73. Mcconville C, Friend DR, Clark MR, Malcolm K. Preformulation and development of a once-daily sustained-release tenofovir vaginal tablet tablet containing a single excipient. Journal of Pharmaceutical Sciences. 2013;102(6):1859-68.
74. Garg S, Goldman D, Krumme M, Rohan LC, Smoot S, Friend DR. Advances in development, scale-up and manufacturing of microbicide gels, films, and tablets. Antiviral Research. 2010;88:S19-S29.
75. Mauck CK, Allen S, Baker JM, Barr SP, Abercrombie T, Archer DF. An evaluation of the amount of nonoxynol-9 remaining in the vagina up to 4 h after insertion of a vaginal contraceptive film (VCF®) containing 70 mg nonoxynol-9. Contraception. 1997;56(2):103-10.
76. Nelfinavir mesylate Agouron. New Antimicrobial Agents Approved by the US Food and Drug Administration in 1997 and New Indications for Previously Approved Agents. 1998.
77. Mehta HK. A new use of KY jelly as a gonioscopy fluid. British Journal of Ophthalmology. 1984;68(10):765-7.

78. Cutler B, Justman J. Vaginal microbicides and the prevention of HIV transmission. The Lancet Infectious Diseases. 2008;8(11):685-97.
79. Weber J, Desai K, Darbyshire J, Programme MD. The development of vaginal microbicides for the prevention of HIV transmission. PLoS Medicine. 2005;2(5):e142.
80. Gilliam ML, Derman RJ. Barrier methods of contraception. Obstetrics and Gynecology Clinics of North America. 2000;27(4):841-58.
81. Hicks D, Martin L, Getchell J, Heath J, Francis D, Mcdougal JS, et al. Inactivation of HTLV-III/LAV-infected cultures of normal human lymphocytes by nonoxynol-9 in vitro. The Lancet. 1985;326(8469):1422-3.
82. Bourinbaiar A, Fruhstorfer E. The efficacy of nonoxynol-9 from an in vitro point of view. AIDS. 1996;10(5):558-9.
83. Miller C, Alexander N, Gettie A, Hendrickx A, Marx P. The effect of contraceptives containing nonoxynol-9 on the genital transmission of simian immunodeficiency virus in rhesus macaques. Fertility and Sterility. 1992;57(5):1126-8.
84. Kreiss J, Ngugi E, Holmes K, Ndinya-Achola J, Waiyaki P, Roberts PL, et al. Efficacy of nonoxynol 9 contraceptive sponge use in preventing heterosexual acquisition of HIV in Nairobi prostitutes. Jama. 1992;268(4):477-82.
85. Roddy RE, Zekeng L, Ryan KA, Tamoufe U, Weir SS, Wong EL. A controlled trial of nonoxynol 9 film to reduce male-to-female transmission of sexually transmitted diseases. New England Journal of Medicine. 1998;339(8):504-10.
86. Van Damme L, Ramjee G, Alary M, Vuylsteke B, Chandeying V, Rees H, et al. Effectiveness of COL-1492, a nonoxynol-9 vaginal gel, on HIV-1 transmission in female sex workers: a randomised controlled trial. The Lancet. 2002;360(9338):971-7.
87. Stafford MK, Ward H, Flanagan A, Rosenstein IJ, Taylor-Robinson D, Smith JR, et al. Safety study of nonoxynol-9 as a vaginal microbicide: evidence of adverse effects. Journal of Acquired Immune Deficiency Syndromes. 1998;17(4):327-31.
88. Fichorova RN, Tucker LD, Anderson DJ. The molecular basis of nonoxynol-9-induced vaginal inflammation and its possible relevance to human immunodeficiency virus type 1 transmission. Journal of Infectious Diseases. 2001;184(4):418-28.
89. Krebs FC, Miller SR, Catalone BJ, Welsh PA, Malamud D, Howett MK, et al. Sodium dodecyl sulfate and C31G as microbicidal alternatives to nonoxynol 9: comparative sensitivity of primary human vaginal keratinocytes. Antimicrobial Agents and Chemotherapy. 2000;44(7):1954-60.
90. Peterson L, Nanda K, Opoku BK, Ampofo WK, Owusu-Amoako M, Boakye AY, et al. SAVVY®(C31G) gel for prevention of HIV infection in women: a phase 3, double-blind, randomized, placebo-controlled trial in Ghana. PloS One. 2007;2(12):e1312.
91. Olsen JS, Easterhoff D, Dewhurst S. Advances in HIV microbicide development. Future Medicinal Chemistry. 2011;3(16):2101-16.
92. Ongradi J, Ceccherini-Nelli L, Pistello M, Specter S, Bendinelli M. Acid sensitivity of cell-free and cell-associated HIV-1: clinical implications. AIDS Research and Human Retroviruses. 1990;6(12):1433-6.
93. Olmsted SS, Dubin NH, Cone RA, Moench TR. The rate at which human sperm are immobilized and killed by mild acidity. Fertility and Sterility. 2000;73(4):687-93.
94. Zeitlin L, Hoen TE, Achilles SL, Hegarty TA, Jerse AE, Kreider JW, et al. Tests of Buffergel for contraception and prevention of sexually transmitted diseases in animal models. Sexually Transmitted Diseases. 2001;28(7):417-23.
95. van de Wijgert J, Fullem A, Kelly C, Mehendale S, Rugpao S, Kumwenda N, et al. Phase 1 trial of the topical microbicide BufferGel: safety results from four international sites. Journal of Acquired Immune Deficiency Syndromes. 2001;26(1):21-7.
96. Mayer KH, Peipert J, Fleming T, Fullem A, Moench T, Cu-Uvin S, et al. Safety and tolerability of BufferGel, a novel vaginal microbicide, in women in the United States. Clinical Infectious Diseases. 2001;32(3):476-82.

97. Karim SSA, Richardson BA, Ramjee G, Hoffman IF, Chirenje ZM, Taha T, et al. Safety and effectiveness of BufferGel and 0.5% PRO2000 gel for the prevention of HIV infection in women. AIDS (London, England). 2011;25(7):957.
98. Neurath A, Strick N, Li Y-Y. Anti-HIV-1 activity of anionic polymers: a comparative study of candidate microbicides. BMC Infectious Diseases. 2002;2(1):1.
99. Mitsuya H, Looney DJ, Kuno S, Ueno R, Wong-Staal F, Broder S. Dextran sulfate suppression of viruses in the HIV family: inhibition of virion binding to CD4+ cells. Science. 1988;240(4852):646-9.
100. Keller MJ, Zerhouni-Layachi B, Cheshenko N, John M, Hogarty K, Kasowitz A, et al. PRO 2000 gel inhibits HIV and herpes simplex virus infection following vaginal application: a double-blind placebo-controlled trial. Journal of Infectious Diseases. 2006;193(1):27-35.
101. Mayer KH, Karim SA, Kelly C, Maslankowski L, Rees H, Profy AT, et al. Safety and tolerability of vaginal PRO 2000 gel in sexually active HIV-uninfected and abstinent HIV-infected women. AIDS. 2003;17(3):321-9.
102. Joshi S, Dutta S, Bell B, Profy A, Kuruc J, Fang G, et al. Documenting intermenstrual bleeding in a vaginal microbicide study: case reports and lessons learned. AIDS Research & Human Retroviruses. 2006;22(3):294-6.
103. McCormack S, Ramjee G, Kamali A, Rees H, Crook AM, Gafos M, et al. PRO2000 vaginal gel for prevention of HIV-1 infection (Microbicides Development Programme 301): a phase 3, randomised, double-blind, parallel-group trial. The Lancet. 2010;376(9749):1329-37.
104. Abdool Karim SS. Results of effectiveness trials of PRO 2000 gel: lessons for future microbicide trials. Future Microbiology. 2010;5(4):527-9.
105. Perotti M-E, Pirovano A, Phillips DM. Carrageenan formulation prevents macrophage trafficking from vagina: implications for microbicide development. Biology of Reproduction. 2003;69(3):933-9.
106. Bollen LJ, Blanchard K, Kilmarx PH, Chaikummao S, Connolly C, Wasinrapee P, et al. No increase in cervicovaginal proinflammatory cytokines after Carraguard use in a placebo-controlled randomized clinical trial. Journal of Acquired Immune Deficiency Syndromes. 2008;47(2):253-7.
107. Kilmarx PH, van de Wijgert JH, Chaikummao S, Jones HE, Limpakarnjanarat K, Friedland BA, et al. Safety and acceptability of the candidate microbicide Carraguard in Thai Women: findings from a Phase II Clinical Trial. Journal of Acquired Immune Deficiency Syndromes. 2006;43(3):327-34.
108. Skoler-Karpoff S, Ramjee G, Ahmed K, Altini L, Plagianos MG, Friedland B, et al. Efficacy of Carraguard for prevention of HIV infection in women in South Africa: a randomised, double-blind, placebo-controlled trial. The Lancet. 2008;372(9654):1977-87.
109. Anderson RA, Feathergill KA, Diao X-H, Cooper MD, Kirkpatrick R, Herold BC, et al. Preclinical evaluation of sodium cellulose sulfate (Ushercell) as a contraceptive antimicrobial agent. Journal of Andrology. 2002;23(3):426-38.
110. Schwartz JL, Mauck C, Lai J-J, Creinin MD, Brache V, Ballagh SA, et al. Fourteen-day safety and acceptability study of 6% cellulose sulfate gel: a randomized double-blind Phase I safety study. Contraception. 2006;74(2):133-40.
111. Malonza IM, Mirembe F, Nakabiito C, Odusoga LO, Osinupebi OA, Hazari K, et al. Expanded Phase I safety and acceptability study of 6% cellulose sulfate vaginal gel. AIDS. 2005;19(18):2157-63.
112. Van Damme L, Govinden R, Mirembe FM, Guédou F, Solomon S, Becker ML, et al. Lack of effectiveness of cellulose sulfate gel for the prevention of vaginal HIV transmission. New England Journal of Medicine. 2008;359(5):463-72.
113. Fichorova RN, Yamamoto HS, Delaney ML, Onderdonk AB, Doncel GF. Novel vaginal microflora colonization model providing new insight into microbicide mechanism of action. mBio. 2011;2(6):e00168-11.
114. van de Wijgert JH, Shattock RJ. Vaginal microbicides: moving ahead after an unexpected setback. AIDS. 2007;21(18):2369-76.
115. Maeda K, Nakata H, Ogata H, Koh Y, Miyakawa T, Mitsuya H. The current status of, and challenges in, the development of CCR5 inhibitors as therapeutics for HIV-1 infection. Current Opinion in Pharmacology. 2004;4(5):447-52.

116. Fletcher P, Herrera C, Armanasco N, Nuttall J, Romano J, Shattock R, editors. Anti-HIV activity of the candidate microbicide maraviroc, a CCR5 receptor antagonist. 5th IAS Conference on HIV Pathogenesis, Treatment and Prevention; 2009.
117. Kish-Catalone TM, Lu W, Gallo RC, DeVico AL. Preclinical evaluation of synthetic− 2 RANTES as a candidate vaginal microbicide to target CCR5. Antimicrobial Agents and Chemotherapy. 2006;50(4):1497-509.
118. Tsai C-C, Emau P, Jiang Y, Agy MB, Shattock RJ, Schmidt A, et al. Cyanovirin-N inhibits AIDS virus infections in vaginal transmission models. AIDS Research and Human Retroviruses. 2004;20(1):11-8.
119. Veazey RS, Klasse PJ, Schader SM, Hu Q, Ketas TJ, Lu M, et al. Protection of macaques from vaginal SHIV challenge by vaginally delivered inhibitors of virus–cell fusion. Nature. 2005;438(7064):99-102.
120. Lewi P, Heeres J, Arien K, Venkatraj M, Joossens J, Van der Veken P, et al. Reverse transcriptase inhibitors as microbicides. Current HIV Research. 2012;10(1):27-35.
121. Patton D, Sweeney YC, Balkus J, Rohan L, Moncla B, Parniak M, et al. Preclinical safety assessments of UC781 anti-human immunodeficiency virus topical microbicide formulations. Antimicrobial Agents and Chemotherapy. 2007;51(5):1608-15.
122. Di Fabio S, Van Roey J, Giannini G, Van den Mooter G, Spada M, Binelli A, et al. Inhibition of vaginal transmission of HIV-1 in hu-SCID mice by the non-nucleoside reverse transcriptase inhibitor TMC120 in a gel formulation. AIDS. 2003;17(11):1597-604.
123. Tintori C, Brai A, Dasso Lang MC, Deodato D, Greco AM, Bizzarri BM, et al. Development and in Vitro Evaluation of a Microbicide Gel Formulation for a Novel Non-Nucleoside Reverse Transcriptase Inhibitor Belonging to the N-Dihydroalkyloxybenzyloxopyrimidines (N-DABOs) Family. Journal of Medicinal Chemistry. 2016;59(6):2747-59.
124. Mahalingam A, Simmons AP, Ugaonkar SR, Watson KM, Dezzutti CS, Rohan LC, et al. Vaginal microbicide gel for delivery of IQP-0528, a pyrimidinedione analog with a dual mechanism of action against HIV-1. Antimicrobial Agents and Chemotherapy. 2011;55(4):1650-60.
125. Tsai C-C, Follis KE, Sabo A, Beck TW, Grant RF, Bischofberger N, et al. Prevention of SIV infection in macaques by (R)-9-(2-phosphonylmethoxypropyl) adenine. Science. 1995;270(5239):1197-9.
126. Mayer KH, Maslankowski LA, Gai F, El-Sadr WM, Justman J, Kwiecien A, et al. Safety and tolerability of tenofovir vaginal gel in abstinent and sexually active HIV-infected and uninfected women. AIDS. 2006;20(4):543-51.
127. Hillier SL, Justman J, Joshi S, Hosely C, Cyrus-Cameron E, Mâsse B, et al., editors. Safety and acceptability of daily and coitally dependent use of 1% tenofovir over six months of use. Microbicides 2008 Conference New Delhi, India; 2008.
128. Karim QA, Karim SSA, Frohlich JA, Grobler AC, Baxter C, Mansoor LE, et al. Effectiveness and safety of tenofovir gel, an antiretroviral microbicide, for the prevention of HIV infection in women. Science. 2010;329(5996):1168-74.
129. Marrazzo JM, Ramjee G, Richardson BA, Gomez K, Mgodi N, Nair G, et al. Tenofovir-based preexposure prophylaxis for HIV infection among African women. New England Journal of Medicine. 2015;372(6):509-18.
130. Rees H, Delany-Moretlwe S, Baron D, Lombard C, Gray G, Myer L, et al., editors. FACTS 001 phase III trial of pericoital tenofovir 1% gel for HIV prevention in women. Conference on Retroviruses and Opportunistic Infections (CROI); 2015.
131. Newman L, Rowley J, Vander Hoorn S, Wijesooriya NS, Unemo M, Low N, et al. Global estimates of the prevalence and incidence of four curable sexually transmitted infections in 2012 based on systematic review and global reporting. PloS One. 2015;10(12):e0143304.
132. Cates W, Wasserheit JN. Genital chlamydial infections: epidemiology and reproductive sequelae. American Journal of Obstetrics and Gynecology. 1991;164(6):1771-81.
133. Spaargaren J, Schachter J, Moncada J, De Vries HJ, Fennema HS, Peña AS, et al. Slow epidemic of lymphogranuloma venereum L2b strain. Emerging Infectious Diseases. 2005;11(11).

134. Haggerty CL, Gottlieb SL, Taylor BD, Low N, Xu F, Ness RB. Risk of sequelae after Chlamydia trachomatis genital infection in women. Journal of Infectious diseases. 2010;201(Supplement 2):S134-S55.
135. Cohen CR, Brunham RC. Pathogenesis of Chlamydia induced pelvic inflammatory disease. Sexually Transmitted Infections. 1999;75(1):21-4.
136. Fleming DT, Wasserheit JN. From epidemiological synergy to public health policy and practice: the contribution of other sexually transmitted diseases to sexual transmission of HIV infection. Sexually Transmitted Infections. 1999;75(1):3-17.
137. Galvin SR, Cohen MS. The role of sexually transmitted diseases in HIV transmission. Nature Reviews Microbiology. 2004;2(1):33-42.
138. Mabey D. Interactions between HIV infection and other sexually transmitted diseases. Tropical Medicine & International Health. 2000;5(7):A32-A6.
139. Plummer FA. Heterosexual transmission of human immunodeficiency virus type 1 (HIV): interactions of conventional sexually transmitted diseases, hormonal contraception and HIV-1. AIDS Research and Human Retroviruses. 1998;14:S5-10.
140. Rotchford K, Strum WA, Wilkinson D. Effect of Coinfection With STDs and of STD Treatment on HIV Shedding in Genital-Tract Secretions: Systematic Review and Data Synthesis. Sexually Transmitted Diseases. 2000;27(5):243-8.
141. Ho JL, He S, Hu A, Geng J, Basile F, Almeida M, et al. Neutrophils from human immunodeficiency virus (HIV)-seronegative donors induce HIV replication from HIV-infected patients' mononuclear cells and cell lines: an in vitro model of HIV transmission facilitated by Chlamydia trachomatis. Journal of Experimental Medicine. 1995;181(4):1493-505.
142. Moulder JW. Interaction of chlamydiae and host cells in vitro. Microbiological Reviews. 1991;55(1):143-90.
143. Dautry-Varsat A, Subtil A, Hackstadt T. Recent insights into the mechanisms of Chlamydia entry. Cellular Microbiology. 2005;7(12):1714-22.
144. AbdelRahman YM, Belland RJ. The chlamydial developmental cycle. FEMS Microbiology Reviews. 2005;29(5):949-59.
145. Marais D, Gawarecki D, Allan B, Ahmed K, Altini L, Cassim N, et al. The effectiveness of Carraguard, a vaginal microbicide, in protecting women against high-risk human papillomavirus infection. Antiviral Therapy. 2011;16(8):1219.
146. Lampe M, Rohan L, Skinner M, Stamm W. Susceptibility of Chlamydia trachomatis to excipients commonly used in topical microbicide formulations. Antimicrobial Agents and Chemotherapy. 2004;48(8):3200-2.
147. Neurath AR, Strick N, Li Y-Y, Lin K, Jiang S. Design of a “microbicide” for prevention of sexually transmitted diseases using “inactive” pharmaceutical excipients. Biologicals. 1999;27(1):11-21.
148. Sater AAA, Ojcius DM, Meyer MP. Susceptibility of Chlamydia trachomatis to the excipient hydroxyethyl cellulose: pH and concentration dependence of antimicrobial activity. Antimicrobial Agents and Chemotherapy. 2008;52(7):2660-2.
149. Osaka I. *In vitro* Susceptibility of *Chlamydia Trachomatis* to LPS-Binding Polyamines and Cellulose Ether Polymers: Towards the Development of a Microbicide Agent Against Chlamydia Infection. Dissertation, University of Kansas, 2013.
150. Lackman-Smith C, Osterling C, Luckenbaugh K, Mankowski M, Snyder B, Lewis G, et al. Development of a comprehensive human immunodeficiency virus type 1 screening algorithm for discovery and preclinical testing of topical microbicides. Antimicrobial Agents and Chemotherapy. 2008;52(5):1768-81.
151. Georgiev VS. "NIAID: Programs in HIV Prevention." National Institute of Allergy and Infectious Diseases, NIH. Humana Press; 2009. p. 363-73.
152. Fichorova RN, Anderson DJ. Differential expression of immunobiological mediators by immortalized human cervical and vaginal epithelial cells. Biology of Reproduction. 1999;60(2):508-14.

153. Stanley M. Pathology and epidemiology of HPV infection in females. Gynecologic Oncology. 2010;117(2):S5-S10.
154. Morrow KM, Underhill K, van den Berg JJ, Vargas S, Rosen RK, Katz DF. User-identified gel characteristics: A qualitative exploration of perceived product efficacy of topical vaginal microbicides. Archives of Sexual Behavior. 2014;43(7):1459-67.
155. Mahan ED, Zaveri T, Ziegler GR, Hayes JE. Relationships between perceptual attributes and rheology in over-the-counter vaginal products: a potential tool for microbicide development. PloS One. 2014;9(9):e105614.
156. Hoffman S, Morrow KM, Mantell JE, Rosen RK, Carballo-Diéguez A, Gai F. Covert use, vaginal lubrication, and sexual pleasure: a qualitative study of urban US Women in a vaginal microbicide clinical trial. Archives of Sexual Behavior. 2010;39(3):748-60.
157. Schneider G, Baringhaus K-H. "De Novo Design: From Models to Molecules." De novo Molecular Design. Weinheim: John Wiley & Sons; 2013. p. 1-55.
158. Selassie C, Verma RP. History of quantitative structure–activity relationships. Burger's Medicinal Chemistry and Drug Discovery. 2003.
159. Lipinski CA, Lombardo F, Dominy BW, Feeney PJ. Experimental and computational approaches to estimate solubility and permeability in drug discovery and development settings. Advanced Drug Delivery Reviews. 2012;64:4-17.
160. Slovic AM, Kono H, Lear JD, Saven JG, DeGrado WF. Computational design of water-soluble analogues of the potassium channel KcsA. Proceedings of the National Academy of Sciences of the United States of America. 2004;101(7):1828-33.
161. Huynh L, Grant J, Leroux J-C, Delmas P, Allen C. Predicting the solubility of the anti-cancer agent docetaxel in small molecule excipients using computational methods. Pharmaceutical Research. 2008;25(1):147-57.
162. Jorgensen WL, Duffy EM. Prediction of drug solubility from structure. Advanced Drug Delivery Reviews. 2002;54(3):355-66.
163. Bergström CA, Norinder U, Luthman K, Artursson P. Experimental and computational screening models for prediction of aqueous drug solubility. Pharmaceutical Research. 2002;19(2):182-8.
164. Lill MA, Danielson ML. Computer-aided drug design platform using PyMOL. Journal of Computer-Aided Molecular Design. 2011;25(1):13-9.
165. Looger LL, Dwyer MA, Smith JJ, Hellinga HW. Computational design of receptor and sensor proteins with novel functions. Nature. 2003;423(6936):185-90.
166. Clark LA, Boriack-Sjodin P, Eldredge J, Fitch C, Friedman B, Hanf KJ, et al. Affinity enhancement of an in vivo matured therapeutic antibody using structure-based computational design. Protein Science. 2006;15(5):949-60.
167. Carlson HA, McCammon JA. Accommodating protein flexibility in computational drug design. Molecular Pharmacology. 2000;57(2):213-8.
168. Sotriffer C, Klebe G. Identification and mapping of small-molecule binding sites in proteins: computational tools for structure-based drug design. Il Farmaco. 2002;57(3):243-51.
169. Röthlisberger D, Khersonsky O, Wollacott AM, Jiang L, DeChancie J, Betker J, et al. Kemp elimination catalysts by computational enzyme design. Nature. 2008;453(7192):190-5.
170. Siegel JB, Zanghellini A, Lovick HM, Kiss G, Lambert AR, Clair JLS, et al. Computational design of an enzyme catalyst for a stereoselective bimolecular Diels-Alder reaction. Science. 2010;329(5989):309-13.
171. Jiang L, Althoff EA, Clemente FR, Doyle L, Röthlisberger D, Zanghellini A, et al. De novo computational design of retro-aldol enzymes. Science. 2008;319(5868):1387-91.
172. Bolon DN, Mayo SL. Enzyme-like proteins by computational design. Proceedings of the National Academy of Sciences. 2001;98(25):14274-9.
173. Fjell CD, Hiss JA, Hancock RE, Schneider G. Designing antimicrobial peptides: form follows function. Nature Reviews Drug Discovery. 2011;11(1):37-51.

174. Dantas G, Kuhlman B, Callender D, Wong M, Baker D. A large scale test of computational protein design: folding and stability of nine completely redesigned globular proteins. Journal of Molecular Biology. 2003;332(2):449-60.
175. Park S, Yang X, Saven JG. Advances in computational protein design. Current Opinion in Structural Biology. 2004;14(4):487-94.
176. Qian N, Sejnowski TJ. Predicting the secondary structure of globular proteins using neural network models. Journal of Molecular Biology. 1988;202(4):865-84.
177. Roughton BC, Iyer LK, Bertelsen E, Topp EM, Camarda KV. Protein aggregation and lyophilization: Protein structural descriptors as predictors of aggregation propensity. Computers & Chemical Engineering. 2013;58:369-77.
178. Caflisch A. Computational models for the prediction of polypeptide aggregation propensity. Current Opinion in Chemical Biology. 2006;10(5):437-44.
179. Agrawal NJ, Kumar S, Wang X, Helk B, Singh SK, Trout BL. Aggregation in protein-based biotherapeutics: Computational studies and tools to identify aggregation-prone regions. Journal of Pharmaceutical Sciences. 2011;100(12):5081-95.
180. Eslick JC, Ye Q, Park J, Topp EM, Spencer P, Camarda KV. A computational molecular design framework for crosslinked polymer networks. Computers & Chemical Engineering. 2009;33(5):954-63.
181. Lin C-C, Metters AT. Hydrogels in controlled release formulations: network design and mathematical modeling. Advanced Drug Delivery Reviews. 2006;58(12):1379-408.
182. Fichorova R, Bajpai M, Chandra N, Hsiu J, Spangler M, Ratnam V, et al. Interleukin (IL)-1, IL-6, and IL-8 predict mucosal toxicity of vaginal microbicidal contraceptives. Biology of Reproduction. 2004;71(3):761-9.
183. Córdoba EV, Arnaiz E, Relloso M, Sánchez-Torres C, García F, Pérez-Álvarez L, et al. Development of sulphated and naphthylsulphonated carbosilane dendrimers as topical microbicides to prevent HIV-1 sexual transmission. AIDS. 2013;27(8):1219-29.
184. Scidmore MA. Cultivation and laboratory maintenance of Chlamydia trachomatis. Current Protocols in Microbiology. 2005:11A. 1.1-A. 1.25.
185. Riss TL, Moravec RA. Use of multiple assay endpoints to investigate the effects of incubation time, dose of toxin, and plating density in cell-based cytotoxicity assays. Assay and Drug Development Technologies. 2004;2(1):51-62.
186. Decker T, Lohmann-Matthes M-L. A quick and simple method for the quantitation of lactate dehydrogenase release in measurements of cellular cytotoxicity and tumor necrosis factor (TNF) activity. Journal of Immunological Methods. 1988;115(1):61-9.
187. Gerlier D, Thomasset N. Use of MTT colorimetric assay to measure cell activation. Journal of Immunological Methods. 1986;94(1-2):57-63.
188. Cummins Jr JE, Doncel GF. Biomarkers of cervicovaginal inflammation for the assessment of microbicide safety. Sexually Transmitted Diseases. 2009;36(3):S84-S91.
189. Scott ME, Wilson SS, Cosentino LA, Richardson BA, Moscicki A-B, Hillier SL, et al. Interlaboratory reproducibility of female genital tract cytokine measurements by Luminex: implications for microbicide safety studies. Cytokine. 2011;56(2):430-4.
190. Fichorova RN. Guiding the vaginal microbicide trials with biomarkers of inflammation. Journal of Acquired Immune Deficiency Syndromes. 2004;37(Suppl 3):S184.
191. Trifonova R, Doncel G, Fichorova R. Polyanionic microbicides modify Toll-like receptor-mediated cervicovaginal immune responses. Antimicrobial Agents and Chemotherapy. 2009;53(4):1490-500.
192. Fichorova R, Zhou F, Ratnam V, Atanassova V, Jiang S, Strick N, et al. Anti-human immunodeficiency virus type 1 microbicide cellulose acetate 1, 2-benzenedicarboxylate in a human in vitro model of vaginal inflammation. Antimicrobial Agents and Chemotherapy. 2005;49(1):323-35.
193. Trifonova RT, Bajpai M, Pasicznyk J-M, Chandra N, Doncel GF, Fichorova RN. Biomarkers of leukocyte traffic and activation in the vaginal mucosa. Biomarkers. 2007;12(6):608-22.

194. Doncel GF, Chandra N, Fichorova RN. Preclinical assessment of the proinflammatory potential of microbicide candidates. Journal of Acquired Immune Deficiency Syndromes. 2004;37:S174-S80.
195. Osaka I, Hills JM, Kieweg SL, Shinogle HE, Moore DS, Hefty PS. An automated image-based method for rapid analysis of Chlamydia infection as a tool for screening antichlamydial agents. Antimicrobial Agents and Chemotherapy. 2012;56(8):4184-8.
196. Grammen C, Augustijns P, Brouwers J. In vitro profiling of the vaginal permeation potential of anti-HIV microbicides and the influence of formulation excipients. Antiviral Research. 2012;96(2):226-33.
197. Zhang T, Sturgis TF, Youan B-BC. pH-responsive nanoparticles releasing tenofovir intended for the prevention of HIV transmission. European Journal of Pharmaceutics and Biopharmaceutics. 2011;79(3):526-36.
198. U. S. Environmental Protection Agency. 1996. Product Properties Test Guidelines. OPPTS 803.7840. Water Solubility: Column Elution Method; Shake Flask Method. EPA712-C-96-041, Prevention, Pesticides and Toxic Substances, Washington DC.
199. Rohan LC, Moncla BJ, Ayudhya RKN, Cost M, Huang Y, Gai F, et al. In vitro and ex vivo testing of tenofovir shows it is effective as an HIV-1 microbicide. PLoS One. 2010;5(2):e9310.
200. Tien D, Schnaare RL, Kang F, Cohl G, McCormick TJ, Moench TR, et al. In vitro and in vivo characterization of a potential universal placebo designed for use in vaginal microbicide clinical trials. AIDS Research & Human Retroviruses. 2005;21(10):845-53.
201. Lai BE, Xie YQ, Lavine ML, Szeri AJ, Owen DH, Katz DF. Dilution of microbicide gels with vaginal fluid and semen simulants: effect on rheological properties and coating flow. Journal of Pharmaceutical Sciences. 2008;97(2):1030-8.
202. Owen DH, Peters JJ, Katz DF. Rheological properties of contraceptive gels. Contraception. 2000;62(6):321-6.
203. Mahalingam A, Smith E, Fabian J, Damian FR, Peters JJ, Clark MR, et al. Design of a semisolid vaginal microbicide gel by relating composition to properties and performance. Pharmaceutical Research. 2010;27(11):2478-91.
204. Owen DH, Peters JJ, Lavine ML, Katz DF. Effect of temperature and pH on contraceptive gel viscosity. Contraception. 2003;67(1):57-64.
205. Kieweg SL, Katz DF. Squeezing flows of vaginal gel formulations relevant to microbicide drug delivery. Journal of Biomechanical Engineering. 2006;128(4):540-53.
206. Andrews GP, Gorman SP, Jones DS. Rheological characterisation of primary and binary interactive bioadhesive gels composed of cellulose derivatives designed as ophthalmic viscosurgical devices. Biomaterials. 2005;26(5):571-80.
207. Jones DS, Woolfson AD, Brown AF. Textural, viscoelastic and mucoadhesive properties of pharmaceutical gels composed of cellulose polymers. International Journal of Pharmaceutics. 1997;151(2):223-33.
208. Toğrul H, Arslan N. Production of carboxymethyl cellulose from sugar beet pulp cellulose and rheological behaviour of carboxymethyl cellulose. Carbohydrate Polymers. 2003;54(1):73-82.
209. Kamel S, Ali N, Jahangir K, Shah S, El-Gendy A. Pharmaceutical significance of cellulose: a review. Express Polymer Letters. 2008;2(11):758-78.
210. Siepmann J, Kranz H, Bodmeier R, Peppas N. HPMC-matrices for controlled drug delivery: a new model combining diffusion, swelling, and dissolution mechanisms and predicting the release kinetics. Pharmaceutical Research. 1999;16(11):1748-56.
211. OLSSON H, AXÉLL T. Objective and subjective efficacy of saliva substitutes containing mucin and carboxymethylcellulose. European Journal of Oral Sciences. 1991;99(4):316-9.
212. Satoh K, Takayama K, Machida Y, Suzuki Y, Nakagaki M, Nagai T. Factors affecting the bioadhesive property of tablets consisting of hydroxypropyl cellulose and carboxyvinyl polymer. Chemical & Pharmaceutical Bulletin. 1989;37(5):1366-8.
213. Kheyfets VO, Kieweg SL. Gravity-driven thin film flow of an ellis fluid. Journal of Non-Newtonian Fluid Mechanics. 2013;202:88-98.

214. Kheyfets VO, Kieweg SL. Experimental and numerical models of three-dimensional gravity-driven flow of shear-thinning polymer solutions used in vaginal delivery of microbicides. Journal of Biomechanical Engineering. 2013;135(6):061009.
215. Szeri AJ, Park SC, Verguet S, Weiss A, Katz DF. A model of transluminal flow of an anti-HIV microbicide vehicle: combined elastic squeezing and gravitational sliding. Physics of Fluids. 2008;20(8):083101.
216. Hu B, Kieweg SL. The effect of surface tension on the gravity-driven thin film flow of Newtonian and power-law fluids. Computers & Fluids. 2012;64:83-90.
217. Spaid M, Homsy G. Stability of Newtonian and viscoelastic dynamic contact lines. Physics of Fluids. 1996;8(2):460-78.
218. Swatloski RP, Spear SK, Holbrey JD, Rogers RD. Dissolution of cellose with ionic liquids. Journal of the American Chemical Society. 2002;124(18):4974-5.
219. Thuresson K, Lindman B, Nyström B. Effect of hydrophobic modification of a nonionic cellulose derivative on the interaction with surfactants. Rheology. The Journal of Physical Chemistry B. 1997;101(33):6450-9.
220. Kulkarni VS, Shaw C. Essential Chemistry for Formulators of Semisolid and Liquid Dosages. London: Elsevier Science; 2015.
221. Acheson DJ. Elementary Fluid Dynamics. Oxford: Oxford University Press; 1990.
222. Neves Jd, da Silva MV, Gonçalves MP, Amaral MH, Bahia MF. Rheological properties of vaginal hydrophilic polymer gels. Current Drug Delivery. 2009;6(1):83-92.
223. Bicerano J. Prediction of Polymer Properties. 3rd ed. New York: Marcel Dekker, Inc.; 2002.
224. R Core Team. R: A language and environment for statistical computing. Vienna, Austria: R Foundation for Statistical Computing; 2014 [update 18 June 2015; cited 30 July 2015]. Avaliable from: http://wwwR-project org.
225. Doelker E. Water-swollen cellulose derivatives in pharmacy. Hydrogels in Medicine and Pharmacy. 1987;2:115-60.
226. Fried JR. Polymer Science and Technology. Pearson Education; 2014.
227. Wira CR, Fahey JV, Sentman CL, Pioli PA, Shen L. Innate and adaptive immunity in female genital tract: cellular responses and interactions. Immunological Reviews. 2005;206(1):306-35.
228. Doncel GF, Clark MR. Preclinical evaluation of anti-HIV microbicide products: new models and biomarkers. Antiviral Research. 2010;88:S10-S8.
229. Köhidai L, Csaba G. Chemotaxis and chemotactic selection induced with cytokines (IL-8, Rantes and TNF-α) in the unicellular Tetrahymena pyriformis. Cytokine. 1998;10(7):481-6.
230. Poli G, Kinter AL, Fauci AS. Interleukin 1 induces expression of the human immunodeficiency virus alone and in synergy with interleukin 6 in chronically infected U1 cells: inhibition of inductive effects by the interleukin 1 receptor antagonist. Proceedings of the National Academy of Sciences. 1994;91(1):108-12.
231. Lane BR, Lore K, Bock PJ, Andersson J, Coffey MJ, Strieter RM, et al. Interleukin-8 stimulates human immunodeficiency virus type 1 replication and is a potential new target for antiretroviral therapy. Journal of Virology. 2001;75(17):8195-202.
232. Lajoie J, Juno J, Burgener A, Rahman S, Mogk K, Wachihi C, et al. A distinct cytokine and chemokine profile at the genital mucosa is associated with HIV-1 protection among HIV-exposed seronegative commercial sex workers. Mucosal Immunology. 2012;5(3):277-87.
233. Chesson HW, Pinkerton SD. Sexually transmitted diseases and the increased risk for HIV transmission: implications for cost-effectiveness analyses of sexually transmitted disease prevention interventions. Journal of Acquired Immune Deficiency Syndromes. 2000;24(1):48-56.
234. Lai BE, Geonnotti AR, DeSoto MG, Montefiori DC, Katz DF. Semi-solid gels function as physical barriers to human immunodeficiency virus transport in vitro. Antiviral Research. 2010;88(2):143-51.

235. Fichorova RN, Rheinwald JG, Anderson DJ. Generation of papillomavirus-immortalized cell lines from normal human ectocervical, endocervical, and vaginal epithelium that maintain expression of tissue-specific differentiation proteins. Biology of Reproduction. 1997;57(4):847-55.
236. Sanford KK, Earle WR, Likely GD. The growth in vitro of single isolated tissue cells. Journal of the National Cancer Institute. 1948;9(3):229-46.
237. Yasin B, Harwig S, Lehrer RI, Wagar EA. Susceptibility of Chlamydia trachomatis to protegrins and defensins. Infection and Immunity. 1996;64(3):709-13.
238. Yamamoto HS, Xu Q, Fichorova RN. Homeostatic properties of Lactobacillus jensenii engineered as a live vaginal anti-HIV microbicide. BMC Microbiology. 2013;13(1):4.
239. Heinrich MC, Kuhlmann MK, Grgic A, Heckmann M, Kramann B, Uder M. Cytotoxic effects of ionic high-osmolar, nonionic monomeric, and nonionic iso-osmolar dimeric iodinated contrast media on renal tubular cells in vitro 1. Radiology. 2005;235(3):843-9.
240. Agrahari V, Youan B-BC. Sensitive and rapid HPLC quantification of tenofovir from hyaluronic acid-based nanomedicine. AAPS PharmSciTech. 2012;13(1):202-10.
241. Kocis GR, Grossmann IE. Computational experience with DICOPT solving MINLP problems in process systems engineering. Computers & Chemical Engineering. 1989;13(3):307-15.
242. Brooke A, Kendrick D, Meeraus A. General Algebraic Modeling System (GAMS). Language Guide: Gams Development Corporation Washington DC; 2012.
243. Chavali S, Lin B, Miller DC, Camarda KV. Environmentally-benign transition metal catalyst design using optimization techniques. Computers & Chemical Engineering. 2004;28(5):605-11.
244. Ostrovsky GM, Achenie LE, Sinha M. On the solution of mixed-integer nonlinear programming models for computer aided molecular design. Computers & Chemistry. 2002;26(6):645-60.
245. Karri S. 2D Thin-Film Flow of a Non-Newtonian Fluid Between Elastic Boundaries. Thesis, University of Kansas; 2011.
246. Alperin M, Feola A, Duerr R, Moalli P, Abramowitch S. Pregnancy-and delivery-induced biomechanical changes in rat vagina persist postpartum. International Urogynecology Journal. 2010;21(9):1169-74.
247. Katz DF, Gao Y, Kang M. Using modeling to help understand vaginal microbicide functionality and create better products. Drug Delivery and Translational Research. 2011;1(3):256-76.
248. Egorov V, Sarvazyan AP. Methods for characterizing vaginal tissue elasticity. Google Patents; 2011.
249. Feller RL, Wilt MH. Evaluation of Cellulose Ethers for Conservation. Getty Publications; 1991.
250. Hostrup M, Harper PM, Gani R. Design of environmentally benign processes: integration of solvent design and separation process synthesis. Computers & Chemical Engineering. 1999;23(10):1395-414.
251. Anwar MR, Camarda KV, Kieweg SL. Mathematical model of microbicidal flow dynamics and optimization of rheological properties for intra-vaginal drug delivery: role of tissue mechanics and fluid rheology. Journal of Biomechanics. 2015;48(9):1625-30.